ABSTRACT

Title of Document:	Identifying Plant and Feedback in Human Postural Control
	Yuanfen Zhang, PhD, 2010
Directed By:	Professor John Jeka, Kinesiology, BioEngineering, Neuroscience and Cognitive Science Program

Human upright bipedal stance is a classic example of a control system consisting of a plant (i.e., the physical body and its actuators) and feedback (i.e., neural control) operating continuously in a closed loop. Determining the mechanistic basis of behavior in a closed loop control system is problematic because experimental manipulations or deficits due to trauma/injury influence all parts of the loop. Moreover, experimental techniques to open the loop (e.g., isolate the plant) are not viable because bipedal upright stance is not possible without feedback. The goal of the proposed study is to use a technique called closed loop system identification (CLSI) to investigate properties of the plant and feedback separately.

Human upright stance has typically been approximated as a single-joint inverted pendulum, simplifying not only the control of a multi-linked body but also how sensory information is processed relative to body dynamics. However, a recent study showed that a single-joint approximation is inadequate. Trunk and leg segments are in-phase at frequencies below 1 Hz of body sway and simultaneously anti-phase at frequencies above 1 Hz during quiet stance. My dissertation studies have investigated the coordination between the leg and trunk segments and how sensory

information is processed relative to that coordination. For example, additional sensory information provided through visual or light touch information led to a change of the in-phase pattern but not the anti-phase pattern, indicating that the anti-phase pattern may not be neurally controlled, but more a function of biomechanical properties of a two-segment body. In a subsequent study, I probed whether an internal model of the body processes visual information relative to a single or double-linked body. The results suggested a simple control strategy that processes sensory information relative to a single-joint internal model providing further evidence that the anti-phase pattern is biomechanically driven.

These studies suggest potential mechanisms but cannot rule out alternative hypotheses because the source of behavioral changes can be attributed to properties of the plant and/or feedback. Here I adopt the CLSI approach using perturbations to probe separate processes within the postural control loop. Mechanical perturbations introduce sway as an input to the feedback, which in turn generates muscle activity as an output. Visual perturbations elicit muscle activity (a motor command) as an input to the plant, which then triggers body sway as an output. Mappings of muscle activity to body sway and body sway to muscle activity are used to identify properties of the plant and feedback, respectively. The results suggest that feedback compensates for the low-pass properties of the plant, except at higher frequencies. An optimal control model minimizing the amount of muscle activation suggests that the mechanism underlying this lack of compensation may be due to an uncompensated time delay. These techniques have the potential for more precise identification of the source of deficits in the postural control loop, leading to improved rehabilitation techniques and

treatment of balance deficits, which currently contributes to 40% of nursing home admissions and costs the US health care system over $20B per year.

IDENTIFYING PLANT AND FEEDBACK IN HUMAN POSTURAL CONTROL

By

Yuanfen Zhang

Dissertation submitted to the Faculty of the Graduate School of the
University of Maryland, College Park, in partial fulfillment
of the requirements for the degree of
Doctor of Philosophy
2010

Advisory Committee:
Professor John Jeka, Chair
Dr. Tim Kiemel
Professor John Scholz
Professor William Levine
Dr. Jae Kun Shim
Professor Mark Rogers

Table of Contents

List of Tables

List of Figures

Chapter 1:

Study Postural Control Using Closed-loop System Identification

Postural control of the human body, which is often approximated as a single-joint inverted pendulum, is challenging, because an inverted pendulum is mechanically unstable. To maintain bipedal stance, the nervous system implements feedback to stabilize the upright human body. The control scheme through which the nervous system combines the musculo-tendon properties of the body (i.e. the plant) with the neural processing of sensory information (i.e. feedback) remains an open question. Within a certain range, increasing neural control and changing body dynamics can both help maintaining upright. One example of changing the body dynamics is modifying the base of support or shifting center of mass. When humanoid robots were designed, the stability problem was always solved by using wide-base feet and/or shifting weights to the lower extremities (e.g. Cornell Efficient Biped and Delft University Denise) (Kuo, 2007). However, these robots were built for tasks other than mimicking human stance. They do not capture the real anatomic features of the human body, which has a small base of support and most of the weight in the upper segment. Subsequently, a sophisticated control system is needed to constantly correct deviation from vertical in order to maintain upright.

Determining the properties of feedback and plant is nontrivial. There are two camps of studies in postural control. One focuses on state estimation with simplifying assumptions about the plant (Peterka, 2000; Mergner, Maurer, & Peterka, 2003;

Horak, Dickstein, & Peterka, 2002). Another camp focuses on the biomechanical perspectives of postural control while trivializing the problem of estimating body dynamics (Winter, Patla, Prince, & Ishac, 1998). The debate around the role of stiffness during quiet stance is a good illustration of this discrepancy. Winter et al. (1998) have argued that stiffness alone is sufficient in maintaining balance without active neural control. On the other hand, models focusing on state estimation often simplified the body as a single-inverted pendulum or a point mass (Peterka, 2004; Carver, Kiemel, van der Kooij, & Jeka, 2005). Both methods may be problematic. The nervous system and the body are mutually dependent. If the assumptions about one are false, then the interpretation about the other could be erroneous. During my graduate studies, I've been working to bridge these two camps.

1. RESEARCH PROJECTS

1.1. Previous projects

1.1.1. Influence of sensory information on two-segment coordination

My first project (chapter 3) investigated the influence of sensory information on inverted pendulum dynamics. The concept of ankle (i.e. a single-link inverted pendulum) and hip strategy (i.e. a double-link inverted pendulum) has been widely accepted in postural control research (Horak & Macpherson, 1996; Runge, Shupert, Horak, & Zajac, 1999; Bardy, Marin, & Stoffergen, 1999). Studies use these two strategies to explain neural and mechanical control in quiet stance. They were thought to be exclusive in postural control. Creath and colleagues (Creath, Kiemel, Horak, Peterka, & Jeka, 2005) have found that these two strategies exist at the same time during quiet stance but in different frequency range: ankle strategy (i.e. in-phase

pattern) at low frequencies; hip strategy (i.e. anti-phase pattern) at high frequencies. The subsequent question would be what the neural and mechanical contribution is for these two patterns. My first project addressed this problem by adding or removing vision and light touch information. We found that sensory information only affects the in-phase pattern, but not the anti-phase pattern. This indicates that the in-phase pattern may be controlled neurally but the anti-phase pattern may be primarily a function of the biomechanics of a two-link pendulum during quiet stance.

1.1.2. Two-segment coordination with bilateral vestibular loss[1]

My second project (chapter 4) applied similar methods to a patient population, analyzing the transition between the in-phase and anti-phase patterns in bilateral vestibular loss (BVL) patients. Although BVLs have severe balance problems, many studies in this population fail to identify the difference between BVLs and healthy subjects during postural control especially during quiet stance or when perturbations were small (Horak & Shupert, 1994; Shupert, Black, Horak, & Nashner, 1988a). We found that BVL patients have high variability of complex coherence (real part) in the transition from in-phase to anti-phase pattern than healthy adults. One implication of these findings is that such methods might be useful to identify the severity or compensation of vestibular sensory loss for this patient population.

1.1.3. A simple control strategy for upright stance control?

Neural control and state estimation play an important role in maintaining upright stance. However, it is not clear whether state estimation considers a multi-link internal model of the body when interpreting sensory information. One observation

[1] This data set was collected by Hamid Bateni, who was a Postdoctoral fellow under the supervision of Dr. John Jeka.

that suggests a relatively simple single-joint control strategy is that most of the power of postural sway is at low frequencies, below ≈0.6 Hz. At these frequencies, the in-phase trunk-leg coordination pattern predominates, suggesting that the nervous system is expending neural resources to maintain this relatively simple configuration of the body. In the third project, my master thesis (chapter 5), we tested more directly whether the nervous system takes into account multi-joint coordination when it interprets visual information. Traditionally, visual information was presented either as a translation or a rotation around the ankle joint with the underlying assumption that human body rotates around the ankle joint as a single-segment inverted pendulum (Peterka & Benolken, 1995; Oie, Kiemel, & Jeka, 2002). The co-existence of the in-phase and anti-phase patterns raises the issue of whether the nervous system interprets visual information in terms of a single- or multi-joint body. In addition to rotation (around the ankle) and translation of the visual stimuli scene, we studied visual rotation around the hip joint. Our results supported our prediction that a single-joint internal model is used to interpret sensory information, at least for vision.

1.2. Unsolved problems

The method that I had been using so far falls into the category of the indirect approach (van der Kooij, van Asseldonk, & van der Helm, 2005). In this approach, frequency response functions (FRFs) from sensory perturbation to body sway were calculated. Gain (i.e. absolute value of the FRF) and phase (i.e. argument of the FRF) were then estimated. Properties characterized by this method are the combination of dynamics of the feedback and the plant (van der Kooij et al., 2005). In figure 1.1., a simple closed loop with only feedback (the controller has been integrated as part of

feedback) and plant is illustrated. Sensory perturbation comes in as u and y is the output (i.e. sway) measured. FRF from u to y represents properties of feedback and plant. If we know the properties of one or the other, then it is relatively easy to attribute what we have characterized to either the feedback or the plant. However, since properties of neither of these are identified, one has to make assumptions for at least one of these components, and offer explanations based on these assumptions.

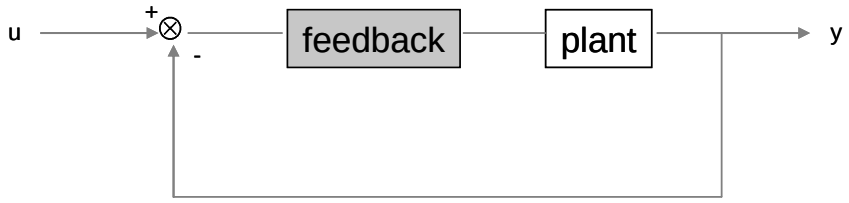

Figure 1.1. A simple closed loop.

The disadvantage of this approach is obvious: explanations might not hold if the assumption has been challenged. For instance, Peterka (2002) has assumed that the plant is a single-link inverted pendulum and attributed the 1 Hz oscillation seen in sway-referencing to sensory reweighting, that is, the feedback. However, recent experiments have shown that a single-joint inverted pendulum approximation is only valid at low frequencies (<1 Hz), while a two-joint inverted pendulum is assumed at high frequencies (>1 Hz) (Creath et al., 2005; Zhang, Kiemel, & Jeka, 2007). The question remains: whether the feedback or the plant accounts for these patterns? Alternatively, if these patterns were a result of both the feedback and plant, then how much does each of them contribute? In the initial attempt to answer this question, we changed sensory information (e.g. light touch, vision), which influenced the transition of phase from in-phase to anti-phase pattern at around 1 Hz. This indicates that feedback plays a major part in the in-phase pattern. The underlying assumption is that

the plant didn't change between conditions. This is a reasonable assumption when we studied healthy young adults with subtle perturbations. On the other hand, it was ambiguous when it came to patient population. To study the role of vestibular information in these patterns, BVL patients were compared to their age-matched controls. Although it is not well documented for BVL patients, patients with similar disease (i.e. Meniere's disease) has been shown to have muscle weakness (http://www.dizzinessbalancedisorders.com.au/images/pdfs/MSharpeVD.PDF). Furthermore, changing sensory information could not provide direct evidence of the contributions of the plant or feedback. We were not able to quantify the contributions of each these components.

In order to have a mechanistic understanding of postural control, we decided to use a mechanistic method, close-loop system identification, to identify the properties of the plant and feedback.

2. CLOSED-LOOP SYSTEM IDENTIFICATION METHOD

2.1. Brief background

In the context of a control theory, the nervous system and the human body correspond to two processes in human postural control: the feedback and plant, respectively. Figure 1.2. shows a conceptual view of the postural control system. Feedback is composed of sensory dynamics, state estimation and control strategy. Note that control strategy has been treated as part of feedback process as compared to the traditional control loop. The plant consists of musculotendon dynamics and body dynamics. Self-motion of the body can be measured through sensory dynamics,

which include vision, somatosensory and vestibular systems. However, this information is not directly available to the nervous system, but rather corrupted by noise and time delay. Therefore, sensory feedback fused from multiple modalities is used to estimate the body's state (i.e., position and velocity) and integrated with the control strategy to generate motor commands, which in turn elicit muscular activity. Torque is generated as a result of muscular activity with body sway as a consequence. The simplest control strategy is a proportional-derivative (PD) control. That is, position (proportional) coupling at low frequencies and velocity (derivative) coupling at high frequencies. The simplest body dynamics is a single inverted pendulum.

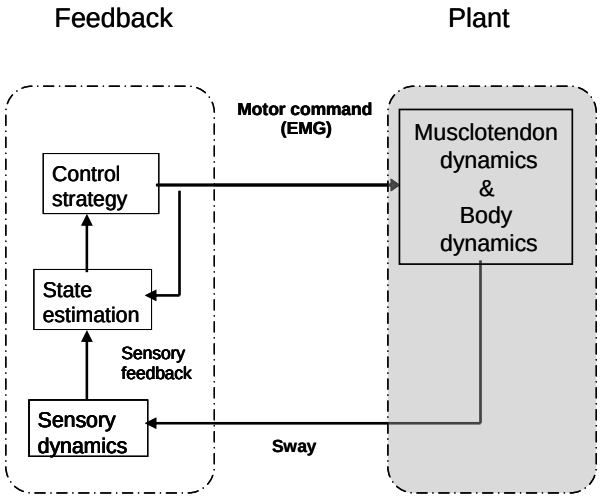

Figure 1.2. A conceptual view of the postural control system.

According to control theory, in order to determine properties of an unknown system, we need to know input into and output from the system. In the case of postural control, plant and feedback have mappings from time-varying inputs to time-varying outputs (figure 1.2.). The motor command is the input to the plant with body sway as the output. Electromyography (EMG) is a common method to measure muscular activity and often taken as a proxy for the motor command (Dai, Liu,

Sahgal, Brown, & Yue, 2001; Kandel, Schwartz, & Jessell, 2000). Body sway is the input to feedback with motor command as the output. However, EMG and sway are mutually dependent and we are still not able to differentiate the inputs and outputs. This is because feedback and plant are in a continuous loop and their inputs and outputs vary with time. In every moment, muscle activity is a combination of input to the plant and output from the feedback. In the same vein, body sway is a combination of output from the plant and input to the feedback. In order solve this problem, we can introduce known continuous sensory or mechanical perturbation and compute frequency response functions.

When a sensory perturbation (e.g. visual motion) is presented to the subject, the subject's feedback system interprets this visual motion as self-motion. This leads to a motor command (i.e. input) to the plant, which in turn generates sway (i.e. output) to compensate for this visual motion. By calculating the frequency response function (FRF) of both sway and EMG with respect to the known sensory perturbation, the common component of these two FRFs can be canceled: the feedback side of the control loop, allowing the properties of the plant to be indentified. Under the assumption of linearity, the plant FRF is calculated by dividing the FRF from visual scene to body sway (i.e. segment angle) by the FRF from visual scene to EMG, with the common feedback component cancelled out in calculation (figure 1.3).

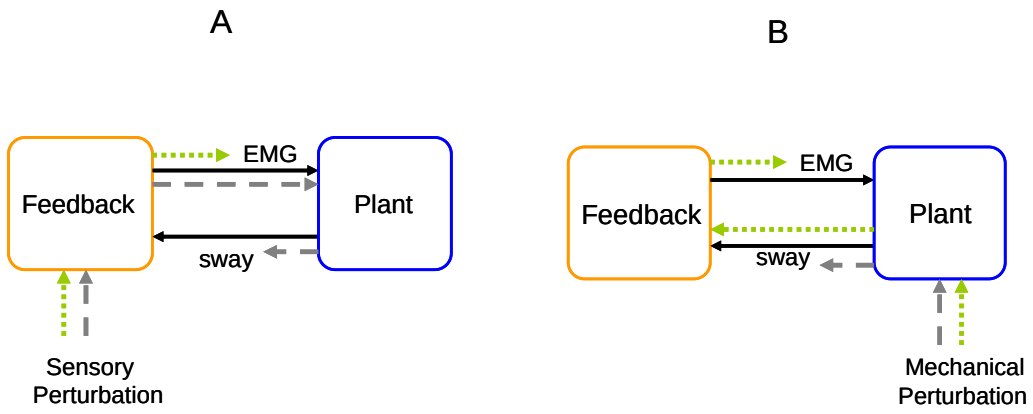

Figure 1.3. Schematics of methods. Sensory (A) and mechanical (B) perturbations are used to identify the plant and feedback, respectively. The gray dashed and green dotted lines are traces of FRFs.

In the same vein, a continuous mechanical perturbation is presented to the plant to induce sway (i.e. input), which is sensed by the feedback system. The feedback system in turn sends out motor command (i.e. output) to correct this body sway. The feedback loop can be computed as the FRF from the mechanical perturbation to muscle activity divided by FRF from motor perturbation to body sway. The plant, as the common component of these two FRFs, is cancelled out in the calculation, allowing the properties of the feedback alone to be identified.

2.2. Mathematical predictions

Predictions are based on a simple plant (i.e. a single inverted pendulum) and a simple controller (i.e. proportional-derivative, PD controller).

2.2.1. Plant

The simplest plant is a single-joint inverted pendulum.

$$\ddot{y} = \gamma y - x \qquad \text{(a. 1)}$$

$$\gamma = \frac{mgh}{J} \qquad \text{(a.2)}$$

Where *y* is sway angle*; x* is motor command*; m* is mass of the inverted pendulum; *g* is gravity acceleration; *h* is height of the center of mass; *J* is moment of inertia. That is, γ depends on mass. When there is no feedback, (a.1) can be simplified as

$$\ddot{y} = \gamma y \qquad \text{(a.3)}$$

When $\ddot{y} = 0$, the pendulum is vertically aligned. This also means that the plant is unstable.

The simplest feedback is a PD control. In this case,

$$x = k_p y + k_D \dot{y} \qquad \text{(a.4)}$$

Let X and Y be the Fourier transforms of *x* and *y*, because $\dot{y}(t) \leftrightarrow sY(s)$

$$X = k_p Y + sk_D Y \qquad \text{(a.5)}$$

Because $\ddot{y}(t) \leftrightarrow s^2 Y(s)$, a(1) can be rearranged as

$$s^2 Y = \gamma Y - X \qquad \text{(a.6)}$$

$$Y = \frac{X}{\gamma - s^2} = \frac{X}{\gamma + (2\pi f)^2} \qquad \text{(a.7)}$$

Where f is frequency. Because plant (A) is the mapping from EMG to sway, it is represented as:

$$A = \frac{Y}{X} = \frac{1}{\gamma + (2\pi f)^2} \qquad \text{(a.8)}$$

According to (a.8), as frequency increases, gain (the absolute value of A) decreases. Phase, the argument of A, should remain 0 across frequencies because A is always real and positive. If the plant is consisted of only body dynamics, then phase should remain constant. However, because the physiological processes underlying a muscular response are often on a slower time scale than a perturbation, muscles act

like low pass filters. Coupled with the inertia of the body, which also acts like a low pass filter, phase of body sway relative to a perturbation tends to decrease as the frequency of the perturbation increases.

2.2.2. Feedback

Feedback (B) is the mapping from sway to EMG. According to (a.5), we have

$$B = \frac{X}{Y} = k_p + sk_D = k_p + 2\pi k_D fi \qquad \text{(a.9)}$$

Therefore, as frequency increases, gain (i.e., absolute value of B) increases. At low frequencies, position coupling is dominant; while at high frequencies, velocity coupling is dominant (Jeka, SchÖner, Dijkstra, Ribeiro, & Lackner, 1997). Because velocity leads position displacement for 90 degrees for an inverted pendulum, phase would increase from 0 to 90 degrees at high frequencies.

3. PROPOSAL

In this proposal, I will apply the close-loop system identification method to characterize both the plant and feedback during quiet stance using a double inverted pendulum model. Two mechanical perturbations (i.e. one for the leg segment, one for the trunk segment) and one sensory perturbation will be used.

Fitzpatrick et al. (Fitzpatrick, Burke, & Gandevia, 1996) were the first to implement this method. However, there were two major problems with their approach. First, they implemented a single joint inverted pendulum model. More recent studies have shown that the in-phase and anti-phase patterns coexist during quiet stance, suggesting that a single link inverted pendulum may not be sufficient to characterize upright body dynamics (Creath et al., 2005; Zhang et al., 2007). Second,

Fitzpatrick et al (1996) applied sensory and mechanical perturbations in separate trials. Because of nonlinear processes such as sensory reweighting, perturbations applied in separate conditions may not be comparable if the system changes as a result of such perturbations (Peterka, 2002). I propose to use simultaneous sensory and mechanical perturbations to identify the feedback and plant properties of a multijoint body.

In the first attempt (my fourth project, chapter 6) to characterize the feedback and plant, we decided to look at two issues: 1). whether reweighting is evident when sensory and mechanical perturbation are used in separate trials; 2). whether a single inverted pendulum is sufficient to characterize the plant and feedback. Weak and continuous mechanical and sensory perturbations were applied both in separate trials and in the same trials. Visual rotation around the ankle joint was used as sensory perturbation. A mechanical perturbation was applied to the subject by attaching a spring between a waistbelt and a linear motor.

The leg and trunk segment yielded different patterns in terms of the plant, consistent with our hypothesis that a single inverted pendulum is insufficient to characterize the plant. The observed feedback properties were different from Fitzpatrick et al. (1996). It is possible that neither Fitzpatrick et al nor us identified the real feedback response. If the feedback has a single input and a single output, then the trunk angle should be a scaled version of the leg angle; while the weighted summation of hip EMG should be a scaled version of the weighted summation of the ankle EMG. In terms of gain and phase, the gain ratio between the two segments should be around 1 and phase difference around 0. However, this prediction was not

consistent with our data, suggesting that two inputs and two outputs are necessary. We used one input (i.e. applying only one mechanical perturbation on waist) and two outputs (i.e. trunk and leg segments) to identify the feedback, while Fitzpatrick used one input and one output (i.e. a one-segment inverted pendulum). The feedback must be designed appropriately for the plant in order to elicit the real feedback response. Therefore, in this proposal study, I am going to apply two mechanical perturbations: one for the leg segment and one for the trunk segment, to test the following hypotheses:

3.1a: The plant can be approximated as the mapping from a single weighted EMG signal to two body segment angles (legs and trunk).

3.1b: Feedback can be approximated as the mapping from two body segments to a single weighted EMG signal.

3.2: The feedback is more than a simple PD control.

3.3: The anti-phase pattern is determined by the biomechanical properties of the plant.

Chapter 2:

A Review of Literature

Postural control may seem like a trivial task during normal daily life. However, the small body sway generated in postural control tells us complicated interaction of the physical body and the nervous system.

1. WHAT IS POSTURAL CONTROL?

1.1. A Classical View of Postural Control

In the late 1800s and early 1900s, Sherrington argued that the nervous system controls the motor system by reflexes, which are stereotyped movements elicited by peripheral receptors, such as muscles or skin (Kandel et al., 2000). Reflexes are simple stimulus-response reactions, in which higher-level central nervous system is not necessary. Reflexes require a minimum of two neurons, a sensory neuron and a motor neuron. Spinal reflexes are typical in postural control. The afferent fibers pass information from peripheral sensors onto the spinal cord, from which the motor neurons send commands to the muscles through efferent fibers. The sensory inputs into the spinal cord either make direct connection to the motor neurons (monosynaptic reflexes, e.g. stretch reflex) or synapse on the interneurons, which connect both ipsilateral flexor muscles and contralteral extensor muscles (polysynaptic reflexes, e.g. flexion and crossed-extension reflex). Spinal reflexes, especially stretch reflexes, serve to resist the lengthening of muscles, thus providing muscle tone, which has even been proposed as the single factor in posture

stabilization (Winter, Patla, Prince, & Ishac, 1998). Other reflexes, such as vestibtulo-spinal and cervico-spinal reflexes are also important. The vestibule-spinal reflexes are activated when the head position is changed, while the cervico-spinal reflexes are used when the trunk is moved (Kandel et al., 2000). They act synergistically to decide whether the head and trunk move together or independently in experiments done on cats. Cervico-spinal reflexes exist only in newborn babies in human.

However, this theory over simplified movement control: it doesn't explain motor control without external perturbation and the adjustment to new environment (Shumway-Cook & Woollacott, 2000). Magnus (1924, 1925) suggested that postural control is a summation of different reflex pathways, which are part of a hierarchical motor control system. This reflex/hierarchical theory became predominant in the 70s. According to this theory, peripheral generators execute a sequence of stereotyped patterns prescribed by the brain (Nashner & Woollacott, 1979). Reflexes are not the only dominant factor of motor control any more (Shumway-Cook et al., 2000), but rather sensory information is thought to be important. The implicit assumption is that the low-level behaviors are nonadaptive and immature, while the high-level behaviors are adaptive and mature (Shumway-Cook et al., 2000). In other words, the basic movement patterns among the limbs, such as muscles and mechanical linkages, are reflexes and fixed; the human body adapts to the environment by prescribing different sequences of patterns (Nashner et al., 1979). However, this sequential organization requires that each step in the sequence to be fast enough, which is conflict with the relative slowness of synaptic processing in the nervous system (Morasso & Sanguineti, 2003).

1.2. A Modern View of Postural Control

As discussed above, the classic view of postural control had at least three assumptions: 1. the "brain" controls all subsystems; 2. the subsystems controlled are static and quiescent; 3. the control is concrete. These assumptions are challenged by the modern view of postural control.

1.2.1. What is controlling?

In 1982, Stein(Stein, 1982) raised the question what muscle variable(s) the nervous system controls in (limb) movements and provided some possible answers. More than 30 commentaries were written in response to his target article with various answers. Kelso & Saltzman were not even satisfied with the question itself by saying the assumption, namely, muscle variables are controlled, is questionable. Here, I want to step back further and focus on the question: is the nervous system controlling? The hierarchical and self-organized schemes would give two extreme answers to this question. In the hierarchical scheme mentioned above, the brain prescribes detailed commands to the lower level systems. While for the self-organization scheme, behavior emerges from multiple subsystems with none of these components controlled by the brain. The role of the brain in this case is giving a rather abstract command to kick off the subsystems. Many other theories, such as the equilibrium point theory (EP), fall in a continuum between these two schemes. EP advocates that a specific descending command or perturbation can trigger a set of preprogrammed functions.

1.2.2. Are the systems being controlled static or dynamic?

Are systems (this term is vague and will be discussed further in the next session) being controlled static or dynamic? Are systems isolated or interacting? The chain-reflex theory pointed out that the conduction in the nervous system is always downstream from sense organ to muscle, and that muscular contraction must always follow promptly on stimulation. This assumes that the nervous system is a quiescent or static system with hardwired reflexes. Almost 50 years later, Lashley (Lashley, 1951) argued that the nervous system is a dynamic, constantly active system and the series of items are internally activated before being externally stimulated.

Furthermore, the components of an active system are not isolated but interactions among them are necessary. This idea was derived from a fairly simple experiment, in which different pairs of legs were amputated from a centipede resulting in different gait patterns. The number of the legs left determined the phase difference between legs.

1.2.3. Is control abstract or concrete?

In the previous session, I used "system" as being controlled. But the level of analysis has been diverse across theories: reflex was used in chain-reflex theory, patterns are the unit of analysis in dynamic theory, and muscles were used in EP. If scientists were satisfied with talking only at their own level of analysis, then there would not have been so many debates like the one around Stein's question. The initial intend of EP theory was to find out a variable, at some level of motor control hierarchy, which would be controlled for all motor tasks. Although this claim is controversy, it does succeed at some level. For example, Bizzi et al. (Bizzi, Polit, & Morasso, 1976) did an experiment on head movement in monkeys and their findings

were consistent with the EP theory. This can be well explained by Latash's (Latash, 1993) comment that the tonic stretch reflex they used in the original experiments was a functional but not a morphological concept. On the other hand, this comment is no more than Sherrington taking reflex as "a simple, if not a probable fiction". That is, control is abstract rather than concrete. This gives theories strength to go beyond where they were derived. For example, the dynamic theory has been used to explain different levels of neural mechanisms from behavioral patterns, neural networks to individual neurons.

Therefore, in a modern view, movement and postural control requires complicated interactions among neural and muscular systems.

2. NEUROLOGY OF POSTURAL CONTROL

Control of posture requires continuous inflow of somatosensory, visual and vestibular information to the motor system. This process involves both the peripheral sensory systems and central nervous system.

2.1. Peripheral Sensory Systems

2.1.1. Somatosensory System

The somatosensory system, including muscle proprioception, joint and cutaneous afferents, serves two roles, it provides information about: 1) the relative position and velocity between body segments and; 2) force and surface properties of the surrounding environment. Proprioception is carried by muscle spindles and golgi tendon organs, which provide information about the velocity and position of the muscle and muscle force respectively. For instance, the length of the ankle muscles

will provide an estimation of the degree of body tilt and hence postural orientation (Horak et al., 1996). The joint receptors are excited by moving the joint to its extremes and sensing flexion and extension of a joint (Matthews, 1988). The cutaneous inputs are important for the phasic information about movement (for a review, see Matthews, 1988). Sudden changes between the support surface and the feet result in stretching and deformation of skin. The rate of firing of the resulted shearing forces informs the velocity of the perturbation (Horak et al., 1996). At the low level of the central nervous system (CNS) hierarchy, the cutaneous inputs are also responsible for reflex movements (Shumway-Cook et al., 2000). In adults, the stimulation of the sole of the feet usually causes the toes to reflex. Because of the fact that somatosensors are distributed throughout the body, they are believed to contribute most to the configuration of the body segments (Horak et al., 1996). When bilateral vestibular loss patients were asked to stand with their eyes closed on a tilting platform, they kept their balance successfully, despite having only somatosensory information as their only resource (Maurer, Mergner, Bolha, & Hlavacka, 2001).

2.1.1. Vestibular

The nervous system uses the vestibular information to detect the position and motion of the head relative to gravity (Horak et al., 1994). The semicircular canals and otoliths are the vestibular sensors involved in the angular and linear acceleration of the head, respectively. These organs are surrounded by membranous and bony labyrinth with perilymph separating the two layers. The membranous labyrinth is filled with endolymph and lined with clusters of hair cells. The relative movement between the endolymph and perilymph caused by the acceleration of the head makes

the hair cells bend, which in turn detects the motion of the head. The otoliths are activated when the head tilts with respect to the gravity. The semicircular canals sense fast head motions (Horak et al., 1996), such as a sudden trip, which indicate that they don't play an important role in quiet stance. Angelaki et al. (Angelaki, McHenry, Dickman, Newlands, & Hess, 1999) have performed an experiment comparing both normal and canal-plugged monkeys. Without damaging the semicircular canals, the monkeys elicited horizontal eye movements in response to translation only but not head tilt conditions. After canal-plugged, the eye movement was related to the resultant acceleration along the naso-occipital, interaural (IA) axis regardless of head tilt or translation. Therefore, information from the canals and otoliths are integrated.

2.1.3. Visual system

Vision is important to identifying the location and shape of objects in space by detecting the relative three-dimensional motion between head and the visual scene, thus guiding movements. It has been indicated that vision input dominates at the low frequencies of body sway (Berthoz, Lacour, Soechting, & Vidal, 1979). However, some other research showed that vision also affects the rapid posture adjustment (Nashner, 1981; Nashner & Berthoz, 1978). Vision is very important in the feedforward control in balance, such as to ovoid an obstacle (Gibson, 1952). Despite vision's important role, it is not absolutely needed. Because when we close our eyes, we can still maintain balance during quiet stance. And sometimes, vision can be misleading when the information of self-motion is not accurate (Shumway-Cook et al., 2000). For instance, two trains stopped next to each other and you are in one of them. If another train moves slightly forward, you may think the train you are on is

moving backward. Self-motion and displacement from external objects can have the same impact on motion, therefore, postural control by vision relies on other sensory information, such as the vestibular information to differentiate them (Guerraz et al., 2000). It is worthy to note that this ambiguity of sensory information also exists in other two sensory modalities.

2.2. Central Systems.

Sensory information passes from the periphery onto the central system, where the input information is processed to control posture. These hierarchically organized systems include spinal cord, brain stem and the cortex. Moreover, basil ganglia and cerebellum also contribute to the planning and execution of postural control. Each level has circuits that can organize or regulate complex motor responses. Sensory information in these systems is operated in parallel (Kandel et al., 2000).

2.2.1. Spinal Cord

The spinal cord is the lowest level of the central nervous system. Spinal cord circuits alone don't produce the organized equilibrium responses in postural control, but mediate reflexes (Kandel et al., 2000; Horak et al., 1996). This was supported by the experiment that adult cats with a complete transection can maintain balance for a short period of time. It was suggested that this might be achieved by local segmental reflex mechanism (Pratt, Fung & Macpherson, 1994, as cited in Horak, et al., 1996).

2.2.2. Brain Stem

The next level of the hierarchy is the brain stem, which obtains inputs from the cerebral cortex and subcortical nuclei and projects to the spinal cord by two descending systems: 1) the medial descending systems, including the reticulospinal,

medial and lateral vestibulospinal and tectospinal tracts, which integrate visual, vestibular and somatosensory information to control postural orientation and equilibrium, and 2) the lateral descending systems, including the rubrospinal tract, which are important for goal directed movement (Kandel et al., 2000). In the brain stem, there are 4 vestibular nuclei projecting to the motor neurons of eye and head movements through the vestibulospinal tract. These connections make vestibule-ocular control possible. When the head moves, the eyes move in a compensatory direction at the same speed as the motion of the head, thus stabilizing images on the retina.

2.2.3. The Cortex

The cerebral hemisphere is the largest region of the human brain. It is organized in 6 distinctive layers from the outmost to the deepest: molecular layer, external granule cell layer, external pyramidal cell layer, internal granule cell layer, and multiform layer. The outmost one is layer I, which is dominated by dendrites of cells from deeper cortex. Connections between different areas are mainly formed in this layer. The cortex is divided into 4 functional lobes: frontal, parietal, temporal and occipital. There are distinct functions involved in each of the lobes. The central sulcus separates the frontal and parietal lobes. The precentral gyrus is the primary motor cortex, which is involved in movement of a joint in a vector. The area rostral to primary motor cortex is motor association cortex, which is involved in motor preparation and programs. The postcentral gyrus and posterior parietal area are part of the primary sensory cortex and unimodal sensory association area, respectively. The occipital cortex is also known as visual cortex.

Efferent inputs from the primary motor cortex and other motor cortexes either control movement by both projections to the spinal cord or regulate the motor tracts derived in the brain stem (Kandel et al., 2000). There are two descending pathways from motor areas in the cortex: 1) the corticobulbar pathways controlling the motor nuclei in the brain stem, primarily involved in movements of the face and tongue and; 2) the corticospinal pathways control the spinal motor neurons that innervate the trunk and limb muscles (Kandel et al., 2000). Neurons in the motor cortex are sensitive to unexpected perturbation of stance. When cats modify gait to avoid obstacles, activity of cells in motor cortex are modulated (Drew, 1993, as cited in Horak, et al., 1996).

2.2.4. Basal Ganglia and Cerebellum

Both basal ganglia and cerebellum are useful for smooth movement and posture. The motor cortex sends information to both of them, which in turn send feedback to the motor cortex via the thalamus. The output of cerebellum is excitatory, while the output of basal ganglia is inhibitory. The basal ganglia don't have direct connections with the spinal cord. Therefore, most of their motor functions are mediated by motor areas in the frontal cortex (Kandel et al., 2000). Parkinsonism is ideal for studying basil ganglia postural disorder. It is characterized by rigidity caused by increased muscle tone (Kandel et al., 2000), which is the force muscle uses to resist lengthening. Furthermore, Parkinsonian patients used the same pattern of muscle activation to respond to surface perturbations, suggesting that basal ganglia are important for the adaptation of motor patterns to context (Horak, Nutt, & Nashner, 1992).

The cerebellar syndromes are characterized by ataxia, evidence for postural coordination function of the cerebellum. The cerebellum influences postural coordination by comparing disparities between intention and action through feedback signals, and by adjusting the operation of motor centers in the cortex and brain stem (Kandel, et al., 2000). It has been showed that the cerebellum generates corrective signals and gradually reduces errors when a movement is repeated, suggesting a role in motor learning.

2.3. Sensory integration

2.3.1. What is sensory integration?

Different modalities of sensory information combine and contribute to movement. The environment or task changes all the time and not all the sensory information is always available, such as entering a dark room or standing on a floating boat. The motor control system needs to adapt to the new environment or task. Redundancy and integration of multisensory are two important aspects in adaptation (Horak et al., 1996). Redundancy means even if one or two of the sources of the sensory information are missing, movement tasks can still be achieved. For example, the CNS uses both vision and proprioception to code the position of our arms during reaching tasks. When vision is not available, it is still possible to reach a target.

2.3.2. Sensory integration in the CNS

Sensory integration mechanism is still an open question. There are many interesting proposals, such as the view from Stein and Meredith. According to them, sensory integration depends on the temporal spatial relationship of the receptive fields

of the two sensory modalities involved in the superior colliculus (SC) (Stein, 1998). If two different sensory stimuli derived from the same location in space, they are more likely to fall within the respective excitatory receptive fields of the same multisenory SC neuron. This results in a synergy effect. On the other hand, if the two stimuli are spatially far away from each other, then integration of these two modalities will be depressed. However, many other aspects other than temporal spatial relationship of the receptive fields, such as reference frame, decision making, are also important in sensory integration.

A single modality of sensory information may be enough to control a specific posture, but the most stable posture requires an integration of sensory information to adjust within a well-defined spatial reference frame (Buchanan & Horak, 1999). All sensory modalities are coded in different coordinate systems. The representation of an object with respect to the body relies not only on where the eyes are looking, but also the relative position of the head to the body (Andersen, Snyder, Bradley, & Xing, 1997). Multiple experiments have indicated that coordinate system transformation is likely to happen in the posterior parietal cortex (PPC).

It has been suggested that the nervous system integrates sensory information according to an internal model. They are two types of internal model: the forward and inverse model. A forward model serves as a fast internal loop that uses the motor command to control the motor system and predicts the next state. Transformation from sensory variables to motor variables is known as internal inverse model, which estimates the motor commands that induce a certain state transition (Wolpert, Ghahramani, & Jordan, 1995). It has been suggested that sensory integration happens

in the forward model to make state estimation, which provides prediction of the next state based on the current state of the arm (Miall & Wolpert, 1996). Errors between the desired state and the actual output of the movement are applied to update the internal model and change motor commands, hence the adaptation process.

Scientists have proposed that internal models are located in all brain areas with synaptic plasticity. For example, Kawato (Kawato, 1999) has proposed an internal model in the cerebellum for ocular following response (OFR).

Many studies have been hypothesized that this adaptation is achieved through changing weights for different sensory modalities, hence the name of sensory reweighting. This process requires a decision making process to decide which sensory modality is more reliable (Jeka, Oie, & Kiemel, 2000). Sensory conflict is common during postural control. For example, you stand on a train while another train is slowly passing by. In this case, you need to figure out whether the other train is moving or the train you are on is moving in the opposite direction. That is, you need to deicide whether vision or proprioception is more reliable. Often times, you might think that the train you are on is moving even though proprioception is more reliable in this case. After you decide which modality is more important, the particular modality gets upweighted and the other sensory modalities get downweighted.

The lateral intraparietal area (LIP) has been shown to be involved in decision making. For example, monkeys were required to decide the movement direction of a cloud of white dots moving against a black background with different fraction of dots moving in one of the two possible directions. The monkeys made a saccade to indicate the movement direction of the white dots. The lateral intraparietal area (LIP)

involves in decision making through encoding a combination of sensory, motor and cognitive signals. Thus, LIP acts as a common currency for mapping of inputs from different sources (Sugrue, Corrado, & Newsome, 2005).

I have provided some views in multisensory integration in the CNS. These views cannot exhaust all the aspects of sensory integration, of course. However, they are enough to point out some weaknesses of Meredith and Stein's (M&S) view.

M & S's proposal is more or less a passive or static view, in which sensory information is simply summed together. This summation only depends on the spatial and temporal properties of sensory information. However, sensory integration could be under modification by many factors, such as experience or cognitive factors. In studies of sensory integration in postural control, a "moving room" paradigm is often used. That is, subjects stand in a visual surround that can be moved in a specified way while the platform the subjects stand on is either fixed or moved. One interesting observation during my experiments was that many subjects usually interpreted the small visual movement as fixed, while thought that the static force platform they stood on was moving. This illusion is very strong even when the subjects were told in advance that the platform was fixed. This can not be explained by M & S's view. On the other hand, in this context, the subject might decide that vision is more reliable than proprioception. Furthermore, sensory integration can be changed as the result of learning and updating of an internal model.

As I have reviewed in the previous session, a lot of brain areas, including SC, LIP, PPC and cerebellum could contribute to multisensory integration. At the mean time, different central functions, such as decision making and reference frame

transformation, also play a role. Evidence so far has pointed to the direction that sensory integration relies on a distributed network rather than a restricted area, such as SC.

2.3.3. Sensory reweighting in postural control

Contribution of different sensory modalities is not identical in sensory integration. Rather, weights of each sensory modality change accordingly to the changing environment following a dynamic process, thence the name sensory reweighting. Peterka (2004) has modeled the dynamic weight change during removing and restoring sensory information. In this study, subjects stood on a fixed platform for 1 min followed by platform sway-referencing for another 1 min and then the platform returned to static again. Eyes were closed through the whole trial. As we can see from the figure 2.1, weights for proprioception (Wp, blue) was higher than graviception (sense of motion with respect to vertical, Wg, red) before the onset of platform sway-referencing. During sway-referencing, Wp dropped to zero, Wg went up to close to 1. In this case, after sway-referencing, Wp went back again and Wg started to decrease. Peterka (2004) is a simplified case of sensory reweighting with the assumption that there is no dynamics between sensory information. In reality, this may not be true.

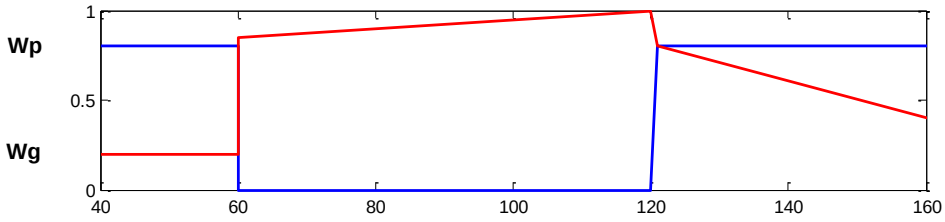

Figure 2.1. Sensory reweighting in Peterka 2004.

In experimental postural control studies, sensory reweighting has been demonstrated through gain and phase of body sway (e.g. COM, segment angle) with respect to the stimuli signals in a moving room paradigm. Methods in these studies assume that the sensory coupling system is linear. That is, response of the motor system is driven by both spatial and temporal structures of the visual stimulus: 1) postural sway is induced in the direction of the visual motion; 2) the coordination patterns are temporally stable, in another word, the coordination patterns are reproducible and sustain inspire of perturbations (SchÖner, 1991).

Following the use of this linear method, interesting nonlinear sensory reweighting has been found. For a linear system, body sway would increase as a function of input stimulus amplitude increases. However, Peterka and Benolken (Peterka et al., 1995) have observed a saturation effect. That is, body sway doesn't increase further as a function of the vision stimulus as the amplitude reaches a saturation level. Healthy subjects with ability of sensory reweighting can downweight the unreliable sensory information and maintain balance. On the other hand, patients with sensory deficit (e.g. bilateral vestibular loss) increase their gains with respect to the stimulus and eventually loss their balance.

2.4. Cognition

Postural control is viewed as the meaningful integration of many different neural systems, including those associated with perception, adaptation, and cognition. Some important aspects of cognition involved in postural control include attention and central set.

Dual task paradigm has been used a lot in studies looking at attention, which is the capacity that an individual processes information. In such a paradigm, subjects are usually asked to perform a secondary task, such as memory task, while standing or walking. The primary task (i.e. postural control or gait) and secondary task should not interact with each other in an experiment of dual task. The assumption is that attention is limited for an individual. Motor tasks share this capacity with other cognitive tasks (Woollacott & Shumway-Cook, 2002). When performing a hard balance task (e.g. a heel-to-toe stance) or for fall-prone people (e.g. elderly person), adding a secondary task deteriorates the balance task. The more complex the secondary task, the more postural control was affected (for a review, see Woollacott, et al., 2002). In a recent study, healthy elderly subjects performed 3 different cognitive tasks during walking (van Iersel, Ribber, Munneke, Borm, & Olde Rikkert, 2007). They were required to subtract 7 from 100 and 13 from 100 in the attention-demanding tasks; citing words starting with "K" or "O" in the verbal fluency task. Subjects reduced gait velocity in order to increase support time and maintain their balance. This effect was most obvious in the verbal frequency task, which is more demanding in attention than the other two tasks. Subtracting 7 from 100, the least demanding among these tasks, affected gait velocity in the least severe way.

Another possible explanation for a dual task paradigm is that neural networks of the frontal and motor cortex interfere with each other (van Iersel et al., 2007). It was found that patients have Parkinson's disease (PD) also have difficulties in dual tasks. For PD patients with freezing (PD-F), antiparkinsonian medications improved their gait parameters but had no effect on dual task performing. It is possible that

these patients might have additional attention deficits in the frontal cortex, thus interfering compensation during dual task (Camicioli, et al. 1998, cited from Wollacott et al, 2002).

Central set involves the modification of automatic motor responses based on expectation of stimulus and task characteristics. That is, subjects' prediction and knowledge about the environment and experiences in the past will affect their postural control (Horak, et al., 1996). For instance, after subjects were exposed to 6-11 trials of small amplitude platform perturbation, they underresponded with smaller initial ankle torques when presented to randomly inserted (unexpected) large amplitude platform perturbation, and vice versa (Horak, Diener, & Nashner, 1989).

3. BODY DYNAMICS AND MUSCULOTENDON DYNAMICS

Postural control is a sensorimotor integration task. Sensory integration and cognition must be compatible with the biomechanics and musculature aspects of the body.

3.1 Single and Double Inverted Pendulum

The human body has been approximated as an inverted pendulum during upright postural control. One of the applications is using ankle and hip strategy to explain both neural and biomechanical perspectives of postural control. The assumption is that the human body is a single-segment and two-segment inverted pendulum in ankle and hip strategy, respectively. In an ankle strategy, the body segments remain aligned, rotating predominantly around the ankle joint. That is, both leg and trunk segment move in the same direction. In a hip strategy, there is a

counter-rotation of the trunk relative to the legs. Leg and trunk segment move in opposite directions.

Traditionally, these two strategies have been taken as centrally selected in response to the perturbations: when perturbation is small, an ankle strategy is used; when perturbation is large, a hip strategy is used (Horak et al., 1996). Selection of ankle and hip strategy depends on intact somatosensory and vestibular information during perturbed stance (Horak, Nashner, & Diener, 1990), respectively. This central selection idea has been challenged by Creath et al. (Creath et al., 2005), who have conducted a study looking at these two strategies during quiet stance with eyes closed. Coexisting in-phase (i.e. ankle strategy) and anti-phase (i.e. hip strategy) pattern between the leg and trunk segment were found: in-phase pattern at frequencies lower than 1 Hz, anti-phase pattern at frequencies higher than 1 Hz. Therefore, these two patterns are not centrally selected from the extremes of a continuum. Rather, they are coexisting fundamental modes. The dominance of either of these depends on available sensory information and task.

The subsequent question is: how sensory information affects these patterns? Vision and light finger touch on the right side led to the shift of transition from in-phase to anti-phase at lower frequencies (Zhang et al., 2007). This indicates that sensory information mainly affects these patterns at frequencies lower than 1 Hz where the in-phase pattern dominates. Compared to age-matched control subjects, who showed consistent transition frequency, bilateral vestibular loss patients had variable transition frequencies ranging from 0.5 to 1.6 Hz (Zhang et al. 2005). One explanation is that sensory information provides precise control of transition between

in-phase and anti-phase pattern. Biomechanical effect on the patterns is in a different frequency range. Adding weighting on the subjects had effects at frequencies higher than 1 Hz, where an anti-phase pattern dominates (Elahi, et al., 2005).

3.2 Muscle dynamics

3.2.1. Functional muscle studies

Studies on functional muscle organization have been focused on the temporal (and spatial) pattern of muscle activation. They usually involved some kind of platform perturbation, for example, translation in different directions. In addition, the support surface length might be changed to destabilize subjects. After the onset of perturbation, muscles in the leg and trunk segment react with phasic activities. Depending on the stimulus, tonic activity might follow the phasic activities. This protocol has been applied to identify ankle and hip strategy (Horak & Nashner, 1986). Subjects stood on a platform (either full or short support surface) that was translated in the forward or backward direction with a constant velocity. Well-practiced subjects standing on full support surface showed a distal-to-proximal muscle activation pattern with shank muscles activated first, followed by thigh muscles and then trunk muscles (i.e. ankle strategy). When they stood on a short support surface, the trunk and thigh muscles activated in a proximal-to-distal pattern without obvious ankle muscles activity (i.e. hip strategy). Mixed ankle and hip strategy were assumed with intermediate length of support surface or right after changed length support surface. These results indicated that there is a continuum muscle coordination pattern with ankle and hip strategy at the two extremes.

A later study by Diener and colleagues (1988) agreed with these results and further argued for these muscle patterns as a result of central pattern generator (CPG). Velocities were changed when keeping the amplitude the same across trials. Keeping either amplitudes or velocity the same while changing the other parameter, the authors assumed that if postural response are centrally programmed, then the response should be independent of sensory stimuli. Subjects experienced backward platform translation. In short duration (75ms) trials, only single burst was observed in gastrocnemius, hamstrings, paraspinal and rectus abdominis muscles independent of velocity and amplitude of the platform perturbation. In longer duration trials, the temporal-spatial relationship of the muscle activation was kept across conditions. The amplitude of early muscle activation was affected by the velocity; while the amplitude of later muscle activation was affected by the amplitude changes. The authors argued that the invariant temporal-spatial relationship indicated a central role of postural control, while the sensory information can be used to scale muscle activity amplitudes.

These two studies have proposed a response of muscle activities to platform perturbation with fixed temporal-spatial relationship of muscle activation. This kind of strategy is very efficient in terms of controlling the muscles. However, a fixed muscle synergy might not be sufficient in postural control. In a more recent study (Henry, Fung, & Horak, 1998), subjects were translated on a platform in 12 equally spaced directions with right translation as 0 degree. 11 left-sided muscles on the shank, thigh and trunk were recorded. Regardless of translation direction, shank and most thigh muscles had a constant temporal activation relationship. Besides this, there

are variable muscle activities in different situation. One thigh muscle (tensor fascia latae, TFL) and two trunk muscle (rectus abdominis, RAB, and erector spinae, ESP) had variable activation latency depending on the perturbation direction. These two trunk muscles with another shank (peroneus longus) and thigh (semimembranosus) had maximum activity in two different directions.

These studies only looked at the onset and amplitude of EMG activities, while ignored a lot of other information containing in EMG activity. A recent study (Saffer, Kiemel, & Jeka, 2008) has shown that soleus and gastrocnemius was in-phase with forward body sway and rectus femoris was in-phase with backward body sway at low frequencies. However, the leg muscles increasingly lagged behind the segment angle as frequency increased. These results indicated that the leg segment is under active muscular control. While the trunk lacks a relationship with muscles at high frequencies suggests a biomechanical effect.

3.2.2. Stiffness

During upright stance, muscles are activated to generate joint torques in order to counteract the effects of gravity (Mergner & Rosemeier, 1998b). The force that muscles use to resist being lengthened is called stiffness, also known as muscle tone (Basmajian & De Luca, as cited in Shumway-Cook, et al., 2000). Muscle and joint stiffness are important to resist displacement from external forces (Horak, et al., 1996). Winter and colleagues even proposed that modulation of muscle stiffness is a simple strategy that the nervous system could use to maintain upright quiet stance (Winter et al., 1998). Directly measurement of the intrinsic ankle stiffness showed that ankle stiffness is not enough to provide the minimal effective stiffness (Loram &

Lakie, 2002). In order to maintain balance, the active changes in muscle produce extra force by stretching the tendon, which is a neural modulation.

Chapter 3:

The influence of sensory information on two-component coordination during quiet stance

Zhang Y., Kiemel T. & Jeka J.

Gait & Posture 26(2007) 263-271

1. ABSTRACT

When standing quietly, human upright stance is typically approximated as a single segment inverted pendulum. In contrast, investigations, which perturb upright stance with support, surface translations or visual driving stimuli have shown that the body behaves like a two-segment pendulum, displaying both in-phase and anti-phase patterns between the upper and lower body. We have recently shown that these patterns coexist during quiet stance; in-phase and anti-phase for frequencies below and above 1 Hz, respectively. Here we investigated whether the characteristics of these basic patterns were influenced by the addition or removal of sensory information.

Ten healthy young subjects stood upright on a rigid platform with different combinations of sensory information: eyes were open or closed with or without light touch contact (<1 N) of the right index fingertip with a 5 cm diameter rigid force plate. The in-phase and anti-phase pattern co-exist in both the anterior-posterior (AP) and medial-lateral (ML) directions of sway. The real part of trunk-leg complex

coherence decreased with the addition of vision and light touch, corresponding to a transition from the in-phase to anti-phase pattern at a lower frequency.

In the AP direction, the decrease was only observed at frequencies below 1 Hz where the in-phase pattern predominates. Additional sensory information had no observable effect at sway frequencies above 1 Hz, where the anti-phase pattern predominates. Both patterns are clearly the result of a double-linked inverted pendulum dynamics, but the coherence of the in-phase pattern is more susceptible to modulation by sensory information than the anti-phase pattern.

2. INTRODUCTION

Human upright stance is often approximated as a single-joint inverted pendulum, pivoting around the ankle during quiet stance (Jeka, Kiemel, Creath, Horak, & Peterka, 2004; Peterka, 2002). When perturbed, additional patterns associated with a double-linked pendulum are then observed, such as the anti-phase hip strategy (Horak et al., 1986). The generally accepted idea is that these basic patterns are centrally selected from a set of motor programs, arising from high-level neural strategies and implemented by complex sensorimotor control processes to most effectively counteract the physical characteristics of the perturbation (Horak et al., 1996). However, recent work has questioned this distinction between quiet and perturbed stance (Creath et al., 2005).

The same in-phase (i.e., ankle strategy) and anti-phase (i.e., hip strategy) patterns between upper and lower body segments observed in response to perturbed stance co-exist at different frequency ranges during quiet unperturbed stance. At

frequencies below approximately 1 Hz, coordination between the trunk and legs assumes an in-phase pattern, while above 1 Hz, an anti-phase pattern predominates.

The co-existence of in-phase and anti-phase body sway during quiet, unperturbed stance raises a number of issues regarding how these patterns arise. These two patterns are clearly a result of double-link inverted pendulum dynamics (McCollum & Leen, 1989), although a neural control system is necessary to maintain upright stability. Thus, even quiet unperturbed stance requires a complex mixture of biomechanical and neural control. In the present study, we investigated how the addition or removal of sensory information influences the co-existing in-phase and anti-phase patterns observed during quiet stance. Are the mechanical characteristics of both in-phase and anti-phase patterns influenced by the addition/ removal of sensory information? We also studied the relationship between upper and lower body segments in both the anterior-posterior (AP) and medial-lateral (ML) directions to determine whether the in-phase and anti-phase patterns co-exist in both directions of sway.

3. METHODS

3.1. Subjects

Ten individuals participated, three women and seven men, ranging in age from 18 to 31 years (mean age = 23.9, S.D. = 4.4). All subjects were right-handed, healthy and physically active, with no known musculoskeletal injuries or neurological disorders that might affect their ability to maintain balance. The procedures used in

the experiment were approved by the Institutional Review Board at the University of Maryland. Informed written consent was obtained from all participants in the study.

3.2. Apparatus

The subjects stood on a rigid platform with their right index finger touching a static touch plate placed in front of the subject's right shoulder. The touch device consisted of a smooth horizontal metal plate (5 cm in diameter) supported by a tripod. The plate was adjusted in height and position to allow subjects to assume a comfortable arm position, typically with ≈10–15º of elbow flexion. When the subjects applied forces of more than 1 N, an auditory alarm sounded. The visual environment consisted of an array of lab equipment against a wall approximately 3 m away, with normal ambient light levels. Kinematics of the shoulder (the scapula), hip (the greater trochanter), knee (the lateral femoral condyle) and ankle (the lateral malleolus) were measured by attaching four LED markers on the left side of the subject and were sampled at 100 Hz using an Optotrak (Northern Digital Inc.) system. Three LED markers were put on the force platform aligned with the corner facing the cameras as a reference, so that the data could be rotated from the cameras' own coordinate system into the subject's global coordinate system later in the data analysis. A bank of three cameras was placed to the left front of the subjects to measure the movements of the markers.

3.3. Procedures

The subjects stood upright with heels 1 cm apart pointed outward at an angle of 15° between each foot and the midline. The floor was marked with tape so that the same foot position could be repeated on each trial and subject. The experimental trials

included two visual conditions, eyes closed or eyes open and two fingertip contact conditions, no contact, or light touch contact, in which the vertical touch force applied on the touch plate by the right index fingertip was limited to 1 N. The four conditions were identified as follows: Neither = eyes closed and no touch contact, Touch = eyes closed and touch contact, Vision = eyes open and no touch contact, Both = eyes open and touch contact.

Subjects began each trial by looking straight ahead at fixation target against a wall approximately 3 m away. In the Touch conditions, subjects were instructed to take as much time as possible to find a comfortable position and keep the fingertip on the same spot on the touch plate throughout the trial. If the alarm sounded, the subjects were told to keep their fingertip in contact with the touch plate while reducing the force at the fingertip. During the no touch trials, the subjects were asked to keep both arms crossed behind their back so that their hands were touching at approximately waist level. This prevented the arms from blocking the markers as subjects faced the camera. Once the subjects felt ready, they said ‘‘yes’’ and the experimenter initiated data acquisition 5 s later.

Each condition was run three times for a total of 12 trials for each subject. All trials were for 240 s, the order of the trials across conditions was randomized for each subject. The subject was asked to sit and rest for 2 min after completing a trial. One trial was discarded due to technical difficulties.

3.4. Analysis

3.4.1. Kinematics

The trunk and leg segment were assumed to lie on the line connecting every two adjacent joints with the knee being ignored, which was based on the fact that knee joints remain approximately stationary during AP sway motions (Alexandrov, Frolov, & Massion, 2001). AP/ML trunk and leg angles with respect to vertical were calculated using the AP/ML and vertical positions of the ankle, hip and shoulder markers. All subsequent analysis was applied separately for the AP and ML directions.

3.4.2. Sway variability

For each segment angle trajectory, a velocity trajectory was calculated using finite differences with a time step of 0.1 s, which was applied to reduce measurement noise for calculation of sway velocity. This was the only filter employed to the data set. Position variability and velocity variability was computed as the standard deviations of the angle trajectory and its velocity trajectory, respectively, and averaged across trials.

3.4.3. Spectral analysis

For each trial means were subtracted fromthe leg and trunk angle trajectories and the power spectral densities (PSDs) of the legs and trunk and cross spectral density (CSD) between the legs and trunk were computed in Matlab using Welch's method with a 20 s Hanning window and 50% overlap. PSDs and CSDs were averaged across the three trials (one subject had only two Touch trials). The 20 s window for spectral analysis produced PSDs and CSDs with a 0.05 Hz frequency step. To increase statistical power, frequency values from0.05 to 3 Hz were divided into 15 bins (4 values per bin), and the PSDs and CSDs were averaged in each bin.

For each subject and condition, complex coherence c12 was computed as

$c_{12} = \frac{p_{12}}{\sqrt{p_{11} p_{22}}}$, where p_{12} is CSD between the legs and trunk, and p_{11} and p_{22} are

PSDs for the leg and trunk segment, respectively.

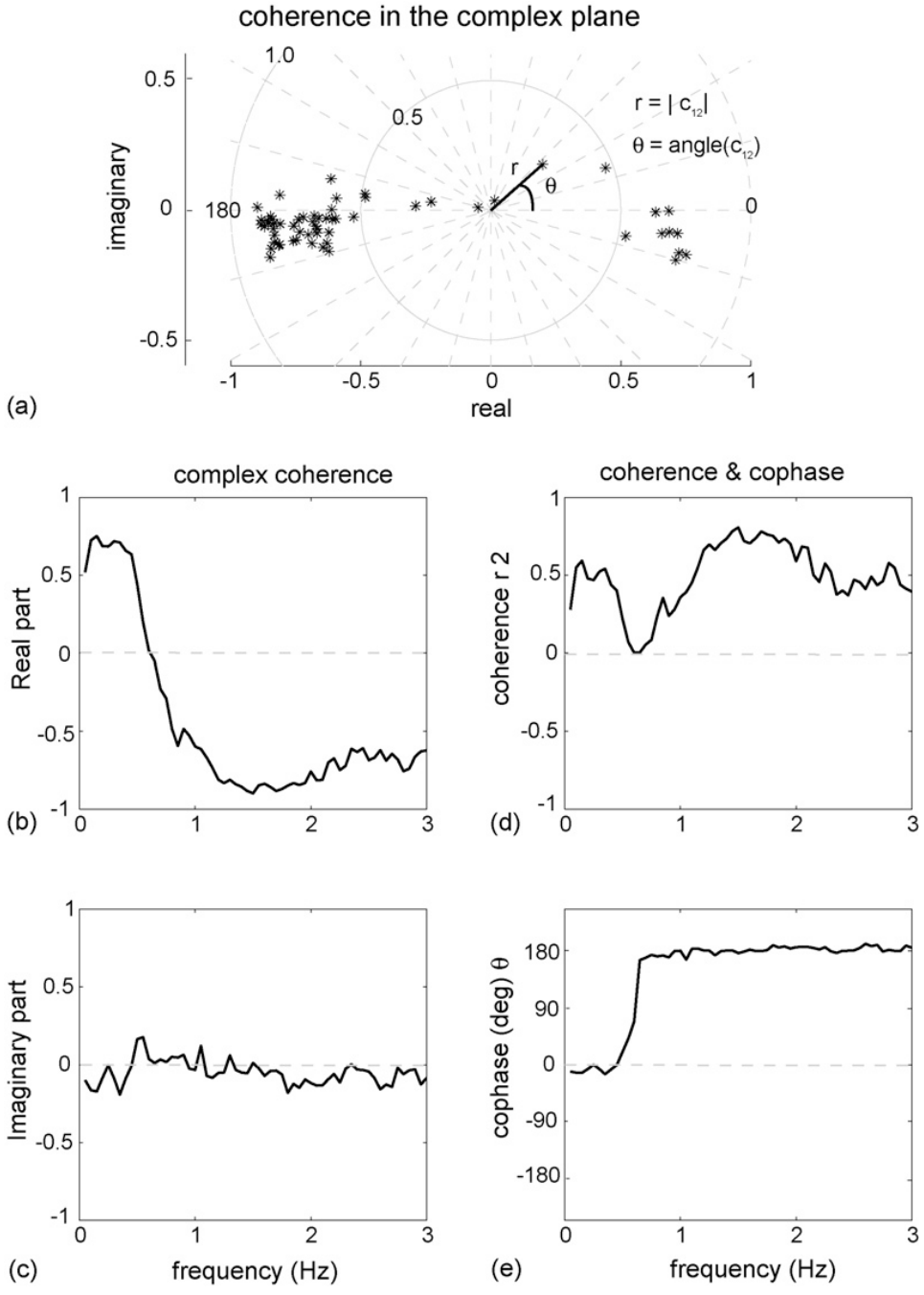

Fig. 3.1. Complex coherence describing the linear relationship between the leg and trunk angles for a single trial in the ML direction. (a) Complex coherence plotted in the complex

plane. Each symbol indicates a different frequency in steps of 0.05 Hz. In the formula for (u), angle refers to the Matlab function; (b, c) complex coherence decomposed into its real and imaginary parts; (d, e) complex coherence decomposed into (magnitude-squared) coherence r2 and cophase u.

Fig. 3.1a shows the trunk-leg complex coherence in the complex plane from a single trial. Each symbol indicates a different frequency in steps of 0.05 Hz. There are two common ways to decompose complex coherence. Fig. 1b and c shows a decomposition into real and imaginary parts. Fig. 1d and e shows a decomposition into (magnitudesquared) coherence r^2 and cophase u, where the distance r and angle u are defined in Fig. 1a. A positive cophase indicates that the leg segment led the trunk segment.

The real–imaginary decomposition of complex coherence was used for two reasons. First, the imaginary part of complex coherence was generally small and changes across frequency were primarily due to the real part (see Section 3). Second, complex coherence was often near the origin of the complex plane at frequencies where the shift from in-phase to anti-phase trunk-leg coordination occurred, leading to highly variable co-phase and complicating its statistical analysis. It will be useful to understand how the real– imaginary and coherence–cophase decompositions of complex coherence are related, since the latter decomposition is often used in the literature (Creath et al., 2005). For example, if the imaginary part of complex coherence remains small while the real part goes from positive to negative with increasing frequency (Fig. 1b and c), then cophase shows a sudden transition from nearly in-phase (0^o) to nearly anti-phase (180^o) accompanied by a drop in coherence at the transition (Fig. 1d and e).

3.4.4. Statistics

The log of the position and velocity variability in both directions was analyzed using Condition x Segment repeated-measure ANOVAs with Greenhouse–Geisser adjusted *p* values. Use of the log transform tends to reduce skewness and deviations from sphericity. Each pair of conditions was tested for a main Condition effect using a mixed model with unstructured covariance, the Tukey–Kramer adjustment for multiple comparisons, and the Kenward– Roger adjustment for reducing small sample bias.

The following statistical analyses were applied separately in the AP and ML directions. The log of the PSDs was analyzed using a Condition x Segment x Frequency repeated-measure ANOVA with Greenhouse–Geisser adjusted *p* values. Then, the log-PSD was averaged across Condition, and paired *t*-tests were used to test for a Segment effect at each of the 15 frequency bins, using the method of Benjamini and Hochberg (Benjamini & Hochberg, 1995) to control the false discovery rate (FDR) at less than 0.05. Because *p* values at different frequencies are dependent, control of the FDR is approximate. For plotting variability and PSDs we used geometric means to be consistent with our use of the log transform in our statistical analyses: the log of the geometric mean equals the arithmetic mean of the logs.

The real and imaginary parts of complex coherence were analyzed separately. First, for each condition and frequency bin, we tested whether the measure was different from zero using a t-test, with the FDR controlled at less than 0.05. Then, we performed a Condition x Frequency repeated-measure ANOVA with Greenhouse–Geisser adjusted p values. Every condition pair was tested for a main Condition effect using a mixed model with unstructured covariance and Tukey– Kramer and

Kenward–Roger adjustments. In those cases with a significant Condition x Frequency interaction, every condition pair and frequency bin were tested for a Condition effect using paired t-tests, with the FDR controlled at less than 0.05.

4. RESULTS

4.1. Sway variability

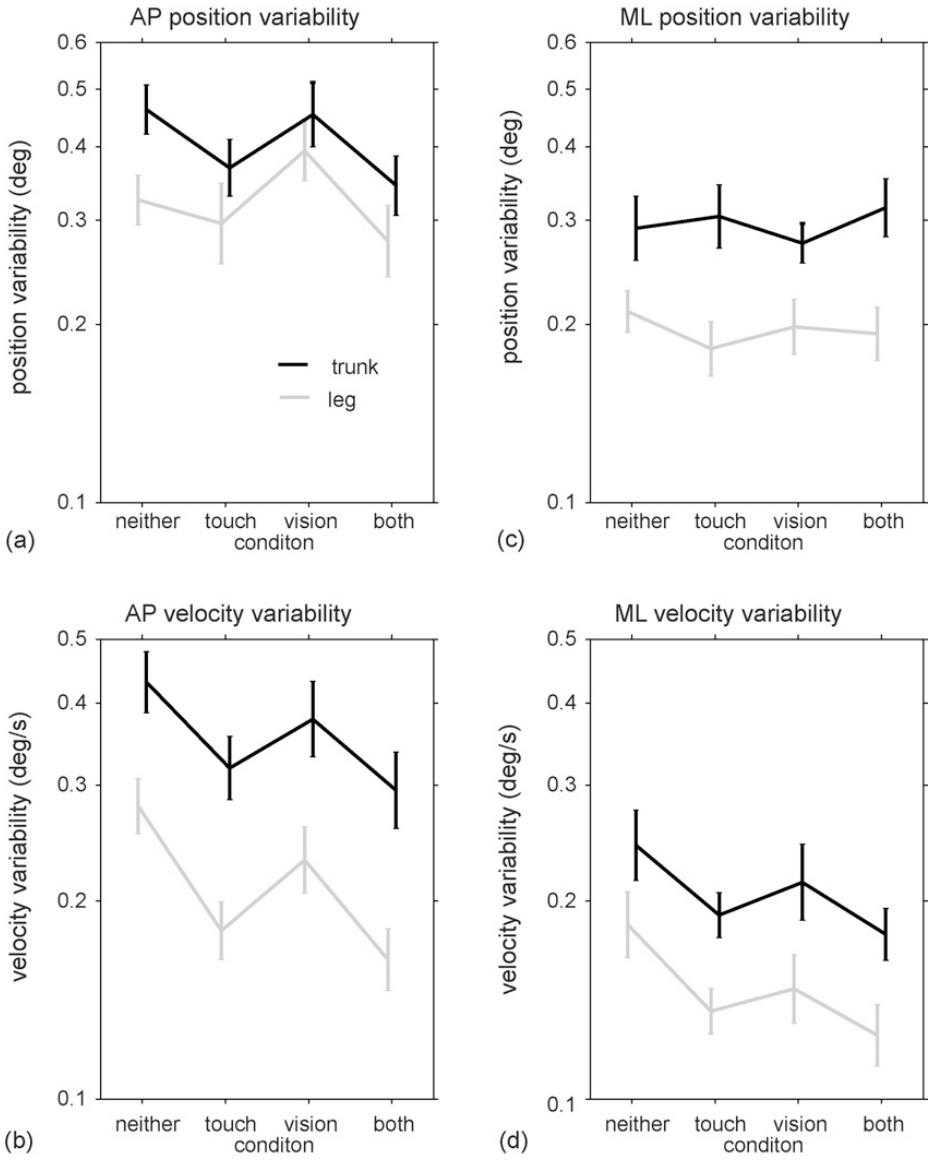

Fig. 3.2. Position viability in the AP (a) and ML (c) directions for each condition. Velocity variability in the AP (b) and ML (d) directions for each condition.

Fig. 3.2 shows the mean position and velocity sway variability in both directions. The variability of the trunk segment was higher than the leg segment, supported by significant main Segment effects ($p < 0.004$). There were highly significant main Condition effects for both AP and ML velocity variability ($p < 0.001$). All conditions were different between each other except for the pairs: Both versus Touch, Touch versus Vision for both segments; and Neither versus Vision for the trunk segment in the AP direction. For the ML direction, Neither was different from the other three conditions in the leg segment and different from the Both condition in the trunk segment. For position variability, the main Condition effect was significant in the AP direction ($p < 0.04$) but not in the ML direction ($p = 0.76$), with differences only between the Vision and Both conditions.

The only significant Condition x Segment interaction was found for AP velocity variability ($p < 0.004$); adding sensory information decreased the log-variability more for the leg segment than for the trunk segment, that is, the percentage decrease in variability was greater for the leg segment. This was supported by the result that the Neither and Vision conditions were significantly different for the leg segment, but not the trunk segment.

4.2. Trunk and legs segment PSDs

Fig. 3.3a–f shows the mean trunk and leg segment PSDs. Repeated-measure ANOVAs revealed significant Condition x Frequency interactions ($p < 0.005$) and Segment x Frequency interactions ($p < 0.0001$) for both directions. All main effects were also significant ($p < 0.02$); the Condition x Segment and Condition x Segment x Frequency interactions were not significant ($p > 0.05$).

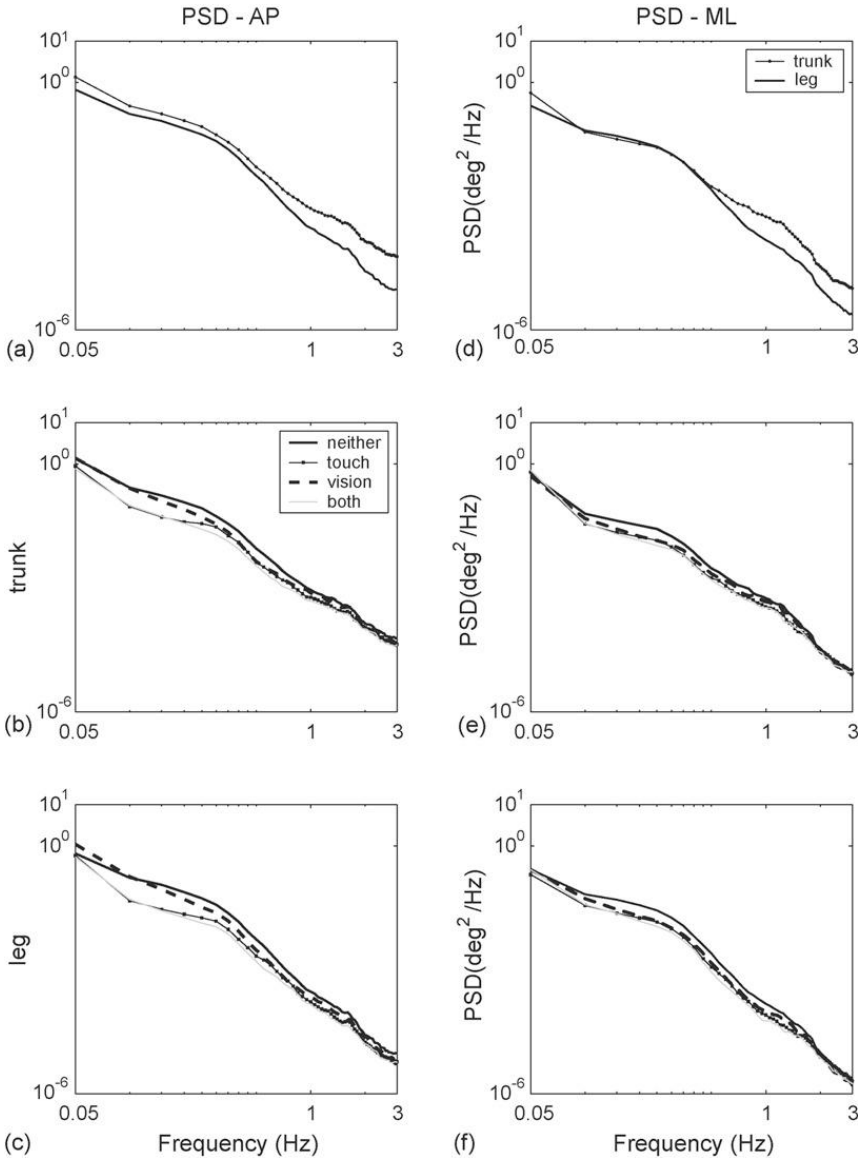

Fig. 3.3. Power spectral density (PSD) of the trunk and leg angle in the (a–c) AP and (d–f) ML directions. PSDs of trunk and leg angle in the (a) and (d) Neither condition; (b, c) and (e, f) in all four conditions.

The presence of a Segment x Frequency interaction for the log-PSD indicates that the percentage difference between PSDs was not uniform across frequency. The trunk PSD tended to be greater than the leg PSD, with the largest percentage differences occurring at the higher frequencies (Fig. 3). To test for segment effects in more detail, we averaged the log-PSD across condition and tested for a segment effect at each frequency bin. For the AP direction, the log-PSD was greater for the trunk

than the legs for all frequency bins (FDR < 0.05; see Section 2). For the ML direction, this was true for all frequency bins except for 0.25–0.40 Hz, where we found no significant difference.

4.3. Trunk-leg coordination

Consistent with a previous study (Creath et al., 2005), Fig. 4 shows the coexistence of trunk-leg in-phase and anti-phase patterns during quiet stance in both directions.

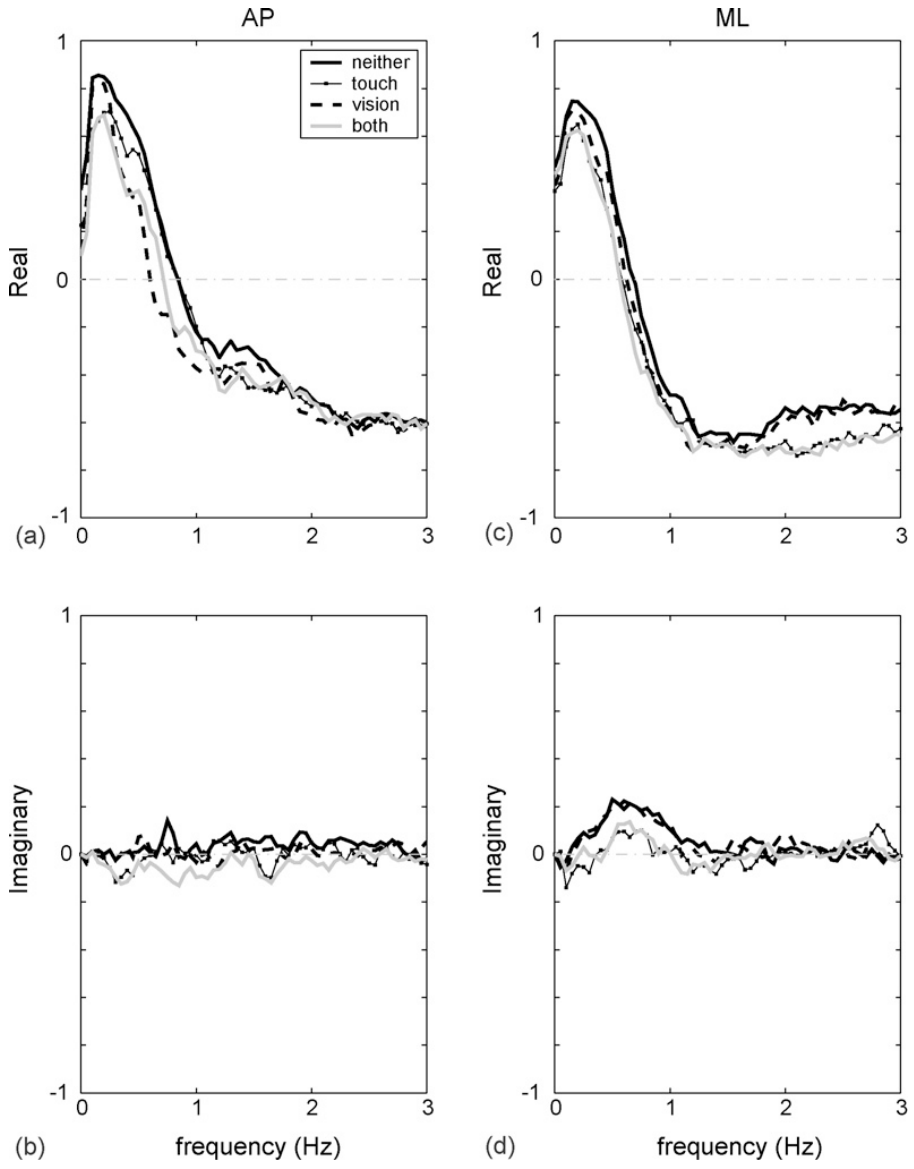

Fig. 3.4. The real and imaginary parts of complex coherence plotted separately in the (a, b) AP and (c, d) ML directions.

Both sway directions show a similar dependence of complex coherence on frequency. The real part (Fig. 3.4a and c) begins close to 0.5 at the lowest frequency, rises slightly, decreases, crosses the x-axis to signify a shift from the right side to left side of the complex plane, and eventually decreases to approximately -0.6. The imaginary part (Fig. 3.4b and d) was approximately zero across all frequencies in both directions, except for a significant increase in the 0.45–0.60 Hz frequency bin for the Neither condition in the ML direction (FDR < 0.05). Recall that this complex coherence pattern corresponds to a shift in cophase from in-phase to anti-phase accompanied by a decrease in magnitude-squared coherence at the transition (Fig. 3.1). Since values of the imaginary part were close to zero, changes in complex coherence across frequency were primarily due to the real part. This was especially true in the AP direction, where the imaginary part did not show any significant dependence on Frequency ($p > 0.35$ for the main Frequency effect and Condition x Frequency interaction). There were significant main Frequency effects for the real part in both directions ($p < 0.0001$) and for the imaginary part in the ML direction ($p = 0.002$).

The real and imaginary parts of complex coherence showed strong Condition effects in both directions. In all cases, there was a significant main Condition effect ($p < 0.005$). The real and imaginary parts tended to decrease significantly ($p < 0.05$) with increasing sensory information (AP real part: Vision & Both < Neither; AP imaginary part: Both < Neither, Touch & Vision; ML real part: Touch, Vision & Both < Neither; ML imaginary part: Both < Vision).

There was a significant Condition x Frequency interaction only for the real part in the AP direction and the imaginary part in the ML direction ($p < 0.004$). Adding vision tended to decrease the real part in the AP direction near the transition from positive to negative (FDR < 0.05: Vision < Neither for 0.45–1.00 Hz; Vision < Touch for 0.45–0.80 Hz). Thus, the transition from in-phase to antiphase occurred at a lower frequency when visual information was available. Adding touch tended to decrease the imaginary part in the ML direction, with Condition effects found in isolated frequency bins in the range 0.25–1.20 Hz.

5. DISCUSSION

The coordination between trunk and leg segment angles during quiet stance was studied to determine how the addition or removal of sensory information influenced their coordinative relationship at different frequencies. We found three main results. First, additional touch or visual information led to a decrease in variability of both the trunk and leg segments. The trunk segment displayed higher variability than the leg segment in all conditions, with the difference in segment variability larger at higher frequencies. Minor differences were observed between the segments due to condition, indicating that additional sensory information led to a similar decrease in segment variability.

Second, co-existing patterns of coordination were found in both directions of sway. At sway frequencies below 1 Hz, the trunk and legs were primarily in-phase in the AP direction. In the ML direction, an increase in imaginary coherence above the horizontal axis (Fig. 3.4d) indicated a trunk-leg pattern that was continually shifting with frequency, traveling above the horizontal axis (Fig. 3.1a). Presently, the

mechanism underlying the difference in phase between the ML and AP directions below 1 Hz is unknown. Above 1 Hz, the AP and ML directions both assume an antiphase pattern.

It has been argued that control of sway in the AP and ML directions are independent, based upon recordings of separate center of pressure profiles under each foot. AP balance is primarily under ankle (plantar/dorsiflexor) control, whereas ML balance is under hip (abductor/adductor) control (Winter, Prince, Frank, Powell, & Zabjek, 1996). Despite different muscular synergies involved in each direction of sway, the present results showing similar patterns of coordination between the trunk and legs suggest that the same control strategy may be realized through different muscular components.

Third, additional touch or visual information decreased the real part of complex coherence, corresponding to a transition from in-phase to anti-phase at a lower frequency. In the AP direction, this decrease depended on frequency and was only observed below 1 Hz, that is, at frequencies near or below the in-phase to anti-phase transition. These condition effects were observed for successive frequency bins, resulting in a relatively wide frequency band of significant differences. In contrast, no effects for the real part of complex coherence were observed above 1 Hz. Above 1 Hz, the phase relationship between the trunk and legs is predominantly anti-phase, suggesting the anti-phase pattern is less influenced by sensory information than the in-phase pattern observed below 1 Hz.

The addition of touch led to an observable decrease in the real part of complex coherence only in the ML direction. This may be related to how the sensory

environment is structured. Placement of the touch plate lateral to the body on the right side emphasized touch information in the ML direction. Previous experiments have shown if the touch plate is placed in front of the body with the hand/arm oriented along the midline of the body, light touch effects sway primarily in the AP direction (Jeka, Ribeiro, Oie, & Lackner, 1998). Similar effects on sway are observed depending on whether the visual display moves in the medial-lateral or anterior-posterior direction (Jeka et al., 2000; Stoffergen, 1985). Even though the touch and visual information in the present experiment was static, the structure of the touch and visual inputs were such that they influenced sway in a particular direction.

5.1. Mechanical versus neural control

These results replicate and add to the recent finding of Creath et al. (Creath et al., 2005), who showed co-existing in-phase (ankle strategy) and anti-phase (hip-strategy) pattern during quiet stance. Rather than viewed as centrally selected from a set of motor programs (Horak et al., 1996), these patterns can be viewed as fundamental modes, either of which may become more prevalent if a perturbation or task excites it preferentially (Alexandrov et al., 2001). The present results add to this view, showing that the inphase pattern is more sensitive to sensory information than the anti-phase pattern.

There are speculative explanations for these results. One possibility is that the sensitivity of the in-phase pattern to sensory changes reflects a greater degree of neural control than the anti-phase pattern, whose underlying basis may be primarily due to the biomechanics of the human body approximated as a double pendulum (McCollum et al., 1989). Recent experiments provide some support for this view.

Biomechanical manipulations such as adding weights to the body have proven to influence coherence at frequencies above 1 Hz, where the anti-phase pattern predominates while having little effect on coherence where the in-phase pattern predominates (Elahi, Kiemel, Saffer, & Jeka, 2005). Moreover, muscle activity during quiet stance has shown a consistent phase relationship between muscles as well as between muscle activity and limb kinematics at lower frequencies below 1 Hz, but no consistent phase at frequencies above 1 Hz (Saffer, Kiemel, & Jeka, 2005). The lack of coherent muscle activity above 1 Hz suggests a diminished role for active neural control of the anti-phase pattern.

Despite such evidence, it is unknown whether the antiphase pattern is actively produced by the control system (feedback), or whether it emerges due to musculotendon and body dynamics (the plant). It is also not known whether state estimation takes such multi-joint coordination patterns into account when interpreting sensory information. State estimation for postural control is generally thought to involve an internal model of the body's dynamics (Kuo, 1995; van der Kooij, Jacobs, Koopman, & Grootenboer, 1999; Kiemel, Oie, & Jeka, 2002; Carver et al., 2005). Because most of the power of postural sway is at low frequencies, state estimation based on a single-joint (ankle) internal model may be sufficient for postural control during quiet stance. Clearly mechanical processes are important in the control of the in-phase and anti-phase coordination modes observed during quiet stance. However, the degree to which neural processes and state estimation play a role in each pattern may differ substantially.

Another possible explanation is that changes in coherence reflect changes in the sensory noise level as sensory information is added/removed. However, it is unclear why such changes are only observed below 1 Hz where the inphase pattern predominates. One possibility is that the signal-to-noise ratio is lower at frequencies above 1 Hz, making it difficult to detect changes due to sensory manipulation.

5.2. Summary

From the perspective of the current literature, our view is one of a schism between biomechanical and nervous system accounts of human postural control. Certain research groups focus on the complicated biomechanical problem of controlling the multi-joint human body while ignoring how the nervous system solves the problem of estimating the position and velocity of the individual body segments (Lenzi, Cappello, & Chiari, 2003; Luporini, Fleury, & Weber, 2003; Popovic et al., 2000). We and other groups have concentrated on the problem of estimating body dynamics using a simplified single-joint (ankle) model of body mechanics (Peterka, 2002; Kiemel et al., 2002; Carver et al., 2005; van der Kooij, Jacobs, Koopman, & van der Helm, 2001). The few multi-joint models that include state estimation require further analysis (Kuo, 1995; van der Kooij et al., 1999; Kuo & Zajac, 1993; Kuo, 2005).

The present results emphasize the need to resolve the biomechanical and neural control problem of upright stance. The origin of the in-phase and anti-phase patterns remains controversial (Horak et al., 1986). Biomechanical accounts have been offered (McCollum et al., 1989), but such accounts do not satisfy how the two-linked approximation of the human body assumes different patterns depending upon:

type of perturbation (mechanically or with sensory information); the presence of neurological deficit; and even cognitive influence (Horak et al., 1996). The co-existence of these patterns during quiet stance changes the prevailing view that coordinative patterns are centrally ‘‘selected’’ and suggests the patterns observed when the body is perturbed reflect an excitation of patterns already present in the unperturbed state.

Chapter 4:

The influence of vestibular information on two-component coordination during quiet stance – a study with bilateral vestibular loss patients

1. INTRODUCTION

Three modalities of sensory information are essential in postural control: vision, somatosenosry and vestibular information. The role of vestibular information in quiet stance has been studied by comparing patients with bilateral vestibular loss (BVL) to healthy subjects. It has been shown that vestibular information is not important for postural control or can be compensated by other sensory modalities(Nashner, Black, & Wall, 1982), especially for patients with good compensation. As long as the support surface is stable, BVL patients are able to maintain balance (Mergner et al., 1998b).

However, vestibular function in hip strategy when human body is approximated as an inverted pendulum remains ambiguous. When exposed to a short base platform, BVL patients failed to trigger hip strategies, suggesting that vestibular information is critical in the use of hip strategy (Horak et al., 1990). This conclusion has been questioned by Runge et al. (Runge, Shupert, Horak, & Zajac, 1998) by pointing out that the short base platform used in previous study changed body biomechanics and vestibular information is not necessary to trigger a hip strategy on an unaltered support of surface. A further complication derives as recent study (Creath et al., 2005) has showed that ankle (in-phase pattern) and hip (anti-phase

pattern) strategies co-exist during quiet stance: in-phase pattern at frequencies lower than 1 Hz and anti-phase at frequencies higher than 1 Hz. Furthermore, the coexistence of in-phase and anti-phase pattern during quiet stance is not only a function of biomechanics, but also a function of neural control. Vision and somatosensory (i.e. light touch) affect the transition from in-phase to anti-phase pattern in the anterior-posterior and medial-lateral direction, respectively (Zhang, Kiemel, & Jeka, 2006). Questions have risen. Does anti-phase pattern exist in BVL patients during quiet stance? If the answer is yes, does vestibular information affect the transition from in-phase to anti-phase?

The vestibular system functions by controlling head position and provides information about the position and motion of the head relative to gravity. Study has demonstrated that control of head position is abnormal in vestibular-loss patients in situations that require hip strategy (Shupert, Black, Horak, & Nashner, 1988b). In this study, we also investigated whether head control is different between BVL patients and healthy controls in ankle/hip strategy.

2. METHODS

2.1. Subjects

Seven bilateral vestibular loss patients, two women five men (mean age = 51.4 years, SD 4.7), participated. They all had severe bilateral loss of vestibular function as a result of antibiotics treatment. Medical records of these subjects showed strong clinical evidence for profound bilateral loss of peripheral vestibular function. Seven age-matched individuals (mean age = 50.0 years, SD = 6.8), four women and three

men, were recruited. These control subjects were healthy, with no known musculoskeletal injuries or neurological disorders that might affect their ability to maintain balance. The procedures used in the experiment were approved by the Institutional Review Board at the University of Maryland. Informed written consent was obtained from all participants in the study.

Subject	BVL1	BVL2	BVL3	BVL4	BVL5	BVL6	BVL7
Gender	Male	Male	Male	Male	Female	Male	Female
Age	46	54	47	52	51	60	55
Duration of loss (months)	36	78	80	38	108	78	42
Cause of loss	Ototoxic	Ototoxic	Ototoxic	Ototoxic	Ototoxic	Ototoxic	Ototoxic

Table 4.1. Charateristics of the BVL subjects.

2.2. Apparatus

Kinematics information of the subjects was captured by Optotrak (Northern Digital, Inc., Waterloo, Ontario, Canada), an active infrared position tracking system. The Optotrak uses a bank of three cameras, which were placed to the right of and behind subjects to measure movements of the markers. The shoulder (the scapula), hip (the greater trochanter), knee (the lateral femoral condyle) and ankle (the lateral malleolus) were measured by attaching four LED markers on the right side of the subject. Three markers were placed on a 10x10x10 cm triangle board with one marker on each corner. The triangle board was then attached on the subject's right side of head to measure head movements. Another three markers were put on a fixed platform, which the subjects stood on, aligned the corner facing the cameras and used

as a reference to rotate the data from the camera's coordinate system to the subject's coordinate system. The markers were sampled at 100 Hz. A safety harness was put on the subjects without affecting their balance.

2.3. Procedures

Subjects stood with feet apart at a distance of 11% of her/his height between the toes and an angle of 14 degrees between the mid line and each foot on a fixed platform (McIlroy & Maki, 1997). The floor was marked with tape so that the same foot position was used in each trial for the same subject. During all the trials, subjects were instructed to stand as still as they can without locking their knees. The experiment included only one condition: eyes closed. Subjects were asked to keep their heads as if they were looking straight ahead and keep both arms crossed at about waist level. Each subject finished 8 trials (one BVL subject had 7 trials). All trials were 125 seconds, with at least 2 minutes sitting rest between trials.

2.4. Analysis

2.4.1. Kinematics.

The trunk and leg segments were determined by connecting shoulder and hip, hip and ankle joint respectively. The knee was not analyzed because previous studies have showed that knee movement contributes very little to overall variability during quiet stance in the anterior-posterior (AP) direction (Alexandrov et al., 2001). AP trunk and leg angles relative to earth vertical were calculated by using AP and vertical segment displacements. For the head segment, Cardan angles were used (ref needed here). Basically, any rotation is equivalent to a sequence of three rotations, one about the x axis, one about the y axis and one about the z axis. The angles of these three

rotations are the Cardan angles. We focused on rotation about the x axis (AP). For each trial, means were subtracted from the head, trunk and leg angle trajectories.

2.4.2. Sway variability.

For each segment angle trajectory, a velocity trajectory was calculated using finite differences with a time step of 0.1s, which was used to reduce measurement errors. No other filter was used in this data set. Position variability and velocity variability were computed as the standard deviations of the angular and velocity trajectories, respectively, and averaged across trials.

2.4.3. Spectral Analysis.

Power spectral densities (PSDs) of the head, trunk and leg and cross spectral density (CSD) between trunk and head were calculated in Matlab using Welch's method with a 25 second Hanning window and 50% overlap, resulting in a 0.04 Hz frequency step. PSDs and CSDs were averaged across trials for each subject. To increase statistical power, frequency values from 0.04 to 3 Hz were divided into 15 bins, with each bin containing five successive frequency steps, PSDs and CSDs were averaged in each bin. Trunk-leg and trunk-head coordination were analyzed through cophase and coherence. Cophase between segment angles was calculated as the argument of the CSDs. A positive cophase indicates that the head/leg segment led the trunk segment. Coherence was calculated as the absolute value of the CSD squared and divided by the product of the PSDs of the two segments.

2.4.4.Statistics.

The log of the position and velocity variability was analyzed using Group(2) x Segment(3) repeated-measured ANOVA with Segment being the repeated factor. Use of log transform tends to reduces skewness and deviations from sphericity.

Cophase of trunk-leg and trunk-head were analyzed separately using Group(2) x Frequency(3) repeated ANOVA with Frequency being the repeated factor. Difference of variance between two groups was tested by Levene's test, which has been used to test for homogeneity across groups in ANOVA analysis. We tested difference of variance instead of mean because the transition frequency at which cophase shifts from in-phase to anti-phase was more variable in BVL than healthy subjects.

3. RESULTS

3.1. Sway Variability.

Figure 4.1 shows the mean position and velocity sway variability for both BVL and healthy subjects. Both position and velocity variability of the head was higher than both the trunk and leg segments, while the variability of the trunk was higher than the leg segment for both groups of subjects. These results were supported by a highly significant Segment main effect ($p < 0.0001$). No Group (position variability: p=0.4310; velocity variability: p=0.7663) or Segment x Group interaction (position variability: p=0.7396; velocity variability: p=0.9853) effect was found.

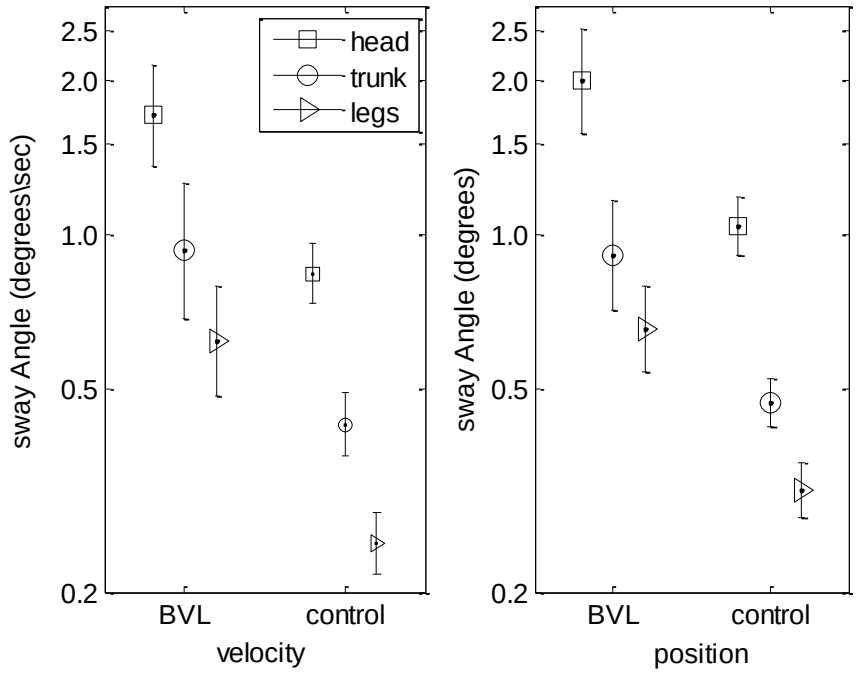

Fig 4.1. Position and velocity sway variability

3.2. Trunk-leg Coordination.

Figure 4.2 shows the co-existing in-phase and anti-phase pattern of trunk-leg coordination for both control and BVL subjects. The cophase (Figure 4.2a,c) for both groups is approximately 0° for lower frequencies and 180° for frequencies above 0.5 Hz. However, lack of vestibular information influenced the shift frequency at which shift from in-phase to anti-phase occurred. For control subjects, the shift consistently initiates around 0.5 Hz. However, for the BVL subjects, the shift frequency varies considerably across subjects. Levene's test showed significant difference of variance in cophase between BVL and healthy subjects at frequencies 0.72-1.92 Hz (p<0.05). Levene's test is traditionally used to test homogeneity between different groups in ANOVA analysis. Basically, it is an ANOVA F test on the absolute difference of the group mean and individual score within the group.

Before the shift from in-phase to anti-phase coordination, coherence has a bell shape with the highest values at approximately 0.2 Hz. Consistent with a previous study (Zhang et al., 2006), coherence then drops to near zero for the shift from in-phase to anti-phase, suggesting a weak relationship between the trunk and leg segment (Figure 2b,d). After the shift, coherence increases. This pattern of coherence change was observed for both BVL and healthy subjects.

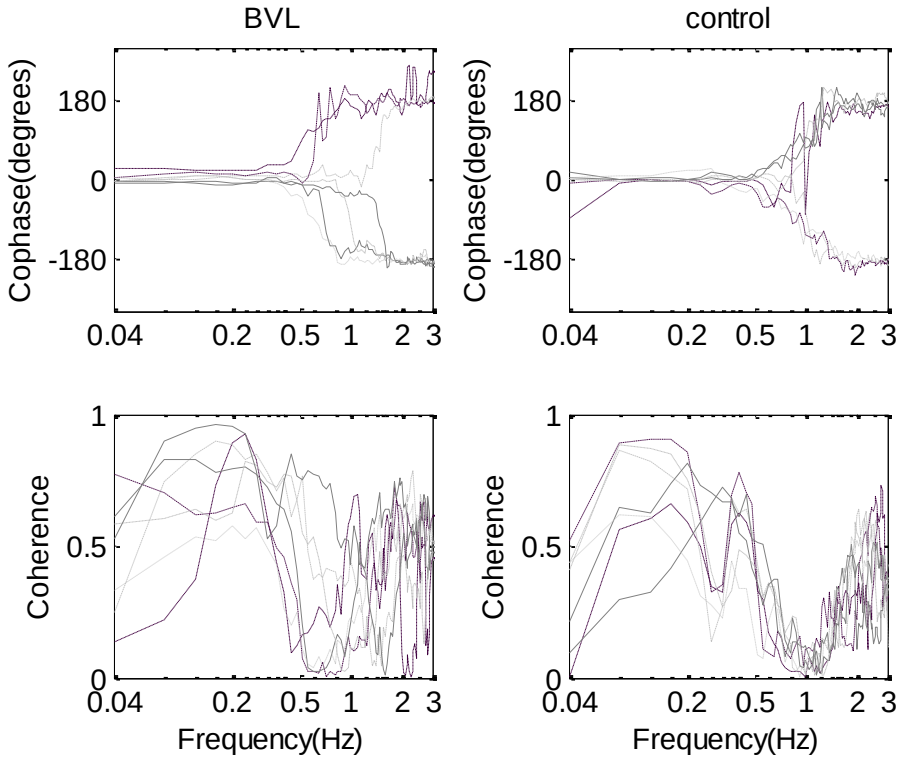

Fig 4.2. Trunk-leg coordination

3.3. Trunk-head Coordination.

BVL and healthy controls have similar trunk-head coordination. For both groups, the trunk-head was mainly in-phase at frequencies below 2 Hz and decreased toward anti-phase at higher frequencies (Figure 4.3). Unlike trunk-leg cophase, which had a very abrupt transition, the shift for trunk-head cophase was gradual. The cophase change is consistent across subjects for both groups, supported by the fact

that the only difference of variance were found at 1.52 Hz (Levene's test, p=0.0305). Coherence increases at low frequencies and decreases at high frequencies with peaks at around 0.2 – 0.5 Hz.

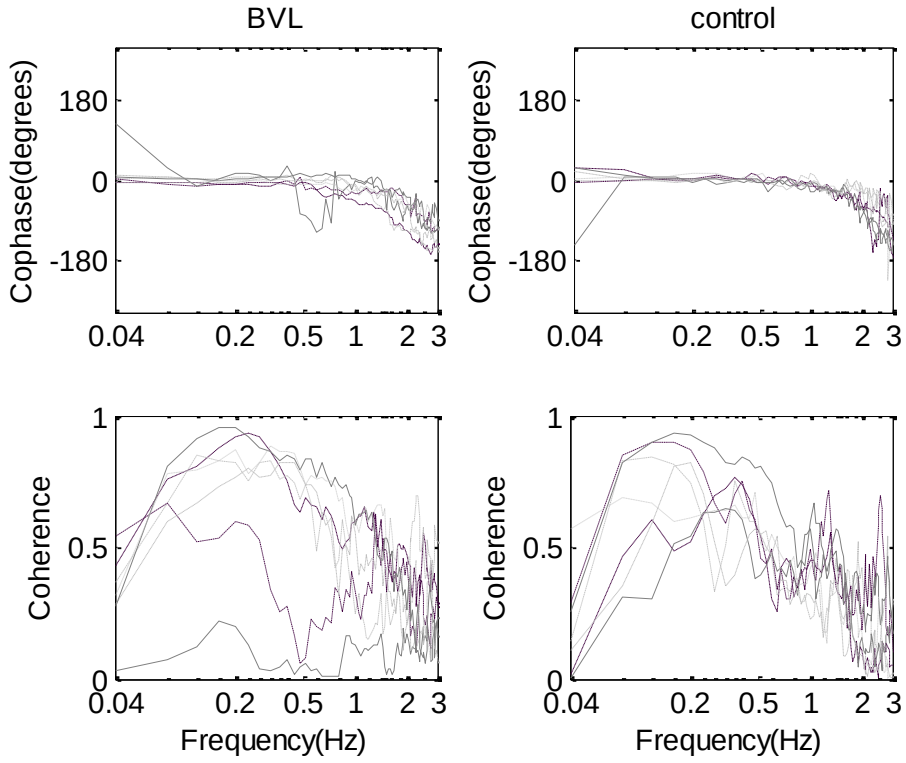

Fig 4.3. Trunk-head coordination

4. DISCUSSION

The coordination between trunk and legs segment, trunk and head segment during quiet stance were studied in both BVL and control subjects to determine the role of vestibular information in ankle and hip strategy. Three main results were found. First, both BVLs and controls showed co-existing coordination patterns in the AP direction: trunk-leg coordination was approximately in-phase at low frequencies and changed to anti-phase at high frequencies. Second, the transition frequency, at which in-phase transfers to anti-phase, was more variable without vestibular

information. The transition frequency for BVLs varied from 0.72 to1.92 Hz. In contrast, the controls showed consistent transition frequency at around 1 Hz. Third, trunk-head coordination in BVL subjects is similar to controls, suggesting that vestibular function contributes to the down-channeling and loss of vestibular information resulted in poor propagation of sensory information to down streams.

Vestibular Function in Quiet Stance

The current thinking is that vestibular function is not critical for stance, especially for patients who are well compensated. For example, BVLs have been showed to perform as well as controls during unperturbed stance or when either visual (e.g. eyes closed/ visual sway referencing) or somatosensory information (e.g. platform sway referencing) was not reliable (Horak et al., 1994). Furthermore, vestibular information was not necessary to trigger a hip strategy with full support and translating platform (Runge et al., 1998).

Our results suggested that loss of vestibular information may not affect the overall amount of sway, but does influence the fine-tone of trunk-leg coordination. Consistent with previous studies showing similar amount of sway for both BVLs and controls, we didn't find any difference in mean position and velocity sway variability between these two groups of subjects for head, trunk and leg segments. BVLs were also able to excite hip strategy at high frequencies. However, while transition frequency at which in-phase shifts to anti-phase was consistent across control subjects, the transition frequency for BVLs spanned a wide range from 0.72 to 1.92 Hz. In previous study, addition of static vision and light touch information decreased the transition frequency from in-phase to anti-phase in healthy young adults in the

anterior-posterior and medial-lateral direction, respectively (Zhang et al., 2006). One explanation is that sensory information provides precise control of transition between in-phase and anti-phase pattern. The loss of vestibular information leads to uncertainty and large variability of transition frequency. It is also possible that the BVLs sacrifice their control of transition between patterns to achieve the overall stability.

These results also add to previous study, that is, the in-phase and anti-phase pattern is not only a function of biomechanics but also a function of sensory information (Zhang et al., 2006). Despite clear biomechanics contribution to these coordination patterns, these results indicated consistent sensory influence on the transition at low frequencies.

The same head-trunk cophase pattern for both BVLs and controls challenges the view that loss of vestibular information results in different head control, especially for the tasks that require hip strategy (Horak & Diener, 1994). It has been suggested that the nervous system might stabilize the head with respect to gravity, but with respect to the trunk when vestibular information is not available (Nashner et al.,1985 as cited in (Horak et al., 1994)). In a later study by Shupert (Shupert et al., 1988a), no head-trunk coordination was found for BVLs when they stood on a narrow bean both with eyes closed and eyes open. Neither were the BVLs able to elicit a hip strategy in such conditions (Horak et al., 1990).

Surprisingly, control of head does not suffer from loss of vestibular information in the current experiment, supporting by similar head-trunk cophase pattern for BVLs and controls. This was true not only for cophase at low frequencies,

but also at high frequencies where an anti-phase pattern (i.e. hip strategy) existed. This could be explained by the up- and down-channeling theory (Mergner & Rosemeier, 1998a). Having reliable proprioception from their feet, BVLs generated a normal head-in-space estimate. However, their deficit led to a poor propagation of vestibular information to the lower segments, resulting in variable transition frequencies from in-phase to anti-phase.

Chapter 5:

Postural Coordination Patterns: Visual Rotation and Translation

1. ABSTRACT

Flow of the visual field is an important component of upright stance control, enabling compensatory corrections to small deviations from vertical. Movement of the visual flow field is typically imposed experimentally as a translation, with the underlying assumption that body sway consists primarily of rotation around the ankle (i.e., inverted pendulum). However, recent evidence has shown that in-phase and anti-phase patterns of trunk-leg coordination co-exist during quiet stance. The co-existence of these coordinative patterns raises the issue of how they interact with the interpretation of visual flow. Thus, we tested whether a single-link or multi-link internal model is used by the nervous system to interpret translatory versus rotary stimuli relative to the ankle and to the hip.

Fifteen healthy adults were exposed to sum-of-sines visual movement, which was either translated in the AP direction or rotated around ankle or hip joint. Results showed that gain and phase between the trunk and leg angles relative to the visual display showed only minor differences between conditions. Phase between trunk and leg angle showed an in-phase relationship at low frequencies and an anti-phase pattern at higher frequencies. The shift in trunk-leg phase was accompanied by a steady decrease in gain in all conditions. These results suggest that coupling of body

sway to a visual stimulus is dependent not only on the structure of the optic flow field, but also by coordinative patterns. The coupling between sensory information and body sway is highest at low frequencies when the trunk and legs are primarily in-phase. The minor condition effects observed for gain and phase indicate that the nervous system uses an internal model close to a single-link inverted pendulum to interpret visual information. The control strategy tries to align the trunk and leg segment together when making compensatory responses to deviations from vertical.

2. INTRODUCTION

Human perception and action are mutually dependent (Schöner, 1991), more specifically in the context of visual coupling in postural control: the structure of visual scene affects body sway, which in turn may influence visual perception. In this study, we examined the effect of neural interpretation of visual translation and rotation provided that human body is approximated as a single-link or double inverted pendulum.

Vision can either destabilize or stabilize postural sway depending on the structure of visual scene: a static visual scene reduces body sway, while visual motion enhances it. The “moving room” paradigm, introduced by Lee and Lishman (1975), has been very useful to study visual motion. It is achieved by either physically moving the walls of visual environment or by computer simulating visual motion. The visual optic flow field can be decomposed into different components, such as translation and rotation. By looking at these individual components, we can get an insight into the effect of vision on posture with integrated components.

Previous studies have shown that translatory movement can induce the illusion of self-motion (Lee, et al., 1975), similar to walking by a slowly moving train. Peterka and Benolken (1995) compared the rotation (around ankle joint) they used to the small amplitude translational visual surround in the anterior-posterior direction Lee and Lishman used in the 1975, and argued that this translation movement corresponded to a 0.1° visual surround rotation about the ankle joint. However, no evidence was provided for this argument.

Amplitude manipulation is involved in sensory reweighting. Within a certain stimulus amplitude range, there is a linear relationship between visual motion and postural control. As amplitude exceeds saturation, nonlinearity takes place. When the perturbations of vision increased to large amplitudes, healthy subjects were able to down-weight visual information and keep their balance; while bilateral vestibular loss patients increased their sway linearly with the stimulus amplitude (Peterka, 2002).

Frequency manipulation has been used to understand the temporal relationship between postural sway and visual motion (Dijkstra, SchÖner, Giese, & Gielen, 1994). It has become a famous result that phase between body sway and visual motion decreases as the frequencies increase regardless the amplitudes.

The human body is not rigid, but sways in both AP and ML directions. Complications arise considering that upright stance has been approximated as a single inverted pendulum rotating around the ankle joint or a two-segment inverted pendulum rotating around the hip joint. A recent study (Creath, et al, 2005) showed that the ankle and hip synergies co-exist during quiet stance. Which one of these synergies predominates depends on the sensory information and task constraints

(Creath, et al., 2005). More recently (Zhang et al., 2005), we asked how addition or removal of sensory information affects these two synergies. The subjects were instructed to either open eyes looking at a static visual scene or close eyes with or without light touching (< 100g) a touch bar. The relationship between upper and lower body was mainly demonstrated by calculating coherence between leg and trunk vertical angles. Addition of vision decreased the trunk-leg coherence at low frequencies.

In the current study, we investigated whether coupling to a visual stimulus depends on the structure of the visual flow field. Comparison between visual rotation and translation will be provided. Rotation is compatible when we consider the body as a single inverted pendulum. Furthermore, the co-existing coordination pattern makes a rotary visual signal inadequate, a rotation around the hip is needed. Also, we want to know how the nature of the optic flow influences postural coordination patterns. Two alternative hypotheses are promoted.

2.1. Two alternative hypotheses

In the first hypothesis, a multi-link (trunk and legs) internal model of the body is used by the nervous system to interpret visual information. A control strategy attempts to align both the legs and the trunk with respect to the vertical. That is, these two segments respond to the visual information separately. For example, if the nervous system interprets a visual motion around the ankle joint as a self-motion in the opposite direction, then both the trunk and the legs segments will actively try to return to vertical and the body behaves as a single inverted pendulum. If the nervous system represents a visual motion as self-motion around the hip joint, in this case,

because the legs are defined as in vertical, the nervous system will only correct the movement of the trunk and the body rotates around the hip joint. In a third case, if the visual motion is translated in the anterior-posterior (AP) direction, then the trunk is "thought" to be vertical and translating with the legs moving to compensate for this translation. As a result, the legs are activated to adjust for this translation movement.

However, this is not the only possible way that the nervous system responds to these visual stimuli. In the alternative hypothesis, a single link (ankle) internal model of the body is used by the nervous system to interpret visual information. A separate control strategy, one not dependent on visual information, attempts to align the two segments with each other. As a result, no matter the visual stimulus is rotated around the ankle or hip joint, or translated in the AP direction, the nervous system interprets it as rotation around the ankle joint and the body behaves as a single inverted pendulum. Predictions are made according to these hypotheses.

2.2. Predictions

It has been reported that body sway is influenced by visual scene velocity rather than position (Kiemel, Oie, & Jeka, 2006; Sch¨oner, 1991; Dijkstra et al., 1994; Jeka, Oie, & Kiemel, 2000). However, in order to compare results in the literature, position displacements are used in calculation. Furthermore, as an inverted pendulum, the velocity of displacement precedes the position of displacement for 90 degrees. As a result, a 90-degree phase lead between the body segment with respect to the visual scene in terms of position corresponds to an in-phase relationship in terms of velocity. The segment (trunk or legs) that is actively catching the visual stimulus should have a 90-degree phase lead and high gain with respect to the visual motion. For the reason

of simplicity, the phase and gain between leg/ trunk segment and visual motion will be called phase and gain of leg/trunk respectively. Three visual conditions will be tested in this study: 1 = rotation around ankle joint; 2 = rotation around hip joint; 3 = translation in AP direction. All the predictions focus on behaviors at low frequencies.

2.2.1.Predictions for the First Hypothesis. For the first hypothesis, if the visual motion is interpreted as a rotation around the ankle joint, both leg and trunk are predicted to have a 90-degree phase lead and high gains. If the visual motion is interpreted as a rotation around the hip joint, the trunk is predicted to have a 90-degree phase lead and high gain for trunk.

Condition	phase	gain
1	90 degree for both leg and trunk w.r.t visual scene	High gain for both
2	90 degree for trunk w.r.t visual scene	Higher gain for trunk Lower gain for leg
3	90 degree for leg w.r.t visual scene	Low gain for trunk High gain for leg

Table 1. predictions for the first hypothesis

Leg gain will be low and hence the phase relationship is not considered. If the visual motion is interpreted as a translation in the AP direction, leg angle will have a 90-degree phase lead and high gain, while the trunk angle will have low gain and phase cannot be reliably estimated. Please refer to table 1 for a summary of these predictions.

2.2.2. Prediction for the Second Hypothesis. For the second hypothesis, if the visual motion is interpreted as a rotation around the ankle joint, then both trunk and leg are predicted to have 90-degree phase lead and high gain. For visual motions that are interpreted as rotation around the hip joint and for translation in the AP direction,

both legs and trunk will have low gain, therefore, phase relationships cannot be reliably estimated. As an inverted pendulum rotating around ankle joint, the phase relationship between leg and trunk angles will be in-phase. Please refer to table 2 for a summary of these predictions. .

Condition	phase	gain
1	90 degree for both leg and trunk w.r.t visual scene	High gain for both
2	Legs and trunk are in-phase	Low gain for trunk Low gain for leg
3	Legs and trunk are in-phase	Low gain for trunk Low gain for leg

Table 2. predictions for the second hypothesis

3. METHODS

3.1. Subjects

15 subjects (9 males, 6 females) at the University of Maryland, aged 19 – 30 (mean age 21±3), participated in this study. The procedures used in the experiment were approved by the Institutional Review Board at the University of Maryland. All subjects received instructions for the test procedures. Informed written consents were obtained from all participants in the study. All the subjects were physically active, with no known musculoskeletal injuries or neurological disorders that might affect their ability to maintain balance.

3.2. Procedures

3.2.1. Apparatus. A visual cave consists of three screens (Fakespace, Inc, Marshalltown, Iowa, USA): one in the middle, two on either side with seamless corner technique was used in this experiment. Subjects were placed in the middle of

the visual cave facing the font screen at a distance of 3.5 feet and equivalent distance to both sides. The visual display was projected by JVC projectors (Model: DLA-M15U, Victor Company of Japan, Japan) to three mirrors, which reflected and rear-projected to the screens. Each screen consisted of 500 white small triangles on a black background. The triangles were randomly rotated with 3.4x3.4x3 cm on each side. No triangles were displayed within about a horizontal band of ±5 degree in height about the vertical horizontal of the subject's eye height. This procedure can reduce aliasing effects in the fovea region. The visual display was written by using CaveLib software (Fakespace, Inc). The frame rate of the visual display is 60 Hz.

Kinematics information of the subjects was captured by Optotrak (Northern Digital, Inc., Waterloo, Ontario, Canada), an active infrared position tracking system. The Optotrak uses a bank of three cameras, which were placed behind subjects to measure movements of the markers. The shoulder (the scapula), hip (the greater trochanter), knee (the lateral femoral condyle) and ankle (the lateral malleolus) were measured by attaching four LED markers on the right side of the subject. The markers were sampled at 60 Hz. Three markers were placed on a 6x6x6 cm triangle board with one marker on each corner. The triangle board was then attached on the subject's head with the center pointed to the inion. Another three markers were put on the fixed platform, which the subjects stood on, aligned the corner facing the cameras and used as a reference to check the data.

3.2.2. Design. An assumption of the experimental design is that the amplitude of visual flow at eye height determines the postural response. This assumption means that amplitude of visual flow at eye level was scaled in the translation and hip joint

conditions to be equal to the ankle joint condition. Without this assumption, calculation of gain across conditions is problematic. First, the signal in the translation condition is in units of cm, leading to a dimensional gain, while gains in the other two conditions would be dimensionless. Second, because the distance from hip to eye is shorter than ankle to eye, rotation angle at eye level in the hip joint condition would be smaller for a given rotation. This would artificially inflate gain in the hip joint condition.

Subjects were exposed to a sum-of-sines signal: U(t), which was either translated in the AP direction or rotated around the ankle or hip joint. Rotation around ankle was used as the reference condition and the other two conditions were scaled accordingly to maintain an equivalent amplitude of visual flow at eye height in each condition. The sum-of-sines signal consisted of 10 sinusoids, with a vector of frequencies (in Hz) defined as:

f = (3; 7; 13; 23; 43; 73; 113; 179; 263; 367)/125

The numbers in the bracket are cycles that repeat in 125 seconds. Prime numbers insured no common low-order harmonics. The resulted frequencies ranged from 0.024 to 2.936 Hz as prime multiples of a basic frequency of 0.008 Hz. To maintain the same peak velocity across frequency, the amplitudes (A) of the sinusoids were defined as the inverse of frequencies: A divided by f. In a previous experiment (Kiemel, et al., 2006), A was equal to 0.05 cm for the low amplitude condition. Based on the average eye height and ankle height of the subjects and approximating the amplitude as the rotation arc, rotation amplitudes were converted to degrees with A = 0.02. For the last 2 sinusoids, the amplitude of the eighth sinusoid was used due to

previous results which showed gains that were not significantly different from 0 at the same two frequencies (Oie et al., in prep). The sum-of-sines signal had five (even) zero-phase and five (odd) 180 degrees phase-lead sinusoids, so that the summation of the sinusoids started at zero-phase without a large change in phase at the beginning of the trial. For the rotation around the hip condition, the rotation origin was the hip joint and the signal was: U(t) x ((eye height – ankle height) / (eye height – hip height)).The translation signal was scaled as: U(t) x ((eye height – ankle height) x 2 π / 360).

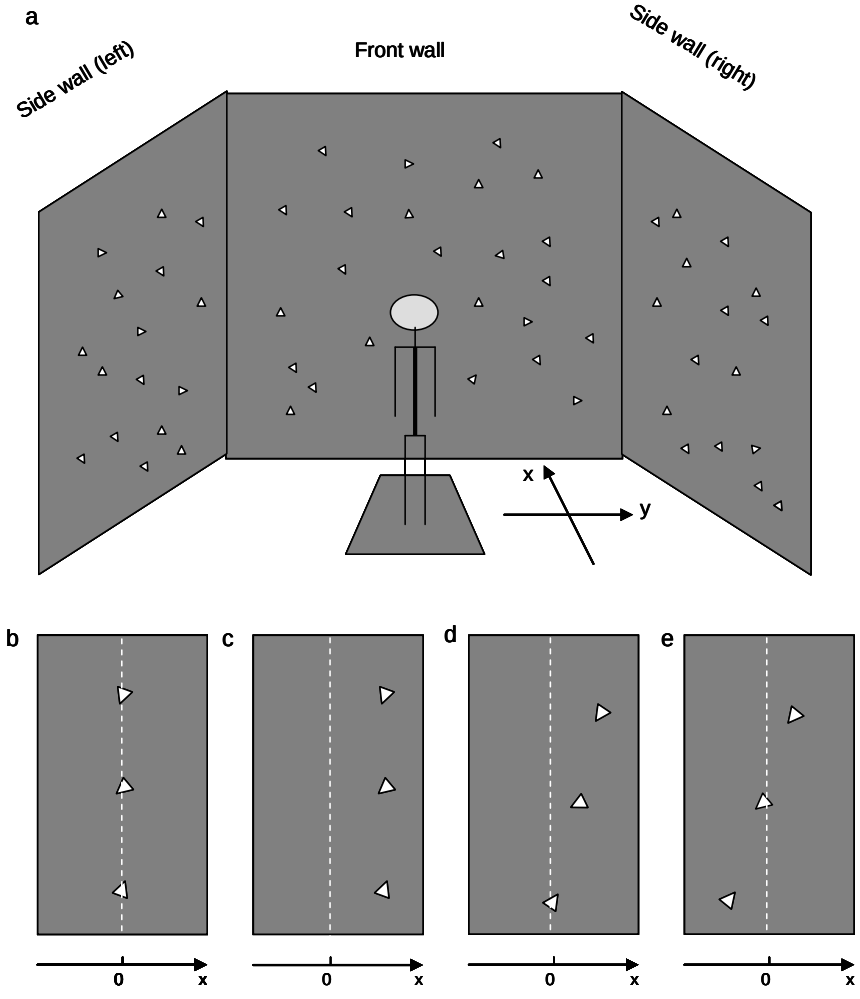

Figure 5.1. Visual stimuli. a) Experimental setup: the subject was placed in a visual cave consisting of three walls. The subject stood on a fixed platform with his/her ankle joint 1.16 m and 1.07 m from the front (x) and side (y) screens, respectively. b – e) Visual stimuli viewed from the left side wall. The triangles on the wall were moving as a whole around an axis (white dash lines) collinear with the subject's ankle joint. Three triangles are shown at the subject's eye height, hip height and ankle height to illustrate the movements of all triangles. b) The initial positions of the triangles. c) Translation; d) Rotation around ankle e) Rotation around hip. Note that the rotation angles are exaggerated to show differences between conditions.

All 12 trials were randomized in blocks for individual subjects with each of these conditions appearing once in each block, four trials per condition. Each trial was 260 seconds including two cycles of the sum-of-sines movements and 5 seconds of quiet stance at the beginning and end. Body sway was analyzed only during visual movement.

Subject stood with feet apart at a distance of 11% of her/his height between the toes and an angle of 14 degrees between the mid line and each foot on a fixed platform (Mcllroy, et al., 1997). Ankle height was measured as the vertical distance between the sole of subject's foot and ankle (the lateral malleolus); hip height was measured as the distance between the sole of the subject's foot and hip (the greater trochanter); eye height was measured as the distance between the sole of the subject's foot and eyes (paropia). The subjects began each trial by looking straight ahead at the visual display with their arms crossed at their chest. Between trials, the subjects were required to sit down for at least 2 minutes to reduce fatigue. All the subjects finished the experiment; one trial and one cycle of the rotation around the ankle condition were discarded due to technical difficulty.

3.2.3. Analysis. The trunk and leg segment were assumed to lie on the line connecting the shoulder and hip and the hip and ankle markers, respectively. The knee marker was ignored based on the previous study showed that knees are static during quiet stance (Alexandrov, Frolov, & Massion, 2001). Trunk and leg angle with respect to vertical were determined by the AP and vertical displacement of the shoulder, hip and ankle marker. We used the average of the three head markers to represent the head displacement. The shoulder and hip marker were used directly for shoulder and hip displacement respectively.

The frequency-response function (FRF) at the stimulus frequency was computed as the Fourier spectra of the time series of output signal divided by the Fourier spectra of the stimulus: U(t), the signal used in the rotation around ankle condition. The output signals used included trunk/leg angle and displacements of head, shoulder and hip. Gain and phase was calculated as the absolute value and the argument of the FRF. A unity gain means the magnitude of body sway at the driving frequency exactly matches the magnitude of the visual motion. A positive phase means that the body segment is leading the visual motion.

Because a large range of stimulus frequencies was probed simultaneously, responses at extremely low or high frequencies tended to have low power. The result is low gains that are centered close to the origin in the complex plane, which can lead to large differences in phase from trial-to-trial because of measurement error. Consequently, two mean values of gain and phase are relevant. Group gain/phase refers to extracting the gain/phase from the average FRF calculated across subjects in a given condition. Mean gain/phase is calculated by averaging gain and phase

extracted from single trial FRFs across subjects. Based on the assumption that the real and imaginary parts of the FRFs have a bivariate normal distribution, we used F statistics to see if the FRFs are significantly different from zero. A significant difference means that the responses are detectable. FRFs of each driving frequency and condition from all the subjects were plotted in the complex plane to determine if all values were roughly in a 90-degree range. If so, then group gain-phase and mean gain-phase are approximately equivalent. If not, then only frequencies that encompass the 90-degree range were used.

Cophase between trunk-leg at the driving frequencies was computed as leg phase minus trunk phase. A positive phase means the leg segment leads the trunk segment. Power spectrum density (PSD) of the trunk/leg segment and cross spectrum density (CSD) between trunk and leg segment were calculated using Welch's method. Complex coherence was computed as CSD divided by the square root of the product of trunk and leg PSDs for each trial. Coherence (also called magnitude squared coherence) was extracted as the absolute value of mean complex coherence averaged across subject at each driving frequencies. Non-driving-frequency cophase is the argument of complex coherence averaged across trials and subjects. Coherence and cophase between hip-shoulder and head-shoulder were calculated in the same manner.

3.2.4. Statistics. Phase and the log of gain was analyzed with a Segment x Condition x Frequency repeated-measure ANOVA analysis with Greenhouse-Geisser adjust *P* value for both trunk/leg angle and displacement of head, shoulder and hip. The use of log transformation for gain reduced the skewness. Follow-up paired *t*-test

was applied to perform the paired comparison. A frequency x condition repeated-measure ANOVA with Greenhouse-Geisser adjust *P* value was used to analyze coherence at the driving frequencies.

For the non-driving-frequency gain and phase, because the frequencies adjacent to the driving frequency (i) may be contaminated, an average of the complex coherence of the i-2^{th} and i+2^{th} frequency is used to compare with the i^{th} driving frequency. The same method applied for FRF is used here.

4. RESULTS

4.1. PSDs.

Figure 2 shows the power spectrum density (PSD) of trunk and leg segment average across subjects. PSDs for both segments decrease from approximately10 to 10^{-5} (degree^2/Hz) across frequencies. Furthermore, although responses to the visual stimulus are detectable across frequencies, FRFs plotted in the complex plane showed that phases for subjects at the 2^{nd} – 7^{th} frequencies were in an approximate 90 degrees range, suggesting consistent responses, while phases at the 1st and highest three frequencies were in a range greater than 180 degrees, indicating unreliable responses. Thus, the analysis focused on the 2^{nd} – 7^{th} stimulus frequencies.

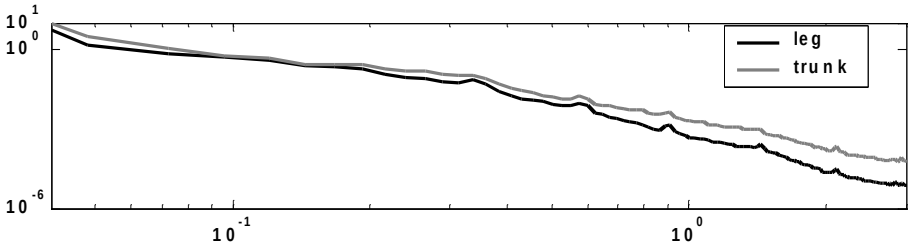

Figure 5.2. PSDs average across subjects.

4.2. Gain of Trunk/leg angle.

Figure 5.3 shows mean gain and phase for both leg and trunk segment relative to the visual movement. Gains are small at low frequencies, rise gradually to a much higher level, typically reaching a peak at the fifth frequency (0.344 Hz), then decrease more abruptly and arrive at values that are lower than the first frequency. All the gains are significantly different from zero ($P < 0.05$). For most of the subjects, the peak gain is greater than 0.5.

There was significant segment x condition effect on gain ($P = 0.0325$, MANOVA). Follow-up paired *t*-test revealed that trunk gain was significantly different between translation and rotation around ankle at the 2^{nd}, 4^{th} and 5^{th} frequency. No effects for gain were observed for the leg segment.

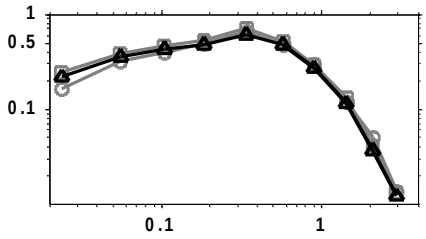

Figure 5.3. group average of gain, phase and trunk-leg phase. a) and c) are gain and phase for the leg segment; b) and d) are gain and phase for the trunk segment. e) is the trunk-leg cophase.

4.3. Phase of trunk/leg angle.

Consistent with previous studies, the phase of both leg and trunk segments with respect to the visual scene decreased as frequency increased for all the conditions. In general, an approximate 90-degree phase lead is seen at the first one or two frequencies. The phases then decreased below 0 degrees at higher frequencies, indicating a phase lag between the body segments and the visual scene. A segment x frequency interaction effect (P =0.0052, MANOVA) and main condition effect (P = 0.0066) were found. Follow-up paired t-tests showed that differences existed for pairs: translation and rotation around ankle, translation and rotation around hip for both segments. Figure 4 shows the phase and gain differences for condition

comparisons. The pattern of gain difference is consistent with predictions for the second hypothesis – a single-link internal model for both trunk and leg segment.

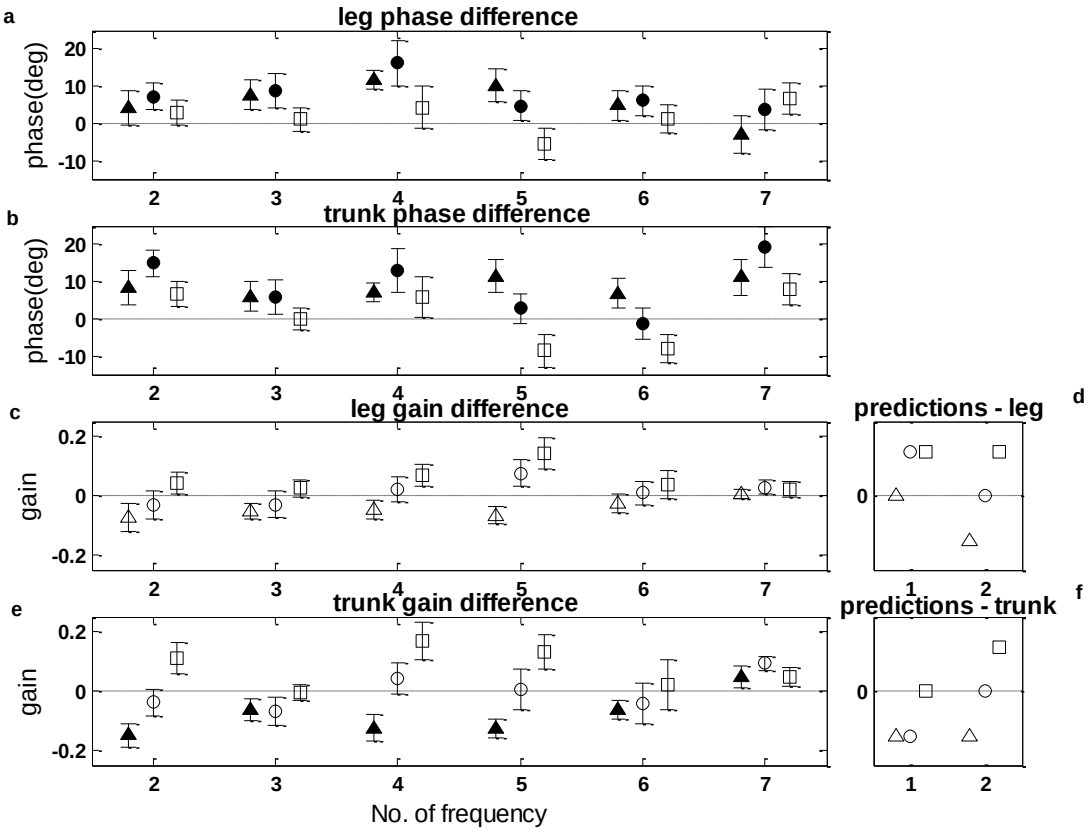

Figure 5.4. Phase and gain differences between conditions. The triangles (Δ) represent the differences between translation and rotation around ankle; the circles (O) are the differences between translation and rotation around hip; the squares (□) show the differences between rotation around ankle and rotation around hip. The pairs with filled markers were significantly different from each other. For both a) and b), translation has higher phase than the two rotation conditions. For e), rotation around ankle has higher gain than translation. d) and f) are predictions for the first and second hypothesis (y axis). If the pairs are not different from each other, then the value is on the zero line; a value above or below the zero line represents the first condition of the pair has a higher or lower gain than the second condition.

4.4. Gain of Displacement.

Gain for displacement of head, shoulder and hip reflect their geometric positions with hip gain the lowest and head gain the highest at the low frequencies (Figure 5.5). This was confirmed by a main Condition effect ($P = 0.0022$). However, gain at the high frequencies merge close to each other, supported by a Segment x Frequency effect ($P = 0.0020$).

4.5. Phase of Displacement.

A Segment x Frequency ($P = 0.0142$) and main Condition effect was found for phase ($P = 0.0004$). These results are further explored in terms of cophase below.

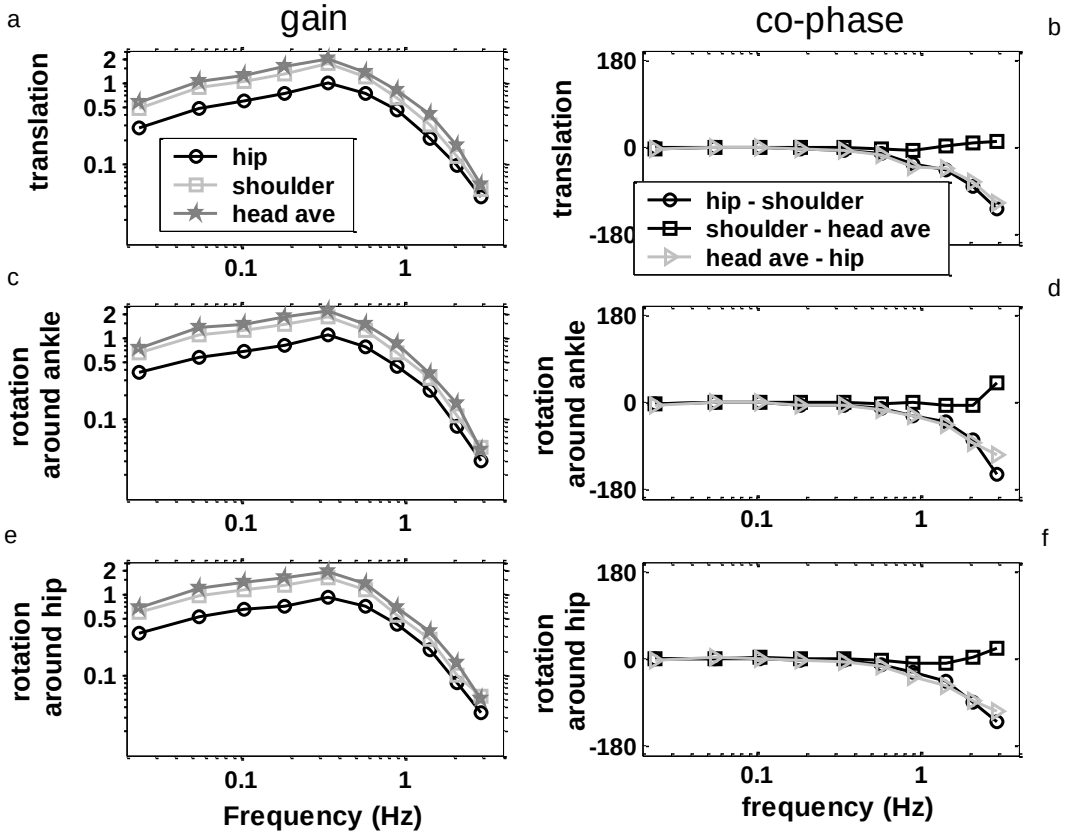

Figure 5.5. (a, c, e) Gain and (b, d, f) cophase for head, shoulder and hip displacement. At low frequencies, head, shoulder and hip are in-phase. At higher frequencies, head and shoulder were in-phase, while the hip lagged both the head and shoulder.

4.6. Trunk-leg Coordination.

Trunk-leg cophase, shown in Figure 6, for all three conditions was approximately 0 degrees at low frequencies up until the fifth frequency (0.344 Hz) and then gradually decreased at the high frequencies towards 180 degrees, with the trunk leading the leg segment. Non-driving-frequency trunk-leg cophase was in-phase at low frequencies and anti-phase at high frequencies. No Condition effect was found for coherence.

Displacement cophase, shown in Figure 5, indicated that head and shoulder were in-phase across frequencies. Hip was in-phase with both head and shoulder at low frequencies, but lagged behind them at high frequencies.

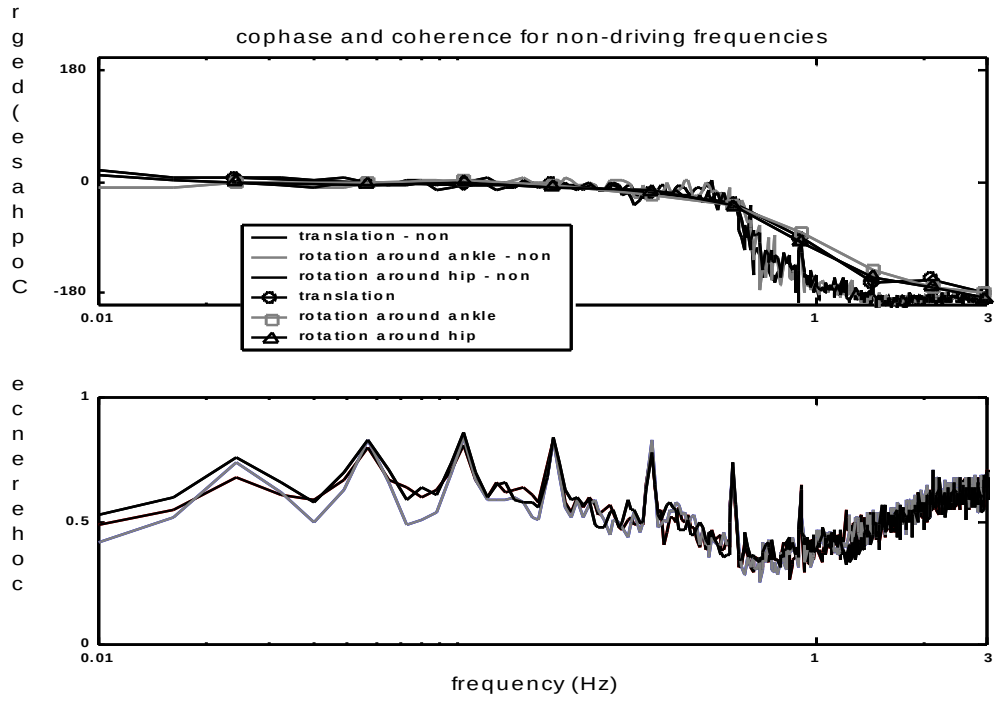

Figure 5.6. Cophase and coherence at the non-driving frequencies. The lines without markers are for non-driving frequencies (a&b).

Cophase at the driving frequencies and non driving frequencies were different at the 7^{th}, 8^{th} and 9^{th} frequency ($P < 0.05$). Coherence was different at the first 7 frequencies ($P < 0.05$).

5. DISCUSSION

We tested whether a single-joint or multi-joint internal model of upright stance is used to interpret different types of visual flow. The visual signal was either translated in the AP direction or rotated around subject's ankle or hip joint in three separate conditions. Systematic gain and phase changes were found for both the trunk and leg segments relative to visual movement. However, only minor differences were observed as a function of the visual display structure. Such results support the second hypothesis: a single-link internal model is used by the nervous system to interpret visual motion with the trunk and leg segment aligned to each other.

5.1. A Single-link Internal Model

The key of our second hypothesis is that the nervous system uses a single-link internal model interpretation in all the conditions. Our prediction was based on extreme situations. Therefore, if only small deviations from the prediction were found, our hypothesis is still supported. The first support comes from the results that the pattern of gain difference for both segments is coherent with predictions of the second hypothesis (Figure 4). With a single-link internal model, one would expect gains in the rotation around ankle would be higher than translation and rotation around hip condition for both trunk and leg segment. Because both translation and rotation around hip condition have low gains, the differences between these two

conditions would be small. Moreover, phases for all conditions at the first one or two frequencies have a 90-degree phase lead between body segment position and visual motion. This is consistent with our prediction for the second hypothesis that body segment leads the visual scene for 90 degrees at low frequencies. Further and more direct evidence comes from trunk-leg phase: the trunk and leg were in phase at low frequencies. That is, the body uses a single-link inverted pendulum.

The common view of motor control is that the nervous system tends to use simple interpretations to control the motor system, especially when ankle and hip synergies are used to explain sensory coupling. For example, somatosensory and vestibular information is important for ankle and hip synergy, respectively. Somatosensory loss subjects showed only hip synergy, while bilateral vestibular loss patients showed only ankle synergy when the subjects were exposed to perturbed surface (Horak, Nashner, & Diener, 1990). The argument was that this behavior is related to the sensor locations. The implicit assumption is that the nervous system controls the trunk and leg segment separately when responds to perturbation. That is, sensors of vestibular information are located in the head; the loss of vestibular information makes control of the trunk segment impossible so that only the leg segment is controlled. Likewise, proprioception comes from feet and is related to the ankle synergy. However, our results suggest that the subjects always tried to align these two segments together when responding to either visual rotation or translation. Although this is far from conclusive that vestibular and somatosenosry information would have the same impact, it indicates that the nervous system may try to control human body as a whole when responds to visual perturbation.

A single-link model has an advantage for feedback control: it reduces time delay, which is usually considered as a constraint for feedback control. A long time delay might destabilize the system. The more degree of freedom the nervous system needs to control, the more time delay. A single-link model simplifies the segments needed to be controlled. The control strategy may try to align both segments together when respond to the visual motion. For example, tonic muscle activity might be used to create stiffness and damping at the hip. This adds to the view that although an ankle synergy is more energy efficient, trunk vertically may have precedence (Horak, et al., 1996).

5.2. Coexisting Postural Coordination Patterns

Coexisting postural coordination patterns were found: phase between the trunk and leg segment was around 0 degree at low frequencies and gradually increased towards 180 degrees at high frequencies, consistent with previous study (Creath et al., 2005). This coexisting pattern argues against the generally accepted view that the ankle and hip synergies are centrally selected before the perturbations based on current sensory information and prior experience (Horak et al., 1990). Different sensory information manipulations and patient population showed consistent co-existing coordination pattern from studies in our lab: platform sway-referencing, foam surface (Creath, et al., 2005), light touch and bilateral vestibular loss patients (Zhang, et al., 2005). Furthermore, mechanical manipulation by adding weights to the subjects didn't change the pattern either (Elahi, et al., 2005). These results replicate the view that the ankle and hip synergies are basic coordination

patterns, the predominance of which depends on the sensory information available (Alexandrov et al., 2001).

Non-driving-frequency cophase and cophase are different at high frequencies. Non-driving-frequency cophase changed abruptly from in-phase; while cophase decreased gradually and did not reach 180 degrees at the highest frequency. Some studies in our lab have shown this different transition from in-phase to anti-phase between conditions (i.e., Creath, et al., 2005) or direction (i.e., Zhang et al., 2005). The mechanism is not yet clear, a model is needed.

Associated with the shift in trunk-leg phase above approximately 0.6 Hz was a steady decrease in gain for all the subjects in all the conditions. Gains increased gradually at the low frequencies and usually reached a peak at the fifth frequency, around which the trunk-leg phase started to shift from in-phase and gradually changed to anti-phase. These results suggest that coupling of body sway to a visual stimulus is dependent not only on the structure of the optic flow field, but interacts with the coordinative patterns that may reflect biomechanical constraints (Creath et al., 2005; Zhang et al., 2005).

The cophase of head, shoulder and hip displacement confirmed that trunk and head moved in the same direction and in opposite direction to the hip at the high frequencies. The anti-phase relationship of head and hip at the high frequencies emphasized the view that head actively tracking visual information, thus leading the whole trunk segment counter-rotating with the hip in a hip synergy (Horack, et al., 1996).

5.3. Visual Rotation and Translation

As mentioned before, Peterka et al. (1995) stated that visual translation and rotation have the same influence on postural sway without providing evidence. The logic was that the arc of rotation could be approximated to the translation amplitude mathematically. In order to test this, we kept the amount of stimuli the same at eye level. As part of the experiment, we asked subjects if they detected how the visual display was moving and the difference between conditions after they finished the trials. None of our participants was able to tell how many conditions were in the experiment, not to mention the difference between conditions. The only main Condition effect for gain was found between translation and rotation around ankle in the trunk segment. Phase differences between these two conditions were found for both the leg and trunk segment. As a result, although these two conditions are mathematically the same, one needs to be cautious when it comes to neural representation of these two visual motions.

There is the possibility that lack of differences between conditions were due to lack of power to detect significant differences. However, this possibility seems unlikely. First, pilot data showed that 15 subjects have enough power to detect differences. Second, gains were significantly different from zero across all the frequencies with peak average gain close to 1. Results showed main condition effects for gain in the leg segment and phase in both segments. Phase differences of approximately 20 degrees were found to be significant, indicating enough sensitivity to detect even small differences.

6. CONCLUSION

The current study emphasized the human body as an inverted pendulum in response to visual motion. Our results support the hypothesis that a single-link inverted pendulum is used to interpret visual motion. This was supported by: 1) the pattern of gain difference between conditions is consistent with predictions of the single-link model hypothesis; 2) an in-phase relationship between trunk and leg angle at low frequencies. The control strategy aligns the trunk and leg segment together while the nervous system tries to bring the body back to vertical. The co-existing coordination patterns argue against the view that ankle and hip synergies are centrally selected. Small gain difference showed between translation and rotation around ankle brings cautions to the argument that translation and rotation are equal.

Chapter 6:

Identifying Postural Control Feedback Using Mechanical Perturbation

1. INTRODUCTION

The human body has been approximated as an inverted pendulum, which is mechanically unstable. An inverted pendulum will fall due to gravity without a control system to compensate for fluctuations. Furthermore, a robust control system must be designed according to the mechanical characteristics of the system. For instance, the base of support and location of center of mass determine the inherent stability of the system. When humanoid robots were designed, the stability problem is always solved by using wide-base feet and/or shifting weights to the lower extremities (e.g. Cornell Efficient Biped and Delft University Denise) (Kuo, 2007). However, these robots were built for tasks other than mimicking human stance. They do not capture the real anatomic features of the human body, which has a small base of support and most of the weight in the upper segment. Subsequently, a complicated and sophisticated control system is needed to constantly correct deviation from vertical in order to maintain upright.

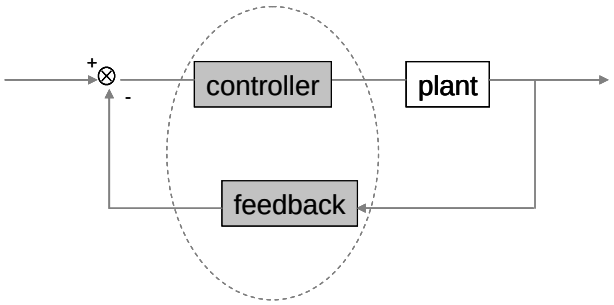

Figure 6.1. The traditional view of a control loop.

A typical control loop is consisted of a controller, feedback and plant (figure 6.1.). We further simplify the system by integrating the controller into feedback, which correspond to the active neural control in the case of quiet standing. The plant is treated as the actuators being controlled. That is, the passive viscoelastic features of the muscles (McMahon, 1984; Kiemel, Elahi, & Jeka, 2008a) and the skeleton structure. Each of these processes has a mapping from time-varying inputs to time-varying outputs (figure 6.2.). Feedback will be characterized with body sway (i.e. legs or trunk segment angles) as input and muscle activity as output. Electromyography (EMG) is a common method to measure muscle activity and will be used here as a proxy for the motor command. Feedback is composed of sensory dynamics, state estimation and the control strategy. Sensory dynamics (i.e. vision, somatosensory and vestibular systems) measures states (e.g. velocity or position) of the body. This information is not directly available to the nervous system, but rather corrupted by noise and time delay. Therefore, the resulting sensory information is estimated, then integrated and sent to the control strategy to generate motor commands. The plant can be characterized with motor command as the input and body sway as the output. It consists of musculotendon dynamics and body dynamics. Musculotendon dynamics receives motor commands and elicits muscle activity. Torque is generated and acts on the body dynamics to generate sway.

Given these mappings, it might seem easy to characterize the feedback and plant. However, the inputs and outputs are not readily accessible. Feedback and plant are in a continuous loop and change at almost the same time frame. Note that the measured EMG serves as an input to the plant and output from the feedback

simultaneously. Measured sway is a combination of input to the feedback and output from the plant. It is not straightforward to tell the proportion of measured EMG due to the feedback or plant. The same situation happens to measured sway. Therefore, we need to figure out the inputs and outputs specific for the feedback or plant.

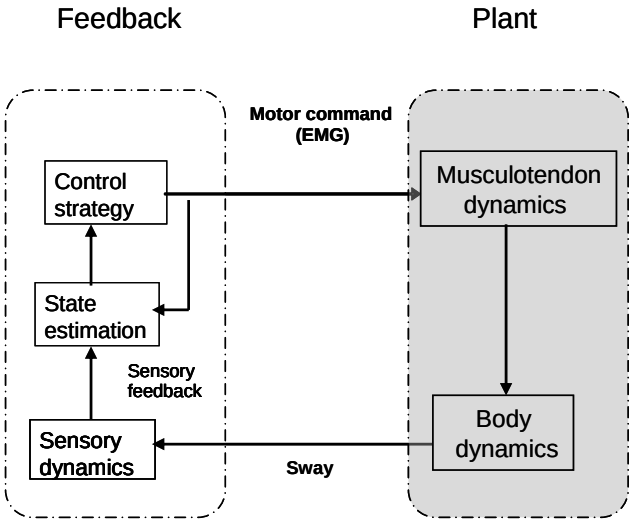

Figure 6.2. A schematic overview of the postural control loop with adaptation of state estimation.

With a physical system, it is relatively easy to characterize the feedback and plant: we might be able to open the loop and measure each component. Early attempts in characterizing a certain biological system separated organs from animal bodies and reconnected them in ways allowing researchers to measure inputs and outputs easily. In the Starling heart-lung preparation, the heart and lung were isolated from the systemic circulation. By adjusting the blood flow into the right atrium, the relationship between the right atrial pressure and cardiac output was investigated (Khoo, 1999). Stark et al. characterized the papillary light reflex in vivo (Stark & Baker, 1958). In a closed-loop condition, increasing the light intensity leads to smaller pupil size, which in turn modifies intensity of the light input. Stark and Baker used a beam of light with diameter smaller than the smallest pupil size so that the

stimulus light was not modified by the pupil and subsequently measured pupil size as a function of the light intensity. Another unusual way of opening the loop included testing a patient with a rare disease (Leigh, Newman, Zee, & Miller, 1982), which was featured by an isolated loss of ability to adjust pupil size in one eye.

Opening the loop is impractical when it comes to the postural control system. The human body is unstable and needs sensory information to maintain an upright position. One possibility of opening the postural control loop would be to remove all sensory information. One can experimentally remove visual information by closing the eyes. However, excluding somatosensory and vestibular information is not feasible experimentally and is only possible in patient populations that are rare. Even if excluding all sensory information were possible, it is not possible to maintain balance without sensory information.

In this experiment, we applied a closed-loop system identification method (van der Kooij et al., 2005). This linear approach relies on introducing known perturbations and computing input-output frequency response functions (FRFs). Fitzpatrick et al. (1996) have implemented this method by using sensory and mechanical perturbation separately in different trials. FRFs were used to characterize the effects of perturbations on the EMG and sway. Then the inferred plant FRF was characterized as the sensory perturbation-to-sway FRF divided by the sensory perturbation-to-EMG FRF; while the inferred feedback FRF was computed as the mechanical perturbation-to-EMG FRF divided by the mechanical perturbation-to-sway FRF (see methods).

Their analysis assumed a single-joint model of the human body and was based on measurements of the ankle angle and muscular activity from the ankle muscle (i.e., soleus). That is, a single-input-single-output (SISO) system was used for both the plant and feedback. However, recent studies have shown that an ankle strategy and a hip strategy co-exist during quiet stance: in-phase pattern (i.e., ankle strategy) of the trunk and leg segment at frequencies lower than 1 Hz; anti-phase pattern (i.e., hip strategy) at frequencies higher than 1 Hz (Creath et al., 2005; Zhang et al., 2007). This indicates that a single inverted pendulum may not be sufficient to characterize the plant. Another limitation of Fitzpatrick et al. (1996) was that mechanical and sensory perturbations were applied in separate trials. Because the perturbations may induce sensory reweighting, the identified feedback or plant may differ between conditions, complicating the interpretation.

In this experiment, feedback was identified with weak mechanical perturbations and measuring multi-joint body segment movements and EMG activity from multiple muscles. If the feedback control is a SISO system, then the feedback identified through perturbations at the hip should be a scaled version of similar perturbations at the shoulder. Visual motion, which has been demonstrated ~~as~~ to be comparable to galvanic stimuli, was used to identify the plant (Kiemel et al. in press). In order to evaluate the role of sensory reweighting when the sensory and mechanical perturbations are applied separately, two perturbations were applied either in the same trial or separate trials.

2. METHODS

2.1. Experimental methods

Subjects. 17 subjects (9 males, 8 females) at the University of Maryland, aged 19 – 31, participated in this study. The procedures used in the experiment were approved by the Institutional Review Board at the University of Maryland. All subjects received instructions for the test procedures. Informed written consents were obtained from all participants in the study. All the subjects were physically active, with no known musculoskeletal injuries or neurological disorders that might affect their ability to maintain balance.

Experiment setup. Weak and continuous mechanical perturbations were applied to the subject by attaching the ends of a spring (with a constant of 0.03N/mm) to the back of a waistbelt worn by the subject on one end and a linear positioning table placed behind the subject on the other end. The subject faced the front wall and stood in the middle of the visual cave 1 m from the front wall and 1.5 m from each side wall. Subjects assumed a foot position with heels at a distance of ~11% of their heights and an angle of 14° between each foot and the midline (McIlroy et al., 1997). The instruction to the subjects was to look straight ahead at the front screen and not to consciously resist any force from the waistbelt.

Kinematics. Kinematics was captured by an Optotrak infrared position tracking system (Northern Digital, Inc.), which was placed behind the subject.. The shoulder (the scapula), hip (the greater trochanter), knee (the lateral femoral condyle) and ankle (the lateral malleolus) were measured by attaching four LED markers on the right side of the subject. The markers were sampled at 120 Hz.

EMG. Muscle activity was measured using a multi-channel telemetric surface EMG system (Noraxon Zerowire). Silver/silver chloride electrodes were placed on

the right lateral gastrocnemius, soleus, tibialis anterior, biceps femoris, rectus femoris, rectus abdominus, erector spinae muscles of the lumbar spine. EMG signals were band passed between 10 and 1000 Hz and sampled at 2160 Hz.

Mechanical and visual perturbation movements. The anterior-posterior displacement of the motor table (the perturbation signal) is a broadband pseudo-random time series with a peak-to-peak displacement of 20 cm and a stimulus cycle of 6.5 seconds, which gives a lowest frequency at 0.15 Hz and no sharp cutoff high frequency. Our data analysis focused on the 10 frequencies below 3 Hz, which have the most power in postural sway. The vector of the ten frequencies was:

f = (0.1538; 0.4615; 0.7692; 1.0769; 1.3846; 1.6923; 2.0000; 2.3077; 2.6154; 2.9)

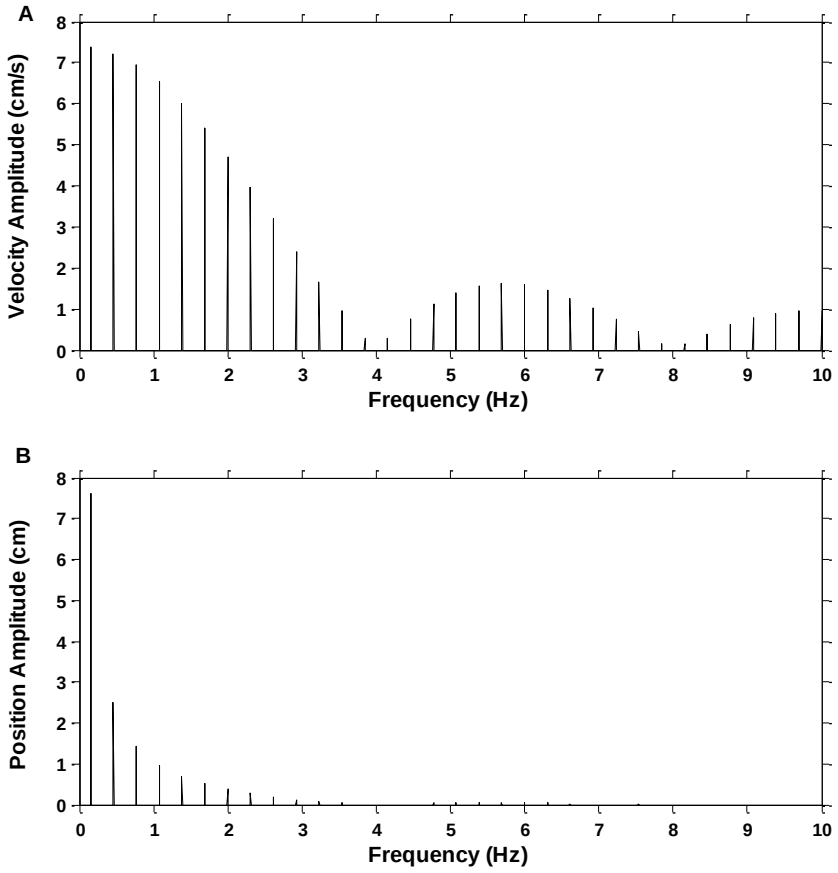

Figure 6.3. The spectral composition of velocity and position amplitudes for the peak-to-peak 20 cm PRTS stimulus signal below 10 Hz.

The visual display was projected by JVC projectors (Model: DLA-M15U, Victor Company, Japan) to three mirrors, which reflected and rear-projected onto a visual cave consisting of three 2.67 x 3.33 m screens (Fakespace, Inc, Marshalltown, Iowa, USA). The visual display consisted of 500 randomly distributed white triangles (3.4x3.4x3 cm) on a black background. To reduce aliasing effects in the foveal region, no triangles were displayed within a horizontal band of ±5 degree at eye height. The visual display was written by using CaveLib software (Fakespace, Inc). The frame rate of the visual display is 60 Hz. A pseudo-random visual signal with the same frequencies as the mechanical perturbation and a peak-to-peak amplitude of 1.5 degrees was displayed as a visual rotation around ankle joint.

Experiment condition. The first trial was a normalization trial for EMG. The subjects were instructed to rotate around their ankle and hip joint forward and backwards as far as possible while keeping their joints aligned in two separate conditions. When leaning to the maximum distance, they were instructed to maintain the position for 5-10 seconds. EMG activity during the maximum was interpreted as maximum contraction. There were four conditions: mechanical perturbation alone, visual perturbation alone, and two combined conditions in which both mechanical and visual perturbations were applied simultaneously with the visual perturbation randomly initiated either forwards (positive) or backwards (negative). In the mechanical perturbation alone condition, the visual scene was static. In the visual perturbation alone condition, the spring between the motor and subject was detached.

The length of each trial was 247 seconds, allowing 38 cycles of stimuli, with 3 trials in each condition.

2.2. Signal processing

Signals. The trunk and leg segment were assumed to lie on the line connecting the shoulder and hip and the hip and ankle markers, respectively. Trunk $\theta_2(t)$ and leg $\theta_1(t)$ angle with respect to vertical were determined by the anterior-posterior (AP) and vertical displacement of the shoulder, hip and ankle marker. For EMG activity of each muscle, the mean was subtracted for the raw EMG and then full-wave rectified, resulting in EMG signals $u_1(t)$, $u_2(t)$, …, $u_7(t)$.

Spectral analysis. The power spectral density (PSD) and cross spectrum density (CSD) of signals were calculated using Welch's method with a 65 sec (10 cycles) Hanning window and 50% overlap. Complex coherence was computed as $C_{xy} = P_{xy} / \sqrt{P_{xx} P_{yy}}$ and (magnitude-squared) coherence is $\left|C_{xy}\right|^2$. Where P_{xx} and P_{yy} are PSDs for signal *x(t)* and *y(t),* and P_{xy} is CSD. For each subject, we defined the closed-loop frequency response function (FRF) from *x(t)* to *y(t)* as $H_{xy} = P_{xy} / P_{xx}$. Gain and phase are the absolute value and the argument (converted to degrees) of the FRF, respectively. A positive phase indicates that *y(t)* leads *x(t).* Taking EMG normalization in consideration, average FRF across subjects was computed as $\bar{H}_{xy} = \bar{C}_{xy} \sqrt{\bar{P}_{yy} / \bar{P}_{xx}}$, where $\bar{C}_{xy}$ is the mean complex coherence and $\bar{P}_{xx}$ and $\bar{P}_{yy}$ are the geometric mean PSDs. In this calculation, if *x(t)* is EMG signal, then its variability only affects the scale of the results but not the pattern of phase or gain change across frequencies. We computed bootstrap 95% confidence intervals for the

log gain and phase of $\bar{H}_{xy}$, using the percentile-*t* method with 4000 boot strap resampling and 400 nested bootstrap resampling for variance estimation.

Weighted EMG signals. Rectified EMG signals of the three ankle muscles (soleus, gastrocnemius and tibialis anterior) were weighted as $u(t) = w_1 u_1(t) + w_2 u_2(t) + w_3 u_3(t)$ based on maximizing the complex coherence between the perturbation (i.e. visual $v(t)$ or mechanical $m(t)$ perturbation) and the weighted EMG response $u(t)$ using the Matlab optimization toolbox to adjust weights w_j. This was done because the plant/feedback control was identified using the FRF from visual/ mechanical perturbation to EMG activity. Average coherence was obtained by averaging C_{vu} and C_{mu} across the conditions identifying the plant and feedback, respectively, (session 3) and then averaging $|C_{vu}|^2$ and $|C_{mu}|^2$ across frequencies. Positive and negative signs of the weights indicate in-phase and anti-phase muscle pairs. $u(t)$ was normalized by dividing by the maximum gain $|C_{vu}|^2$ or $|C_{mu}|^2$ across the ten frequencies for each subject. Using the same method, the weighted hip and all EMG signal were computed using the four hip or lower trunk muscles (i.e. biceps femoris, rectus femories, rectus abdominus and erector spinae) and all seven muscles, respectively.

In order to compare our methods to the traditional EMG normalization technique, EMG normalization was also calculated by dividing EMG activities during the perturbation by the EMG activity in the normalization trial. Muscle activity patterns did not differ between the techniques.

2.3. Identification of the plant and feedback frequency response function

Given a single-input-multiple-output linear system (SIMO), a weighted EMG signal is the input to the plant, with the leg and trunk segment angles as outputs, arranged in a matrix $\theta(t) = [\theta_1(t) \quad \theta_2(t)]^T$ ('T' indicates transpose). The reverse is for the feedback control. Let $V(f)$, $U(f)$, $M(f)$ and $\Theta(f)$ be the Fourier transforms of $v(t)$, $u(t)$, $m(t)$ and $\theta(t)$. Then

$$\Theta(f) = P(f)U(f) + N_v(f), \tag{1}$$

$$U(f) = F(f)\Theta(f) + N_m(f), \tag{2}$$

where $P(f) = [P_1(f) \quad P_2(f)]^T$ is the open-loop FRF of the SIMO plant and $N_v(f)$ is the Fourier transform of a vector sensory noise signal;

$F(f) = [F_1(f) \quad F_2(f)]^T$ is the open-loop FRF of the feedback controller and $N_m(f)$ is the Fourier transform of a vector mechanical noise signal. Since the noise signals were not correlated with the chosen perturbation signals, they should cancel when trials are averaged. Therefore,

$$H_{v\theta}(f) = P(f)H_{vu}(f), \tag{3}$$

$$H_{mu}(f) = F(f)H_{m\theta}(f), \tag{4}$$

Where $H_{v\theta}(f) = [H_{v\theta_1}(f) \quad H_{v\theta_2}(f)]^T$ is the vector closed-loop FRF from the visual scene angle to body segment angles and $H_{vu}(f)$ is the closed-loop FRF from the visual scene angle to the control signal; $H_{m\theta}(f) = [H_{m\theta_1}(f) \quad H_{m\theta_2}(f)]^T$ is the vector closed-loop FRF from the mechanical signal to body segment angles and $H_{mu}(f)$ is the closed-loop FRF from the mechanical perturbation to the control signal. The plant FRF is $P(f) = H_{v\theta}(f) / H_{vu}(f)$ after rearranging equation 3.

Applying methods described in section 2, we used mean closed-loop FRFs across subjects to identify the plant:

$$P(f) = \bar{H}_{v\theta}(f) / \bar{H}_{vu}(f) \quad (5)$$

Using the same methods, the feedback was derived as:

$$F(f) = \bar{H}_{mu}(f) / \bar{H}_{m\theta}(f) \quad (6)$$

Compared to identifying the plant and feedback for each subject and then averaging across subjects, this method reduced errors due to subjects whose coherence between EMG signal $u(t)$ and visual scene angle $v(t)$ or mechanical signal $m(t)$ was low. Coherence intervals for the gains and phase of $P(f)$ were computed using the bootstrap percentile-*t* methods.

Ideally, when mechanical and sensory perturbations are applied simultaneously, these two signals should be uncorrelated in order to detect independent responses to each. These two types of perturbations were highly correlated in any given trial in our experiment since the same signal was applied. Assuming a linear system, the response (e.g., EMG or segment angles) should be a response to the sum of these two stimuli instead of individual stimulus. For example, the FRFs from perturbations to EMG activity are $H_{(v+m)u} = P_{vu} / P_{vv} + P_{mu} / P_{vv}$ and $H_{(-v+m)u} = -P_{vu} / P_{vv} + P_{mu} / P_{vv}$ for vision positive and negative combined conditions, respectively. However, notice that the response to vision has the same values but opposite signs. The average of these two conditions gives $H_{mu} = P_{mu} / P_{uu}$, that is, the true response for mechanical perturbation. The same procedure was used for FRFs from visual and mechanical perturbation to body segment angles and EMG activity.

3. RESULTS

We chose to maximize the average coherence between the EMG signals and visual/mechanical perturbation with the weights allowed to be either positive or negative. In most cases, the weights of the anterior and posterior muscles had the opposite signs: soleus and gastrocnemius weights had the same sign in 13 (vision) and 15 (mechanical perturbation) of 17 subjects; gastrocnemius and tibialis anterior weights had opposite signs in 11 (vision) and 10 (mechanical perturbation) of 17 subjects. A positive sign = active posterior muscles, a negative sign =active anterior muscles. The weighted EMG signal is the sum of muscles with both positive and negative values. The same method was used to calculate a weighted hip EMG signal from the remaining four muscles and a weighted EMG signal from all muscles.

Figure (6.4.) demonstrates the average coherence between visual/mechanical perturbation and the rectified EMG of individual muscles and weighted EMG activities. In general, coherence was higher for gastrocnemius and soleus and lower for tibialis anterior. Coherence for weighted sum of the ankle EMG signals was higher than individual ankle muscles. This coherence improvement was also observed for the weighted sum of hip EMG signals compared to individual hip/lower trunk muscles.

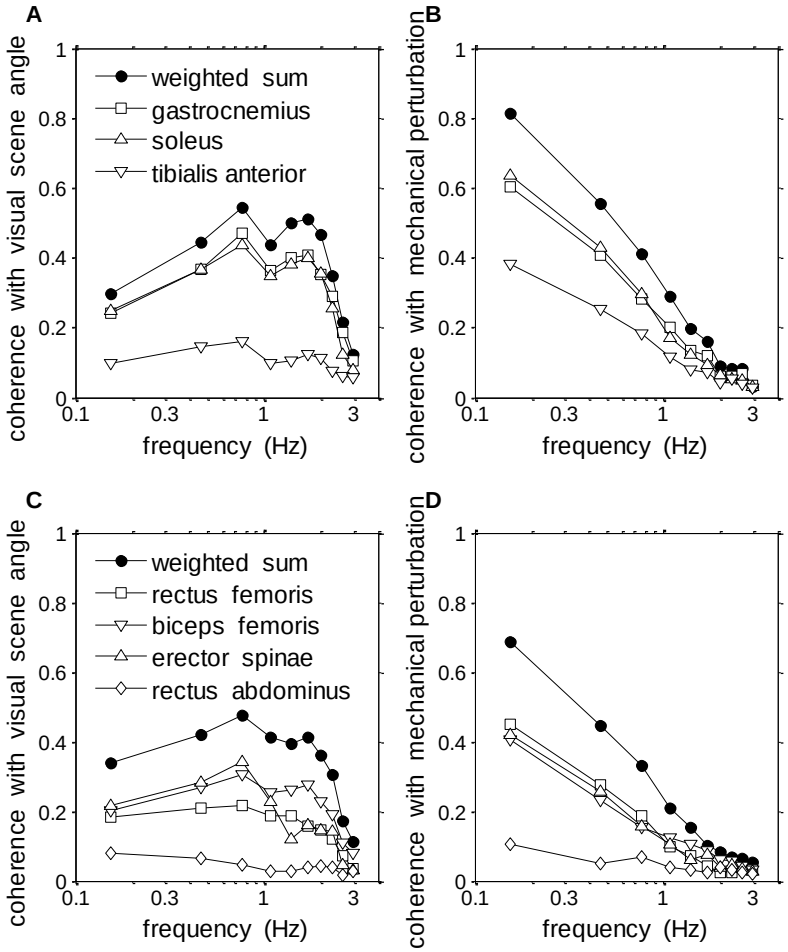

Figure 6.4. Coherence of the visual scene angle with the EMG signals of ankle muscles (A) and hip and lower trunk muscles (C). Coherence of the mechanical perturbation with the EMG signals of ankle muscles (B) and hip and lower trunk muscles (D). Coherence was computed by averaging complex coherence C_{vu} or C_{mu} across both conditions and then averaging coherence $|C_{vu}|^2$ or $|C_{mu}|^2$ across subjects.

3.1. Frequency response functions of the plant

Gain and phase patterns of the closed-loop single-input single-output FRF from visual scene angle to the weighted ankle EMG signal (Fig 6.5.A,B), the closed-loop single-input multiple-output (SIMO) FRF from the visual scene angle to the leg and trunk segment angles (Fig 6.5.C,D), and identification of the open-loop SIMO

FRF from the weighted EMG signal to the body segment angles (Fig 6.5.E,F) were consistent with results from our previous experiment (Kiemel et al. in press) using only a visual perturbation. In addition, there was no differences in gain and phase between the alone and combined conditions, although gains of the FRF from visual scene angle to the EMG signal were slightly but not significantly higher in the combined condition at only a few frequencies. The similar phase response in both conditions demonstrates that we can separate the response to the visual and mechanical perturbation. EMG and segment angle responses exhibited a phase value of ~0 degree at the lowest frequency (0.15 Hz) and lagged behind the visual scene at higher frequencies. This phase lag of the segment angles suggests that the plant is not a direct mapping form EMG to joint torque, which would generate constant phase across frequencies.

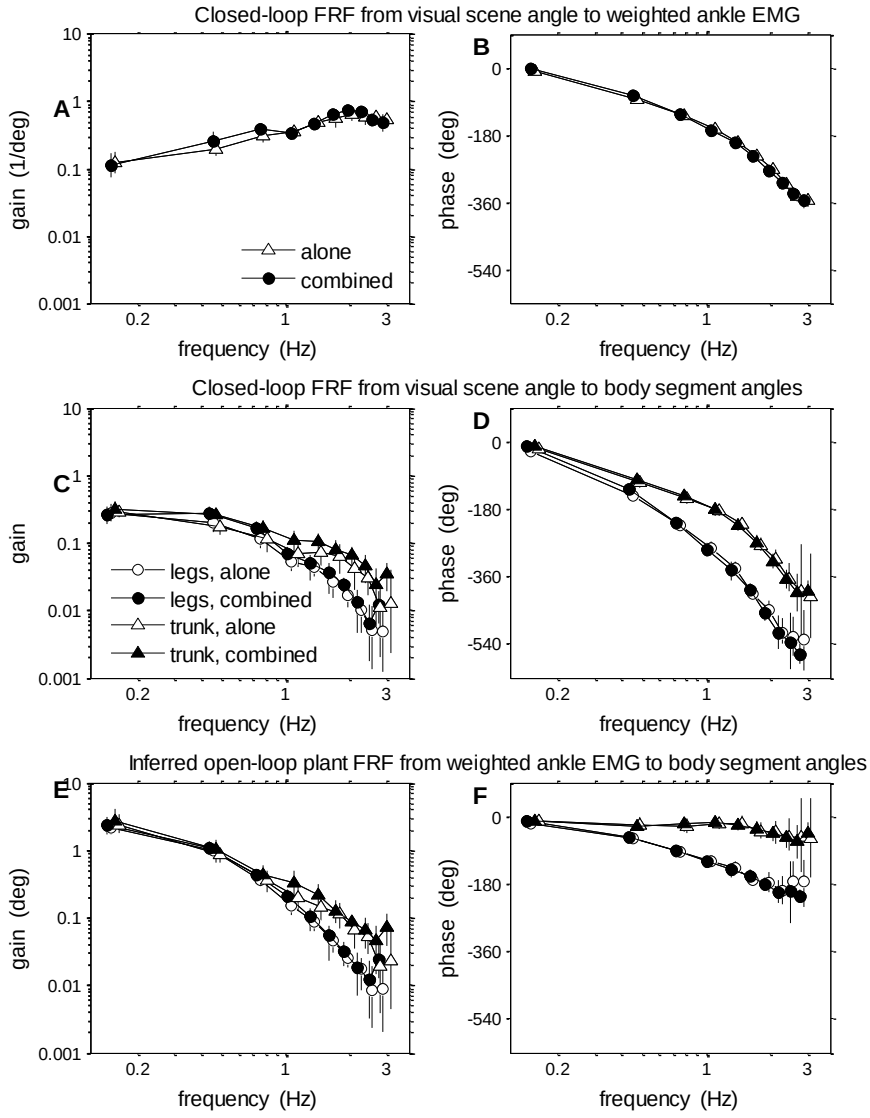

Figure 6.5. Gain and phase of frequency response functions of the plant. The closed-loop FRFs (A-B and C-D) are means across subjects. The inferred open-loop plant (E-F) was computed by dividing the FRF of C-D by the FRF of A-B. Gain of the plant in E equals the gain in C divided by the gain in A. Phase of the plant in F equals the phase in D minus the phase in B. FRFs are shown for both combined and alone visual scene motion. Error bars indicate 95% bootstrap confidence intervals.

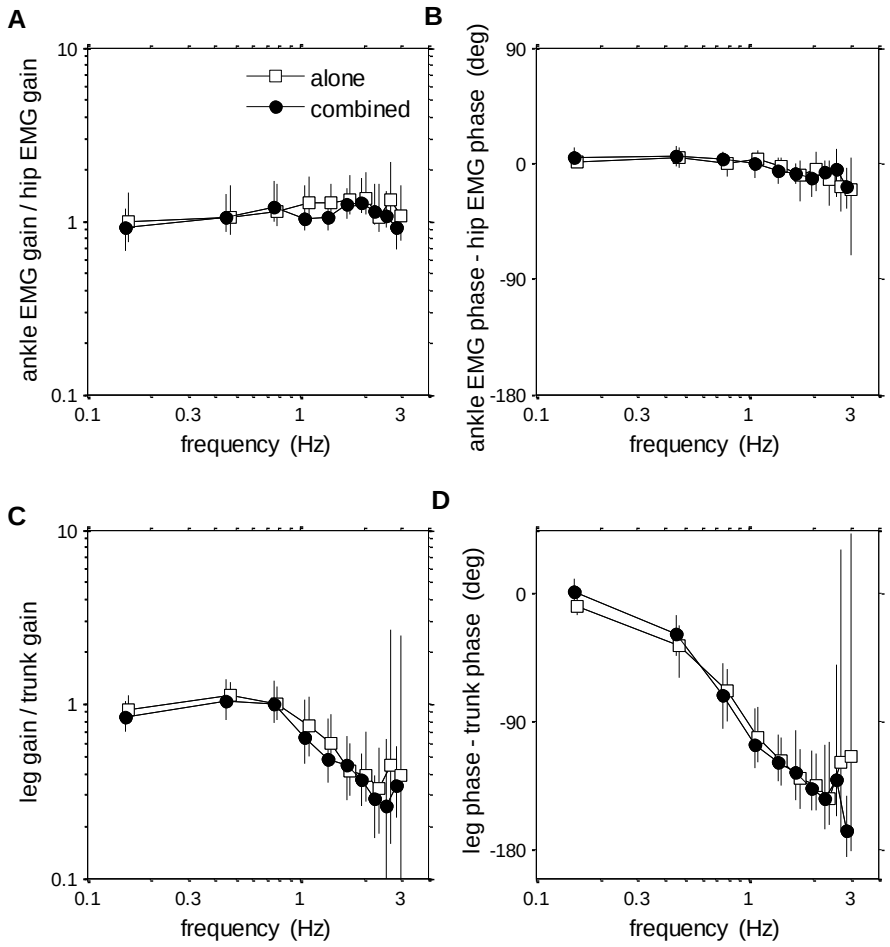

Figure 6.6. Comparison of frequency response functions of the plant. A-B: comparison of the response of the weighted ankle and hip EMG signals to the visual scene angle. C-D: comparison of the responses of the leg and trunk segment angles to the visual scene angle. Error bars indicate 95% bootstrap confidence intervals.

The identification of the open-loop SIMO FRF from the weighted EMG signal to the body segment angles is based on the assumption that the plant can be approximated as having a single input. Comparing the weighted ankle and hip EMG signals to the visual scene angle (Fig 6.6.A,B) supports this assumption. The ratio of the ankle EMG and hip EMG signal remained constant at approximately one across frequencies. The phase difference between the ankle EMG and hip EMG signal

remained approximately zero across frequencies, although there was a phase lag of <20 deg for the ankle EMG at the highest two frequencies. On the other hand, comparison of the two segment angles (Fig 6.6.C,D) indicated a multiple output system. There was large frequency dependence for both gain ratio and phase difference between the leg and trunk segment. The phase difference decreased gradually from about 0 deg at 0.15 Hz to about -160 deg at the highest frequency.

3.2. Frequency response functions of the feedback

The difference between the combined and alone condition was also not observed in feedback control. Fig 6.7. (A,B) shows the closed-loop FRF from mechanical perturbation to the weighted ankle EMG signal, and Fig. 6.7. (C,D) shows the FRF from the mechanical perturbation to the leg and trunk segment angles. Gain and phase in both conditions had similar patterns of change across frequencies.

Dividing the FRF from mechanical perturbation to the EMG signal by the FRF from mechanical perturbation to body segments angles provided an estimate of the feedback FRF (Fig 6.7.E,F). This feedback FRF was different from Fitzpatrick et al. 1996, in which the phase (of the leg segment) increased from around zero at lower frequency to around 180 degrees at 5 Hz. Note that, the FRF of the feedback identified by the leg segment in our case increased initially and reached approximately 70 degrees at 0.7230 Hz, then decreased to slightly below zero. In particular, the phase did not reach 180 deg at high frequencies. The difference could not be explained by the different kinematic measurement used in this experiment. We performed the same calculation using shank angle as described in Fitzpatrick et al. (1996) and obtained similar results. On the contrary, the phase of the trunk segment

increased across frequency and reached approximately 180 deg at 1.7261 Hz and then decreased at higher frequencies. For a proportional-derivative (PD) controller, one would expect phase increases to approximately 90 deg at high frequencies where velocity dominates the response. Our results indicated that postural control involves a mechanism other than or more complicated than PD control.

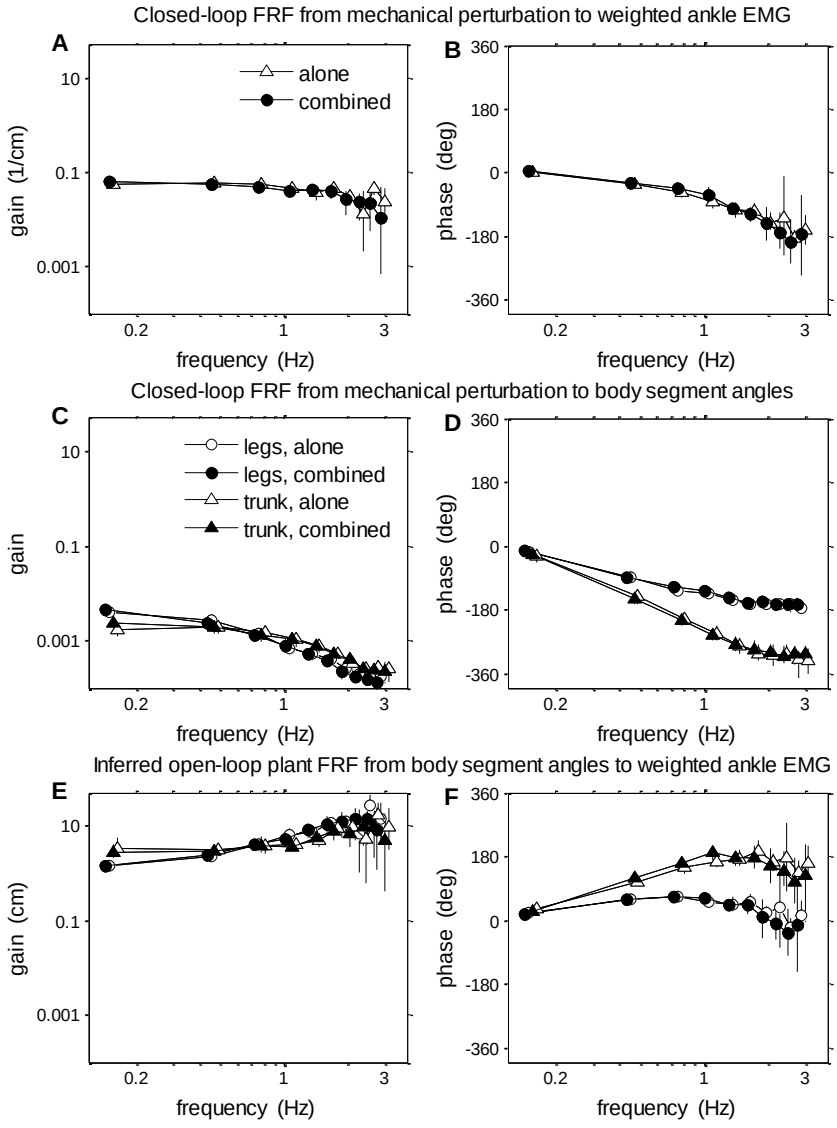

Figure 6.7. Gain and phase of frequency response functions of the feedback. The closed-loop FRFs (A-B and C-D) are means across subjects. The inferred open-loop feedback FRF (E-F) was computed by dividing the FRF of A-B by the FRF of C-D. Gain of the feedback in E equals the gain in A divided by the gain in C. Phase of the feedback in F equals the phase in B minus the phase in D. FRFs are shown for both combined and alone mechanical perturbation. Error bars indicate 95% bootstrap confidence intervals.

Fig 6.8.(C,D) compares the leg and trunk segment to the mechanical perturbation. If the feedback has only one input, then the gain ratio and phase difference of leg and trunk segment angles should remain approximately one and zero across frequencies, respectively. However, this hypothesis is not supported by our results. The gain ratio and phase difference of the leg and trunk responses depended on frequency. The gain ratio started at around 0.4 and became larger and larger as frequencies increased. On the other hand, the phase difference decreased as frequencies increased with the leg lagging the trunk segment. Therefore, the ankle and trunk feedback signal are different and cannot be approximated as a single segment. At lower frequencies (< 1.3846 Hz), the ratio of the ankle and hip EMG signal (Fig 6.8.A,B) remained approximately constant at 0.7. Phase difference decreased from around 0 deg to around -45 degrees at the highest frequency. The gain ratio and phase difference became less consistent at higher frequencies with large variability. This might be due to the low power of the mechanical perturbation signal at high frequencies.

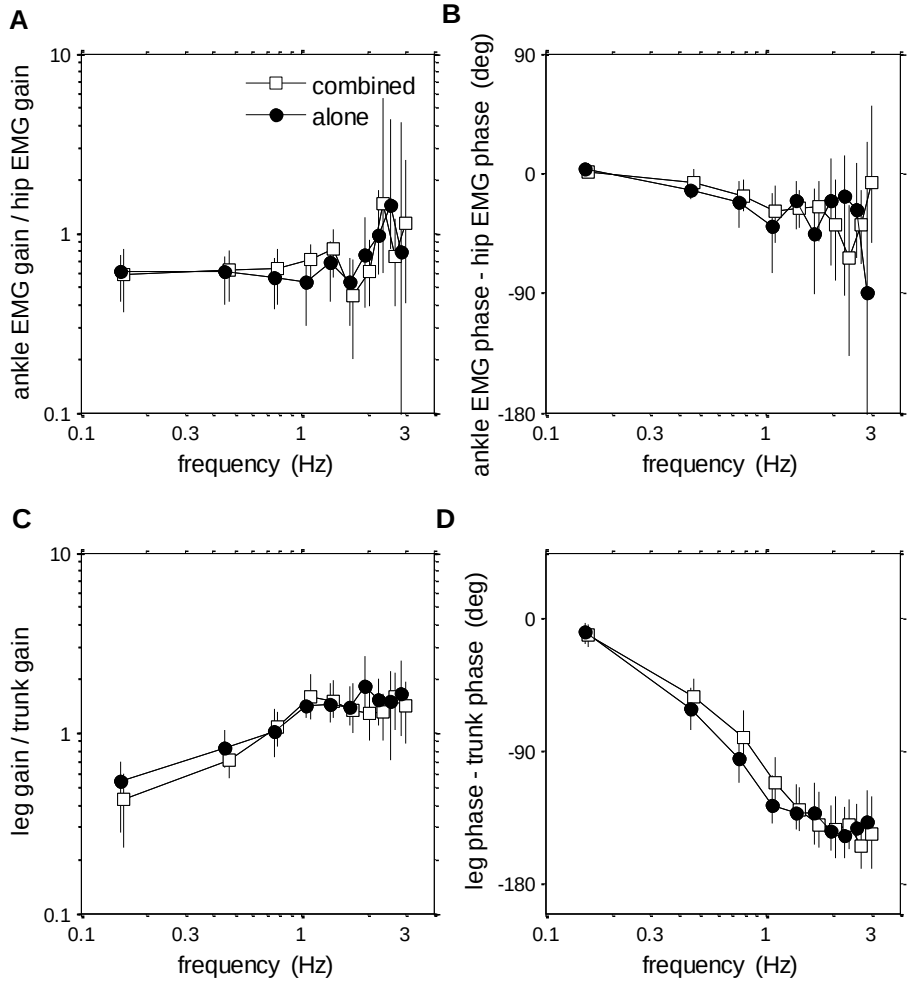

Figure 6.8. Comparison of frequency response functions of the feedback. A-B: comparison of the responses of the weighted ankle and hip EMG signals to the mechanical perturbation. C-D: comparison of the responses of the leg and trunk segment angles to the mechanical perturbation. Error bars indicate 95% bootstrap confidence intervals.

4. DISCUSSION

Mechanical and sensory perturbations were used to characterize the plant and feedback in postural control using the closed-loop system identification method,

focusing on two issues. First, can mechanical and sensory perturbations be used simultaneously within a trial? Fitzpatrick et al. (1996) applied mechanical and sensory perturbations in separate trials, while we have these two perturbations either in separate trials or combined in the same trials. Second, is single-joint or multi-joint body dynamics needed to characterize the plant and feedback? A single-joint inverted pendulum and soleus muscle was used in Fitzpatrick et al., while we used a two-joint inverted pendulum model and weighted EMG activities from 7 muscles. These changes addressed underlying issues related to sensory reweighting and multi-segment coordination.

4.1. Mechanical and sensory perturbation

The concern of using a mechanical perturbation is that the mechanical perturbation itself might physically change the plant, more specifically the trunk-leg coordination, thus changing the system. Results from the present experiment demonstrate that the mechanical perturbation did not have this problem. Phases of FRF from mechanical perturbation to both segment angles were very similar between the separate and combined conditions (figure 6.7.).

In this experiment, trials with mechanical and sensory perturbation were applied separately or combined in one trial. When both plant and feedback are within the linear range of movement, uncorrelated sensory and mechanical perturbations can be applied simultaneously to characterize both components. Phases of the FRFs relative to vision were similar when the motor was stationary or moving simultaneously with the visual stimulus, indicating that we could separate the responses to the visual and mechanical stimuli.

There seemed to be no suggestion of sensory reweighting between conditions, since gains from visual perturbation to EMG and segment angles were similar between conditions. This could be due to: 1) perturbations that were not large enough to elicit non-linearity between conditions; or 2) reweighting might be detected only at frequencies that were lower than those probed (< 0.15 Hz). Even if non-linearity between conditions is not a concern, there are advantages of applying two perturbations together. It is more efficient and can reduce testing time significantly. Consequently, subjects feel more comfortable, reducing the potential for fatigue. This also makes longer trials feasible and increases frequency resolution of the analysis.

4. 2. Two-segment inverted pendulum and the plant

Recent findings have supported that the trunk and leg segment are in-phase and anti-phase pattern coexist during quiet stance (Creath et al., 2005; Zhang et al., 2007). However, the neural and biomechanical aspects of these patterns were not clear. Does the plant or feedback contribute to the in-phase and anti-phase pattern? Results showed that the inputs (i.e., ankle and hip EMG) to the plant were a scaled version of each other, while the outputs (i.e., leg and trunk segment angles) showed a more complicated pattern. That is, with respect to the visual perturbation, the gain ratio of the ankle and hip EMG was close to 1 and the phase difference was approximately 0 across frequencies. On the other hand, the gain ratio of the leg and trunk segment was 1 at low frequencies and decreased as frequency increased; phase decreased from 0 across frequencies. This implies that inputs to the plant (i.e. the motor command) could be approximated as a single input, which agreed with Kiemel

et al. (in press). Since there was one input into the plant but two outputs, the trunk-leg phase difference at higher frequencies is based upon properties of the plant, rather than the neural control associated with feedback. This also compliments a previous study showing that sensory information affected these patterns at low frequencies where the in-phase pattern is observed (Zhang et al., 2007).

The identified plant indicates that musculotendon dynamics is more complicated than a direct mapping from EMG to joint torque. A direct mapping means that there is no delay (i.e., zero phase) between the EMG and joint toque. This was true for the phase at the 1st frequency, whereas phase decreased at higher frequencies. Because the physiological processes underlying a muscular response are often on a slower time scale than a perturbation, muscles act like low pass filters. Coupled with the inertia of the body, which also acts like a low pass filter, the phase of body sway relative to a perturbation tends to decrease as the frequency of the perturbation increases.

4.3. Double inverted pendulum and Feedback Control

The observed feedback properties were different from Fitzpatrick et al. (1996), in which phase increased across frequencies to around 180 degrees at 5 Hz. The phase pattern in this experiment is more complicated. Nevertheless, none of these results agreed with predictions of a simple proportional-derivative (PD) controller (Johansson, Magnusson, & Akesson, 1988; Peterka, 2000). At low frequencies, position coupling is dominant; while at high frequencies, velocity coupling is dominant (Jeka et al., 1997). Because velocity leads position displacement for 90 degrees for an inverted pendulum, phase would increase from 0 to 90 degrees at high

frequencies. Therefore, feedback control is more complicated than a PD controller. A model is needed in order to have more insight what type of controller is plausible.

One of the possible explanations for this discrepancy observed in the feedback is that neither of these experiments identified the real feedback response. If the feedback has a single input and a single output, then the trunk angle should be a scaled version of the leg angle; while the weighted summation of hip EMG should be a scaled version of the weighted summation of the ankle EMG. In terms of gain and phase, the gain ratio between the two segments should be around 1 and phase difference around 0. However, this prediction was not consistent with our data. The identification of both feedback and plant using the leg segment angle was different from trunk segment angle, especially at higher frequencies. This suggests limitations in using a single-joint (i.e. single-input-single-output, SISO) model to understand the control of upright stance. Therefore, a multi-segment inverted pendulum model is necessary.

In order to elicit true responses, the mechanical perturbation should be designed in a way that matches properties of the feedback. We used one input (i.e. applying only one mechanical perturbation on waist) and two outputs (i.e. two segments inverted pendulum) to identify the feedback. While Fitzpatrick et al. used one input and one output (i.e. a single link inverted pendulum). In future studies, we will use two mechanical perturbations, one for the leg segment and one for the trunk segment, instead of one mechanical perturbation.

4.4. Limitations

Due to equipment constraints, relatively high frequencies (with the lowest frequency of 0.1538 Hz) were used in this study. As a result, we were not able to detect responses at low frequencies, which are of great interest in postural studies. On the other hand, frequency components at the highest two frequencies had little power, reflecting by the large error bars at higher frequencies. The lack of power at higher frequencies makes it hard to interpret results at this particular frequency range, which is important in addressing the properties of the feedback. In future studies, we will consider using filtered white noise to allow a wide range of frequency components.

4.5. Conclusions

The relative contribution of neural control and biomechanical aspects is still an open question. We have illustrated that using a closed-loop system identification method could provide useful information in solving this problem. This experiment is a first step. It has: 1) demonstrated that a single-input-single-output system is insufficient to characterize both feedback and plant during quiet stance; and 2) provided further support that the anti-phase pattern between the trunk-leg segments is due to the biomechanical properties of the plant. In the proposed study, two mechanical perturbations will be used to characterize the feedback.

Chapter 7:

Dissertation Study:

Using Two Mechanical Perturbations to Identify Feedback in Postural Control

1. INTRODUCTION

Human upright bipedal stance is a classic example of a control system consisting of a plant (i.e., the physical body and its actuators) and feedback (i.e., neural control) operating continuously in a closed loop. While this sophisticated control system allows for flexible and stable behavior, it remains a scientific challenge to understand the source of control. For example, generation of a corrective torque to stabilize human upright stance can be achieved by changing the plant (increasing stiffness) or altering feedback control (e.g., sensory reweighting). A number of groups have attempted to separate the contribution of these two components to the control of upright stance (Morasso & Schieppati, 1999; Peterka, 2002; Loram et al., 2002), but currently there is no consensus. It has been argued, for instance, that when stiffness is high enough, active feedback control is not necessary to stabilize an inverted pendulum during quiet (undisturbed) stance (Winter et al., 1998). Recent studies, however, have estimated that ankle stiffness contributes from 15-90% of the minimum stiffness necessary to stabilize the plant (Kiemel, Elahi, & Jeka, 2008b; Loram et al., 2002; Peterka, 2002), illustrating that the precise contribution remains controversial. Some have even argued that low stiffness at the ankle joint is an advantage, allowing for flexible control and more resistance to external perturbation (Ishida, Masuda, Inaoka, & Fukuoka, 2008). A reasonable

model of postural control not only captures upright stance behavior, but also takes the properties of the plant and the feedback into account. Here we seek to characterize the properties of the feedback and the plant simultaneously.

The technique of opening-the-loop experimentally to isolate certain components of a control system has been successfully used in a wide variety of systems, including respiration (e.g., Starling heart-lung preparation (Patterson, Piper, & Starling, 1914)) and pupillary reflex (Stark et al., 1958). However, opening the loop by removing sensory information is impractical with the postural control system because without at least one of the three primary sensory inputs (vision, vestbular and proprioception), upright bipedal stance is not possible. Here we used a closed-loop system identification method with continuous small perturbations to identity different components of the control loop (Fitzpatrick et al., 1996; van der Kooij et al., 2005; Fujisawa et al., 2005; Kiemel et al., 2008b).

A conceptual model of the posture control loop is shown in Figure 7.1. Feedback is defined as the mapping from body sway (i.e., body segment angles) to muscle activity, in which electromyography signals (EMG) are used as a proxy for a motor command. Feedback represents active neural control and includes sensory dynamics, state estimation and the control strategy. The plant is defined as a mapping from EMG to body sway, consisting of body dynamics and musculotendon dynamics. An important issue experimentally is to use the appropriate number of inputs, which are under experimental control, to fully characterize the output behavior of the plant and/or feedback. A previous study used a visual perturbation (Kiemel et al., 2008b) to characterize properties of the plant during upright stance. Trunk and leg segment

kinematics as well as the activity of seven muscles (both anterior and posterior) were measured. The results showed that individual muscles behaved similarly, allowing a simplification into two "group" muscles at the ankle and hip. The resulting gain ratio (≈ 1) and phase difference (≈ 0) between ankle EMG and hip EMG muscles (i.e., inputs to the plant) with respect to the visual perturbation were constant across frequency, indicating that ankle and hip muscles were activated simultaneously. Thus, the plant can be approximated as having a single input in response to a visual stimulus. On the other hand, the gain ratio and phase difference between the leg and trunk segment kinematics with respect to the visual perturbation were not constant across frequency. A distinct decrease in gain and a phase difference between the trunk and leg segments were observed at frequencies above 1 Hz, suggesting that the plant has two outputs (i.e. leg & trunk segment) which serve as inputs to feedback. Therefore, in the current study, two mechanical perturbations were applied, one for the trunk segment and one for the leg segment, to characterize properties of feedback.

There is very limited knowledge about the feedback control system for human postural control. Several feedback control mechanisms, such as optimal control (Kiemel et al., 2002; Kuo, 1995; van der Kooij et al., 1999) or proportional-integral-derivative (PID) (Peterka, 2002) have been proposed. These proposals rely on assumptions about the nervous system such as optimality, which assumes that the nervous system tries to minimize a variable such as the center of mass (CoM) (Kuo, 1995) or muscle activity (van der Kooij et al., 1999). These are two very different assumptions of control mechanisms. The current study is meant to identify the properties of feedback so that such assumptions can be tested more rigorously.

2. METHODS

2.1. Experimental Methods

2.1.1. Subjects. 18 subjects (9 males, 9 females), aged 18-27, were recruited at the University of Maryland. The procedures used in the experiment were approved by the Institutional Review Board at the University of Maryland. All subjects received instructions for the test procedures. Informed written consent was obtained from all participants in the study. All the subjects were physically active, with no known musculoskeletal injuries or neurological disorders that might affect their ability to maintain balance.

2.1.2. Experiment setup. Weak and continuous mechanical perturbations were applied to the subject by attaching springs to a waistbelt and shoulder-strap worn by the subject on one end and computer controlled linear motors on the other. The spring constants for the waistbelt and shoulder-strap were 0.04N/mm and 0.0157N/mm. The subjects faced the front wall and stood in the middle of the visual cave 1 m from the front wall and 1.5 m from each side wall. Subjects assumed a foot position with heels at a distance of ~11% of their heights and an angle of 14° between each foot and the midline (McIlroy et al., 1997). The instruction to the subjects was to look straight ahead at the front screen and not to consciously resist any force from the waistbelt and shoulder-strap.

2.1.3. Kinematics. Kinematics were captured by an Optotrak infrared position tracking system (Northern Digital, Inc.), which were placed behind the subject. The shoulder (the scapula), hip (the greater trochanter), knee (the lateral femoral condyle)

and ankle (the lateral malleolus) were measured by attaching four LED markers on the right side of the subject. The markers were sampled at 120 Hz.

2.1.4. EMG. Muscle activity was measured using a multi-channel telemetric surface EMG system (Zerowire, Aurion). Silver/silver chloride electrodes were placed on the right side of the body measuring 11 muscles: lateral gastrocnemius, medial gastrocnemius, soleus, tibialis anterior, biceps femoris, Semitendinosus, rectus femoris, Vastus lateralis, Vastus medialis, rectus abdominus, and erector spinae muscles of the lumbar spine. EMG signals were band passed between 10 and 1000 Hz and sampled at 2160 Hz.

EMG frequency analysis is crucial in the method applied. EMG has been widely used in postural control studies (Henry et al., 1998; Nashner, 1977; Masani, Popovic, Nakazawa, Kouzaki, & Nozaki, 2003). Most of these studies mainly focused on temporal or spatial relationships of EMG signals with respect to a perturbation. Fitzpatrick et al. (1996) applied EMG frequency analysis with a CLSI method in postural control. Reasonable coherence between perturbations (i.e., mechanical and sensory perturbations) and EMG below 5 Hz was reported, suggesting EMG frequency analysis is feasible. Subsequently, Kiemel et al. (2008) showed that the coherence between a visual perturbation and weighted EMG activity could be as high as ~0.7 below 3 Hz.

2.1.5. Mechanical and visual perturbation movements

It is important that perturbation signals are uncorrelated when applying all perturbations simultaneously. In order to achieve this goal, we used filtered white noise generated with two low-pass Butterworth filters for the mechanical

perturbations: a first-order filter with a cutoff frequency of 0.1 Hz and an eighth-order filter with a cutoff frequency of 5 Hz. Power spectrum density (PSD) for the motor signals were kept constant at 4 cm^2/Hz and 2.5 cm^2/Hz respectively for the waist and shoulder. We used different seeds for every trial and subject. The resulting peak-to-peak amplitude for the waist motor and shoulder motor displacement was 13 to 15 cm and 11.5 to 13.5 cm, respectively. The same procedure was used for the visual signal except that the power spectrum density was 4.05 deg^2/Hz and the cutoff frequency of the first filter was 0.02 Hz. These parameters led to visual signals with a root mean square velocity similar to those used in previous studies (Kiemel, Oie, & Jeka, 2006; Kiemel et al., 2006).

The mechanical perturbations were delivered through two linear motors (LX80L, Parker Hannifin Corporation, USA), which were positioned behind the subjects and pulled subjects from their backs. The actual displacements of the motors were used as mechanical perturbation signals.

The visual display was projected by JVC projectors (Model: DLA-M15U, Victor Company, Japan) to three mirrors, which reflected and rear-projected onto a visual cave consisting of three 2.67 x 3.33 m screens (Fakespace, Inc, Marshalltown, Iowa, USA). The visual display consisted of 500 randomly distributed white triangles (3.4x3.4x3 cm) on a black background. To reduce aliasing effects in the foveal region, no triangles were displayed within a horizontal band of ±5 degree at eye height. The visual display was written by using CaveLib software (Fakespace, Inc). The frame rate of the visual display was 60 Hz. A visual signal was displayed as a visual rotation around ankle joint.

2.1.6. Experiment condition

There was only one condition with all the perturbations applied simultaneously. The length of each trial was 240 seconds. Another 5 seconds in the beginning and at the end were added to allow the motors to speed up or slow down. There were 12 trials in total for each subject (one subject had only 10 trials due to some technical difficulties).

2.2. Signal Processing

2.2.1.Signals

The trunk and leg segment was assumed to lie on the line connecting the shoulder and hip, and the hip and ankle markers, respectively. Trunk $\theta_2(t)$ and leg $\theta_1(t)$ angle with respect to vertical were determined by the anterior-posterior (AP) and vertical displacement of the shoulder, hip and ankle marker. For EMG activity of each muscle, the mean was subtracted from the raw EMG and then full-wave rectified, resulting in EMG signals $u_1(t)$, $u_2(t)$, …, $u_{12}(t)$.

2.2.2. Spectral analysis.

The power spectral density (PSD) and cross spectrum density (CSD) of signals were calculated using Welch's method with a 40 sec Hanning window and 50% overlap. Complex coherence was computed as $C_{xy} = P_{xy} / \sqrt{P_{xx} P_{yy}}$ and (magnitude-squared) coherence was computed as $\left|C_{xy}\right|^2$. Where P_{xx} and P_{yy} are PSDs for signal *x(t)* and *y(t),* and P_{xy} is CSD. For each subject, we defined the closed-loop frequency response function (FRF) from *x(t)* to *y(t)* as $H_{xy} = P_{xy} / P_{xx}$. Gain and phase are the absolute value and the argument (converted to degrees) of the FRF,

respectively. A positive phase indicates that *y(t)* leads *x(t)*. Taking EMG normalization into consideration, the average FRF across subjects were computed as $\bar{H}_{xy} = \bar{C}_{xy}\sqrt{\bar{P}_{yy}/\bar{P}_{xx}}$, where $\bar{C}_{xy}$ is the mean complex coherence and $\bar{P}_{xx}$ and $\bar{P}_{yy}$ are the geometric mean PSDs. In this calculation, if *x(t)* is the EMG signal, then its variability only affects the scale of the results but not the pattern of phase or gain change across frequencies. One subject was excluded when computing $\bar{H}_{xy}$ because his EMG response had a different pattern from the other 17 subjects. We computed bootstrap 95% confidence intervals for the log gain and phase of $\bar{H}_{xy}$, using the percentile-*t* method with 4000 boot strap resampling and 400 nested bootstrap resampling for variance estimation.

2.2.3. Weighted EMG signals.

Rectified EMG signals of the four ankle muscles (lateral gastrocnemius, medial gastrocnemius, soleus, tibialis anterior) were weighted as $u(t) = w_1u_1(t) + w_2u_2(t) + w_3u_3(t) + w_4u_4(t)$ based on maximizing the average complex coherence between the perturbations and the weighted EMG response $u(t)$ using the Matlab optimization toolbox to adjust weights w_j. This was because we identified plant/feedback control using FRF from visual/ mechanical perturbation to EMG activity. Average coherence was obtained by averaging C_{vu} and C_{du} across the multiple perturbations, and then averaging $|C_{vu}|^2$ and $|C_{du}|^2$ across frequencies. Positive and negative signs of the weights indicate in-phase and anti-phase muscle pairs. $u(t)$ was normalized by dividing by $\sqrt{\int_{0.025}^{5} S}$, where S is the PSD of weighted

EMG, 0.025 Hz is the first frequency and 5 Hz is the last frequency. Using the same method, we computed the weighted hip and all EMG signal using the seven hip or lower trunk muscles (i.e. biceps femoris, Semitendinosus, rectus femoris, Vastus lateralis, Vastus medialis, rectus abdominus, and erector spinae) and all eleven muscles, respectively.

2.2.4. Frequency binning.

With a 40 second window, we had 200 data points from 0.025 to 5 Hz. PSDs and CSDs were lumped into 10 frequency bins in order to increase power. Frequency binning was done after finishing EMG normalization and weighting, and before calculating FRFs. The basic principle was trying to get 10 equal-spaced bins in a log scale with additional fine adjustments to ensure that responses were significantly different from zero. The resulted frequency bin vector was:

[0.05 0.1375 0.2375 0.35 0.525 0.7875 1.2 1.8375 2.7625 4.15].

2.3. Identification of the Plant and Feedback Frequency Response Function

Given a single-input and multiple-output linear system (SIMO), a weighted EMG signal is the input to the plant, which has the leg and trunk body segment angles as outputs, arranged in a matrix $y(t) = [\theta_1(t) \quad \theta_2(t)]^T$ ('T' indicates transpose). The reverse is for the feedback control. Let $V(f)$, $U(f)$, $D(f)$ and $Y(f)$ be the Fourier transforms of $v(t)$, $u(t)$, $d(t)$ and $y(t)$. Then

$$Y(f) = P(f)U(f) + M(f)D(f) + N_y(f), \quad (1)$$

$$U(f) = F(f)Y(f) + S(f)V(f) + N_u(f), \quad (2)$$

where $P(f)$ is the open-loop FRF of the SIMO plant, $M(f)$ is a FRF characterizing the effect of the mechanical perturbations on body segment angles, $N_y(f)$ is the

Fourier transform of intrinsic noise in the plant output, $F(f)$ is the open-loop FRF of the feedback controller, $S(f)$ is a FRF characterizing the effect of the sensory perturbations on the EMG signals, $N_u(f)$ is the Fourier transform of intrinsic noise in the feedback output. Since the noise signals were not correlated with the chosen perturbation signals, they should be cancelled out when trials are averaged. Solving Eq. (1) and (2), we have

$$H_{vy}(f) = P(f)H_{vu}(f), \quad (3)$$

$$H_{du}(f) = F(f)H_{dy}(f), \quad (4)$$

Where $H_{vy}(f)$ is the closed-loop FRF from the visual scene angle to body segment angles and $H_{vu}(f)$ is the closed-loop FRF from the visual scene angle to the control signals, $H_{dy}(f)$ is closed-loop FRF from the mechanical signals to body segment angles and $H_{du}(f)$ is the closed-loop FRF from the mechanical perturbation to the control signal. Mean closed-loop FRFs across subjects computed as described in session 2.2.2. were used to identify the plant and feedback. From Eqs. (3) and (4), we can identify the plant $P(f)$ and feedback $F(f)$ as

$$P(f) = \bar{H}_{vy}(f)\bar{H}_{vu}(f)^{-1} \quad (5)$$

$$F(f) = \bar{H}_{du}(f)\bar{H}_{dy}(f)^{-1} \quad (6)$$

Compared to identifying the plant and feedback for each subject and then averaging across subjects, this method reduces errors caused by subjects whose coherence between EMG signal $u(t)$ and visual scene angle $v(t)$ or mechanical signal $d(t)$ was

low. Coherence intervals for the gains and phase of $P(f)$ and $F(f)$ were computed using the bootstrap percentile-*t* methods.

3. RESULTS

3.1 Motor characteristics

Figure 7.2 A and B showed an example of the motor response to our desired signal. The gains remained around one to up until 5 Hz. Phases were around 0 at lower frequencies and started to slowly decay until around 130 degrees at 5 Hz.

3.2 Weighted EMG and Coherence

We applied one sensory perturbation and two mechanical perturbations simultaneously in this experiment. At the mean time, we measured body segment angles and EMG signals from 11 muscles. Figure 7.3 showed an example of the time series of these signals for 20 seconds in a single trial. The top three graphs (Figure 7.3 A-C) demonstrated the filtered white noise signals of the visual scene rotation angle, waist motor and shoulder motor displacement. Because we had positive and negative weights, the weighted EMG had both positive and negative components (Figure 7.3 F). This weighted EMG was a summation of eleven muscles. When the weighted EMG signal is visually compared to the leg and trunk angle (Figure 7.3 D and E), the modularity of the EMG signal has a correlation with the forward and backward body sway. When the leg and trunk segment swayed forward, the muscles with positive weights (posterior muscles) became more active; when the leg and trunk segment swayed backwards, the muscles with negative weights (anterior muscles) became more active.

The mean and standard deviation of weights across subjects were listed in Table 7.1. Even though weights can be set to zero, only a few subjects had zero weights for the ankle and hip weighted EMG. For weighted ankle and hip EMG, posterior muscles seemed to be dominant as indicating by the larger total weights of the posterior muscles. The ankle muscles carried more weights than the hip muscles in the all muscle combined case.

Figure 7.4 A and B showed averaged coherence across subjects between perturbations and muscle signals. Perturbation wise, the coherence was highest for the waist motor perturbation at the 2^{nd} to 7^{th} frequency. There was no obvious difference among the three perturbations at other frequencies. Shoulder motor perturbation and vision yielded similar coherence with muscles signals. Coherence was highest for the weighted all-muscle signal with waist motor perturbation. While there was no apparent difference between the coherence of weighted ankle muscle and all-muscle signal for the waist perturbation, the coherence of all-muscle signal was substantially higher than the hip muscle. The coherence of all-muscle, ankle and hip muscle signals was similar in both waist motor and visual perturbation.

Figure 7.4 C and D showed the partial coherence between the waist motor signal and individual muscle EMG signals adjusted for the weighted all-muscle EMG signal. Because there was no quantitative difference among perturbations and waist coherence was the highest among the three perturbations, only partial coherence of waist motor signals was shown. Partial coherence was low for all muscle signals across frequencies. This indicates that the linear relationship between each

perturbation and weighted muscle signals account for most of the coherence seen in figure 7. 4 A and B.

3.2. Frequency Response Function

3.2.1. Plant

Figure 7.5 A and B showed the closed-loop FRF from visual scene angle to weighted ankle and hip EMG. The gains of ankle EMG were higher than the gains of hip EMG with a constant ratio across frequency. The phases of ankle and hip EMG were overlapped with each other, indicating that the phase difference was roughly zero across frequencies. These results were consistent with previous study showing that the plant has a single input (Kiemel et al., 2008b). The closed-loop FRF from visual scene angle to body segment angles was demonstrated in Figure 7.5 C and D. Note that even though the phase of the trunk and leg segments were similar at lower frequencies, leg segment gain had slightly lower values than the trunk segment, indicating that there was movement at the hip joint even at lower frequencies. At higher frequencies, the leg segment had a lower gain and lagged behind the trunk.

Dividing the FRF from visual scene angle to body segment angles by the FRF from visual scene angle to weighted EMG resulted in the inferred open-loop FRF from weighted EMG to body segment angles (Figure 7.5 E & F). Because the identified plant using ankle and hip EMG were expected to have similar values, only the ankle EMG was presented. While both gain and phase decreased as frequency increases, the leg gain and phase decreased more than the trunk at higher frequencies. Gains were around 1 at the lowest frequency and decrease to around 0.001 and 0.01 for the leg and trunk, respectively. Phase values were approximately zero at the first

frequency and decreased to about -90 and -270 degrees at the highest frequency for the leg and trunk, respectively. These results for the plant were similar to those observed in Kiemel et al. (2008) study, which used visual scene rotation without mechanical perturbations. The similarity of the plant in both studies suggested that our mechanical perturbations were small enough so that the plant was not changed in a meaningful way.

3.2.1. Feedback

The gains of closed-loop FRF from waist and shoulder motor perturbations to weighted ankle and hip EMG signal (Figure 7.6A, B) increased slightly across frequencies initially at lower frequencies and then decreased across frequencies. Waist perturbation induced higher gains of ankle EMG than the shoulder perturbation at the lower eight frequencies. Phase values decreased across frequency with the response to the waist perturbation lagging more than the shoulder perturbation at the higher frequencies. The response of the hip muscle to the waist and shoulder perturbations showed larger differences than the ankle muscle. For sway angles, similar gain and phase patterns across frequencies were observed (Figure 7.6C and D). While the leg segment in response to the waist perturbation led the trunk segment at higher frequencies; the trunk segment in response to the shoulder perturbation led the leg segment at higher frequencies.

Dividing the FRF from mechanical perturbations to EMG by the FRF from mechanical perturbations to body segment angles resulted in the FRF from body segment angles to EMG, that is, the inferred open-loop feedback FRF (Figure 7.6E and F). Compared to the plant, these feedback gains and phases had distinctively

different characteristics, suggesting separate plant and feedback responses. Gains for all four FRFs increased from around 1 (1/deg) to 100 (1/deg) across frequencies. Note that the gains of the leg segment to ankle EMG and trunk to ankle EMG were parallel to each other with the leg gains constantly higher than the trunk gain. On the other hand, the gain values of legs to hip EMG and trunk to hip EMG were similar. The phase pattern was more complicated. Phase values first increased from around zero degrees at lower frequencies, peaked at approximately 90 degrees around 1.5 Hz, then decreased to about zero degree at higher frequencies. Phase values among different FRFs displayed minor differences.

In order to look at the gain ratio and phase difference in a more intuitive way, gain ratio and phase difference between the FRFs using ankle and hip muscles were shown in figure 7.7. The gain ratio and phase difference were roughly constant across frequencies. Consistent with observation in figure 7.6, the gain ratio of legs to EMG using ankle and hip EMG fluctuated at around 2 across frequencies. The gain ratio of trunk to EMG using ankle and hip EMG was approximately 1 at the first frequency, decreased to around 0.5 and then gradually increases to approximately one at the highest frequency. The phase difference was close to zero for both leg and trunk relative to EMG.

4. DISCUSSION

In this experiment, we simultaneously determine the properties of the plant and feedback using a closed-loop system identification method. The identified plant and feedback show distinctive gain and phase patterns, indicating that we could

separate the responses to sensory and mechanical perturbations. Furthermore, our plant is similar to Kiemel et al. (2008), in which only a visual perturbation was applied. These results demonstrate that our mechanical perturbations did not change the plant significantly and applying sensory and mechanical perturbations together was feasible. Applying these perturbations in a single trial rather than separate trials not only eliminates the possibility of sensory-reweighting in different conditions (Peterka, 2002), but also is more efficient.

SIMO plant and MISO feedback

In previous study (Kiemel et al. 2008) using visual information, the plant was found to be a single-input multiple-output (SIMO) system, which is similar to what we have observed in this current study (figure 7.5). A constant gain ratio and phase difference between the ankle and hip EMG justifies this finding. Assuming that the number of inputs into the plant and the number of outputs from the feedback is the same, we expect the identified feedback to have a single output (i.e., a simple control strategy). A simple control strategy approximation would predict that the feedback FRFs using ankle and hip EMG are similar to each other. However, the experimental data demonstrates different gain values using ankle and hip EMG. This difference is highlighted by calculating the gain ratio. Even though we did see roughly constant gain ratio and phase difference across frequencies, the gain ratio of leg to EMG was different from the gain ratio of trunk to EMG (figure 7.7). That is, the feedback has two outputs. This indicates that there are limitations in considering human postural control to be a single input-multiple output (SIMO) control system.

The question is what may have led to the observed single-input of the plant. One possible explanation is the properties of a visual scene rotating around the ankle joint, which may not excite the trunk segment movement other than following the leg segment. Vision is processed by sensors located in the head. It is viewed to have a global reference of frame, such as gravity (Dichgans, Held, Young, & Brandt, 1972). In the moving room paradigm, a visual scene at the eye level, be it visual rotation or visual translation, is usually thought to excite the in-phase (ankle) pattern of leg and trunk coordination (Peterka et al., 1995). This interprets the constant ratio between the ankle and hip EMG (Figure 7.5 A and B). Obviously, two types of sensory perturbations are necessary to elicit two inputs into the plant. In addition to the visual rotation we use, the second sensory perturbation needs to excite a hip EMG activity that is different from the ankle EMG.

A plant with single input and multiple outputs would mean that the anti-phase pattern observed is a result of the plant (Kiemel et al., 2008a). It is worth mentioning that the abovementioned limitation (i.e., two outputs from feedback) does not automatically invalidate this hypothesis, especially when visual information is used to identify the plant. The anti-phase pattern during quiet stance is different from that with visual perturbation. During quiet stance, it is known that there is an abrupt transition from in-phase to anti-phase at around 1 Hz (Creath et al., 2005). This transition becomes gradual when visual perturbation is used: it starts at 0.425 Hz and reaches approximately160 degrees at the last frequency. Even though the mechanism of this phase difference is still unclear, it is obvious that visual perturbation is related to this anti-phase change. Further investigation is necessary.

Feedback control

The identified feedback indicated that control is more complicated than a proportional-derivative (PD) controller, which stabilizes the plant based on information of position and velocity of the body sway. At low frequencies, position coupling is dominant; while at high frequencies, velocity coupling is dominant (Jeka et al., 1997). Because velocity leads position displacement for 90 degrees for an inverted pendulum, phase would increase from 0 to 90 degrees at high frequencies. Our feedback phase (figure 7.6) starts from zero at low frequency, peaks around 90 degrees at about 1.5 Hz and then decreases at higher frequencies. These results do not agree with predictions of a simple proportional-derivative controller (Johansson et al., 1988; Peterka, 2000).

Explaining properties seen with the feedback requires modeling. In the model provided by Dr. Tim Kiemel based on this data set, an optimal control with a cost function minimizing COM displacement results in a more complicated gain pattern than our experimental results (figure 7.8): the gain of trunk to EMG is higher than the gain of legs to EMG at lower frequencies, they cross over at around 1.5 Hz with the gain of legs higher at higher frequencies. Physiologically, it is hard to interpret the meaning of minimizing COM displacement. COM is a physical property and abstract. It is not straightforward how the nervous system figures out the COM; the observed behavior of COM is a consequence of joint interaction (Hsu, Scholz, SchÖner, Jeka, & Kiemel, 2007). Furthermore, if the nervous system really tries to minimize COM movement, then a pure anti-phase pattern would be more beneficial. For example, when the leg segment sways backwards, a forward motion of the trunk segment

would minimize the COM displacement; while an in-phase movement of the trunk would further deviate the COM. However, an in-phase pattern at lower frequencies where the feedback is dominant is seen in experiment data (Zhang et al., 2007).

On the other hand, the model shows that an optimal control with time delay could reproduce the experimental data. This optimal control penalizes muscle activities, consistent with the "minimal intervention" principle (Todorov, 2004). In other words, the nervous system is not so concerned about body sway as long as the sway is with a certain boundary and does not cause the body to fall. Muscles are activated only when it is necessary to maintain upright. This kind of behavior has lower energy cost.

Time delay

The estimated time delay with modeling is 200 ms. The time delay shown in this study is pertinent to the debate of the contribution of feedback, feedforward and stiffness in posture control (van der Kooij et al., 2005; Peterka, 2002). If the system is controlled only by stiffness, then in theory, there is no time delay in feedback. Therefore, our data does not support a stiffness control. The identified plant had gains and phases decreased across frequencies. To compensate for this low-pass property, the feedback had increasing gains across frequencies. The feedback phase also increased initially, but decreased at higher frequencies. In an unstable system with a time delay and increasing gain, the system is unstable. The question is how the unstable human body stays upright with such a feedback system? One of the possibilities is that the feedback control is used along with an additional feedforward control. When we use unpredictable perturbations to identify the feedback system, the

feedforward component is largely excluded (van der Kooij et al., 2005; Fujisawa et al., 2005). A forward control could be part of an internal model used to control movements (Loram, Maganaris, & Lakie, 2005; Wolpert & Ghahramani, 2000).

Different from our view, Peterka (2002) pointed out that feedback alone without feedforward control is sufficient. The high stiffness estimated in Peterka (2002) could contribute to this disagreement. The stiffness estimated in his study was always 1/3 higher than necessary to resist the gravity. When stiffness is high, the requirement for neural control decreases. However, a recent study (Kiemel et al., 2008b) identifying the plant has shown that ankle stiffness is about 50% of necessary to maintain standing. The high stiffness in Peterka (2002) may be due to the platform sway-referencing he used. Recently, Creath et al. (not published yet) had investigated platform sway-referencing as a perturbation and found that it caused changes in the plant and possibly affected the stiffness.

Limitations

One could argue that using a two-input two-output system to identify the feedback oversimplifies the problem since there are so many potential segments of the body. It would be fair to say that there are unexplained aspects of the feedback and plant using this simplification. Obviously, the more segments chosen, the more precise it is for both the identified plant and feedback. However, the posture control system is robust; a reasonable approximation of the number of segments may be enough to identify the fundamental properties of the feedback. It is possible that increasing segments used adds some details to the plant or feedback, but the fundamental properties do not change. Fitzpatrick et al. (1996) have identified the

feedback using a single mechanical perturbation. In their study, the feedback phase increased across frequencies to greater than 180 degrees at higher frequencies. This result is contradicted to the common belief of a time delay in the nervous system especially at the higher frequencies (Peterka, 2002; van der Kooij et al., 2005). By adding an additional mechanical perturbation, we showed a feedback with a time delay of 200 ms, which is within a reasonable physiological range for posture control.

Conclusions

We have identified the feedback and the plant simultaneously using a closed-loop system identification method. The inferred feedback has two outputs, indicating that a simple control strategy may not be sufficient. Subsequently, two sensory perturbations that excite both the legs and trunk segments are more appropriate to identify the plant. Modeling for the feedback favored an optimal control minimizing muscle activity with uncompensated time delay.

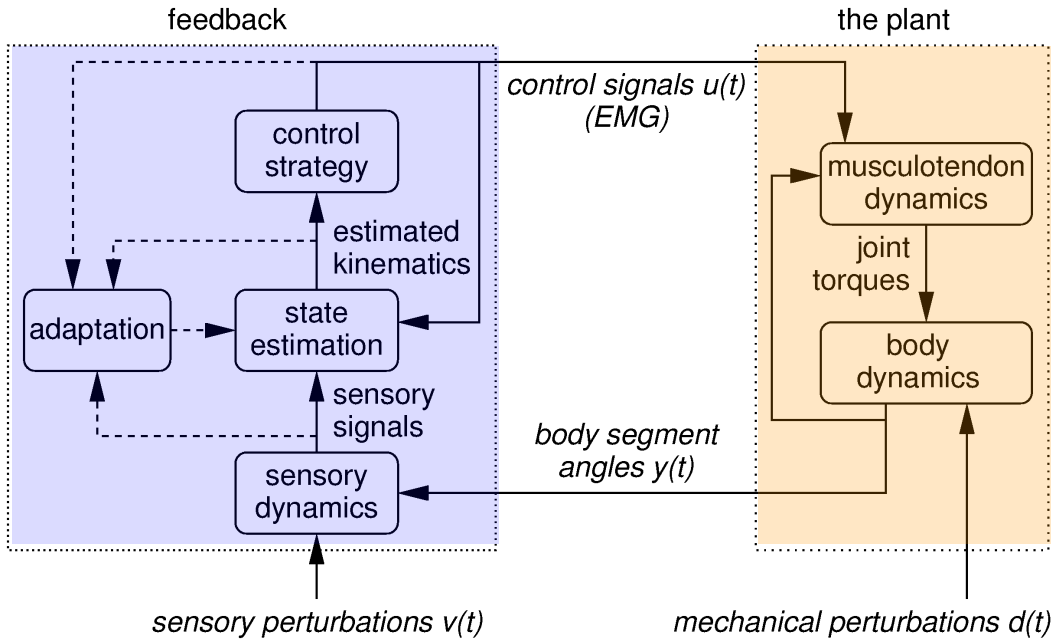

Figure 7.1. model diagram

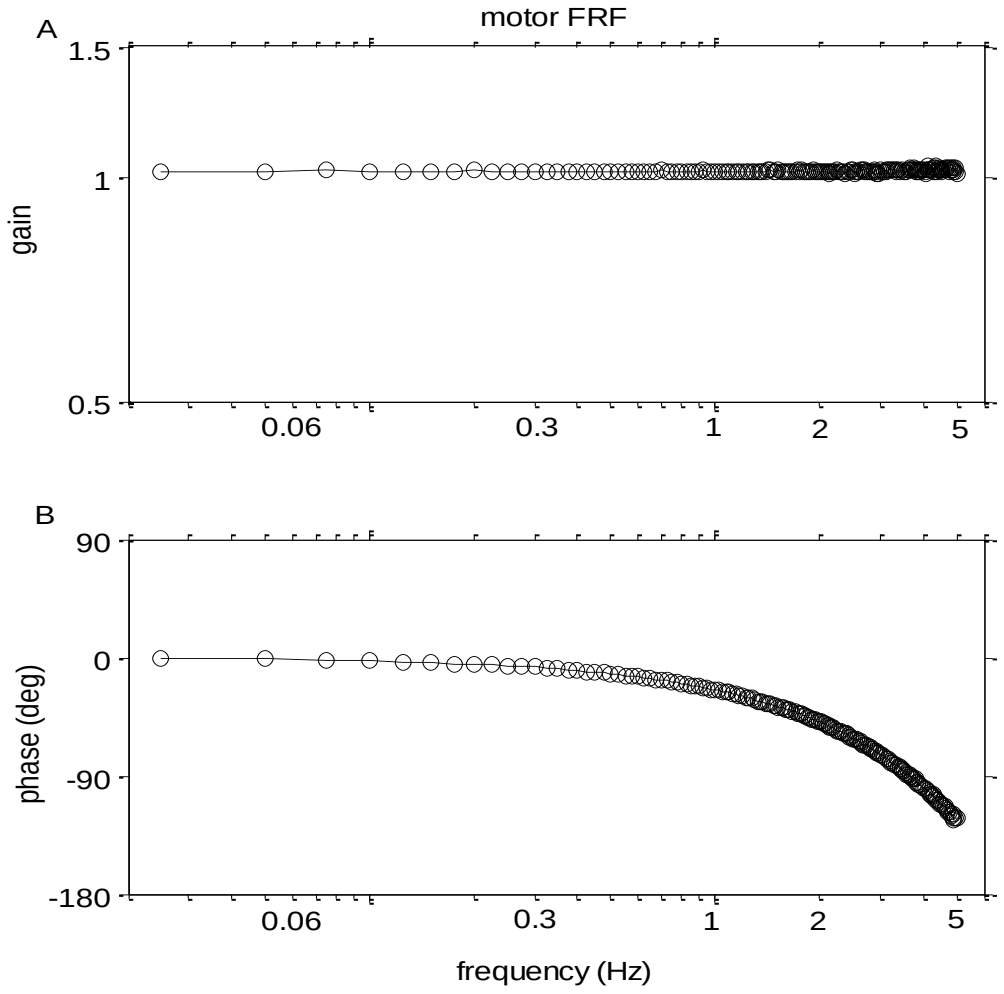

Figure 7.2. Motor FRF. This is an example of the waist motor in response to the desired signal. A. gain; B. phase.

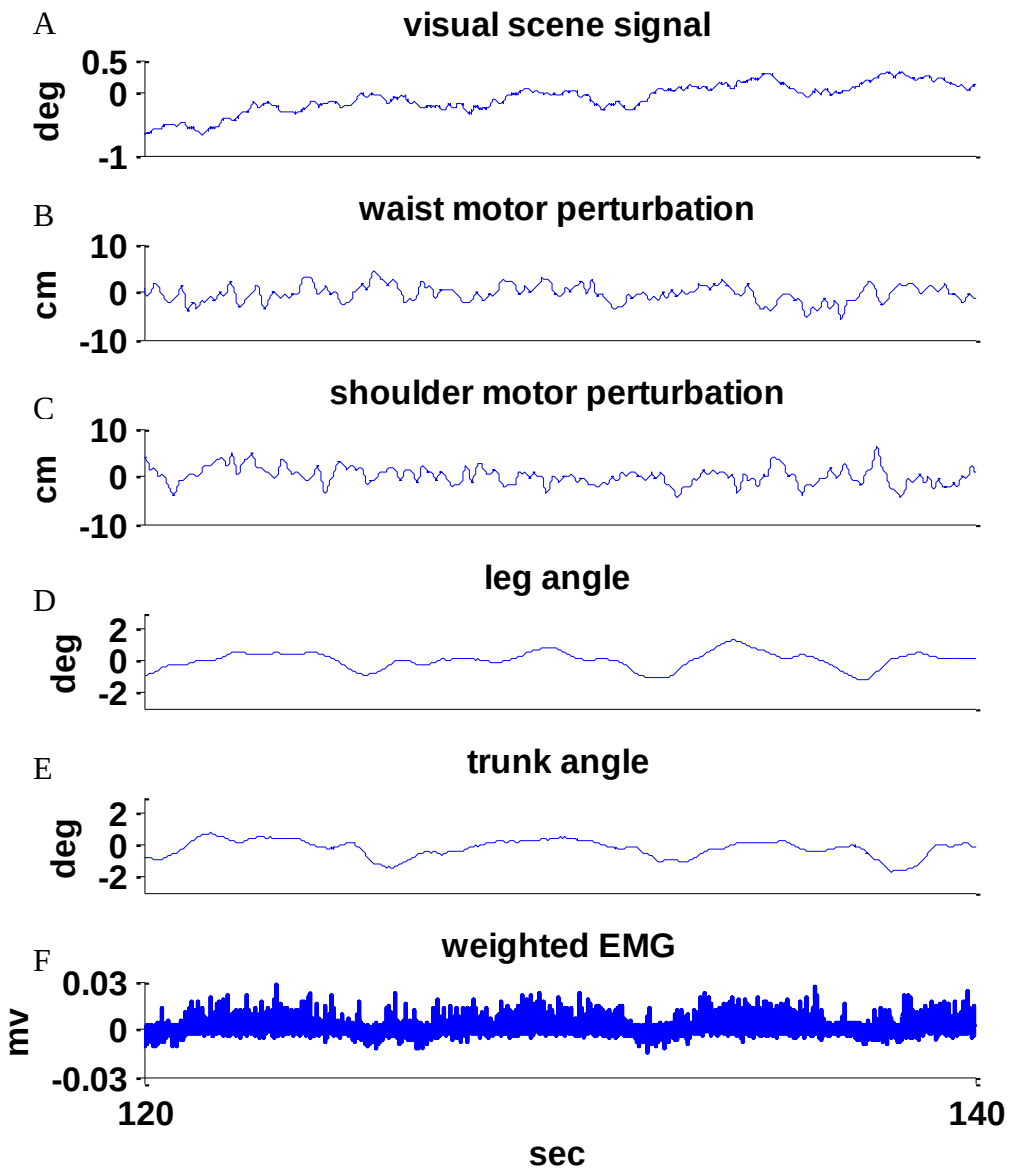

Figure7.3. Example time series from a subject (20 seconds of a single trial). A. visual scene signal; B. waist motor displacement; C. shoulder motor displacement; D. leg angle; E. Trunk angle; F. weight EMG.

	Tibialis anterior	Soleus	Medial gas.	Lateral Gas.	Vastus lat.	Vastus med.	Rectus femoris	Biceps femoris	Semiten diosus	Rectus abdominalis	Erector spinae
Weighted ankle EMG	-0.3235 ±0.1928 (1)	0.3589 ±0.1660 (0)	0.1997 ±0.1311 (1)	0.1179 ±0.1302 (3)	N/A	N/A	N/A	N/A	N/A	N/A	N/A
Weighted hip EMG	N/A	N/A	N/A	N/A	-0.1598 ±0.1260 (0)	-0.0779 ±0.0848 (5)	-0.1092 ±0.1100 (3)	0.2038 ±0.2310 (2)	0.1524 ±0.2506 (5)	-0.1216 ±0.1924 (2)	0.1754 ±0.2124 (2)
Weighted all muscles	-0.1737 ±0.1082 (1)	0.2002 ±0.0955 (0)	0.1226 ±0.0811 (1)	0.0680 ±0.0980 (3)	-0.0633 ±0.0632 (2)	-0.0364 ±0.0405 (5)	-0.04662 ±0.0468 (3)	0.0888 ±0.0987 (2)	0.0710 ±0.1188 (6)	-0.0657 ±0.0888 (2)	0.0637 ±0.0694 (2)

Table 7.1. The mean±SD of weights across subjects for different muscles. The number of subjects with zero weights is included in the parentheses.

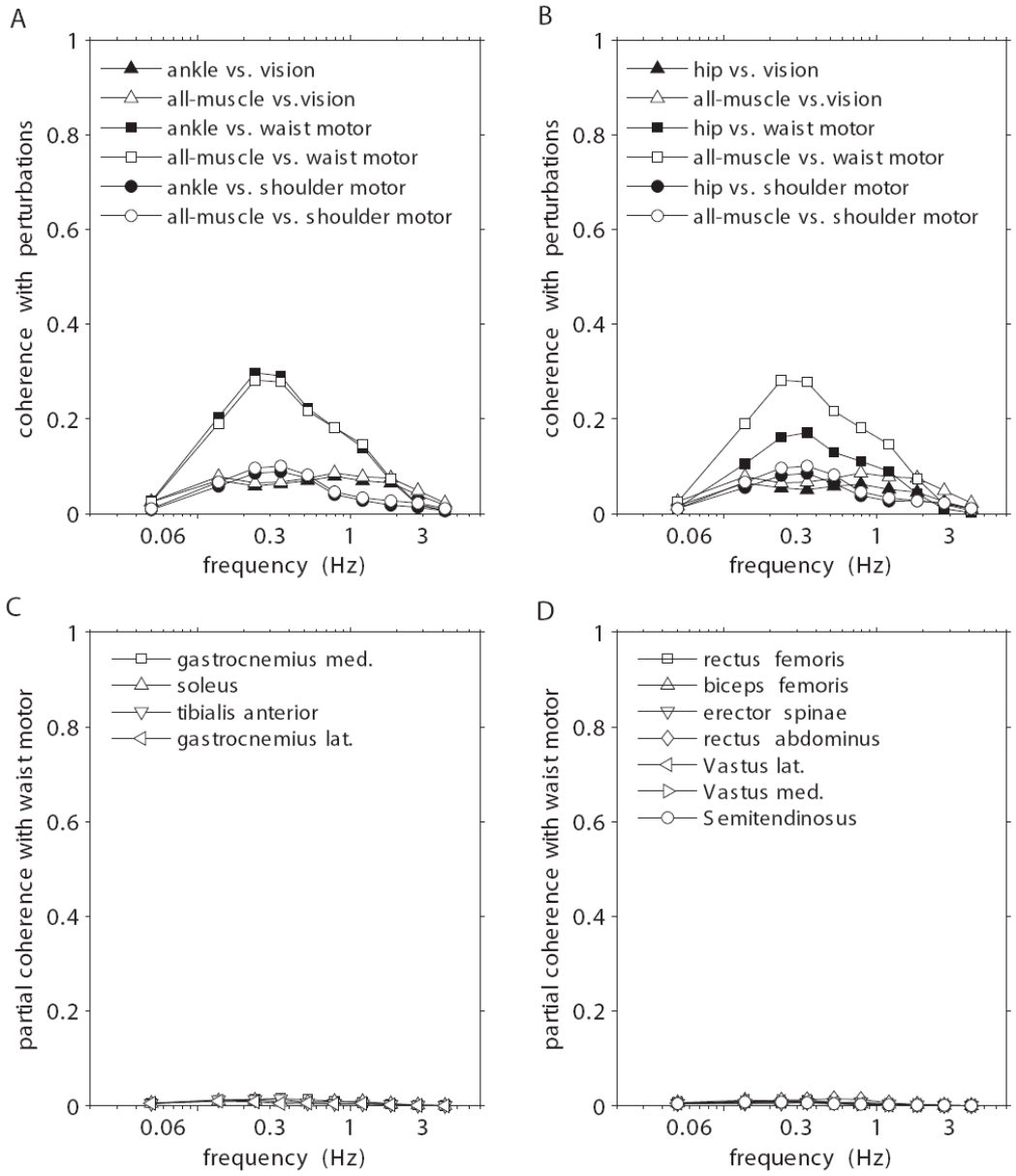

Figure 7.4. Coherence and partial coherence between the perturbations and rectified EMG signals. A. coherence with ankle EMG signals. B. coherence with hip EMG signals. C. partial coherence of vision with ankle EMG signals with ankle EMG signals adjusted for the weighted all-muscle EMG signal. D. partial coherence of vision with hip EMG signals with hip EMG signals adjusted for weighted all-muscle EMG signal.

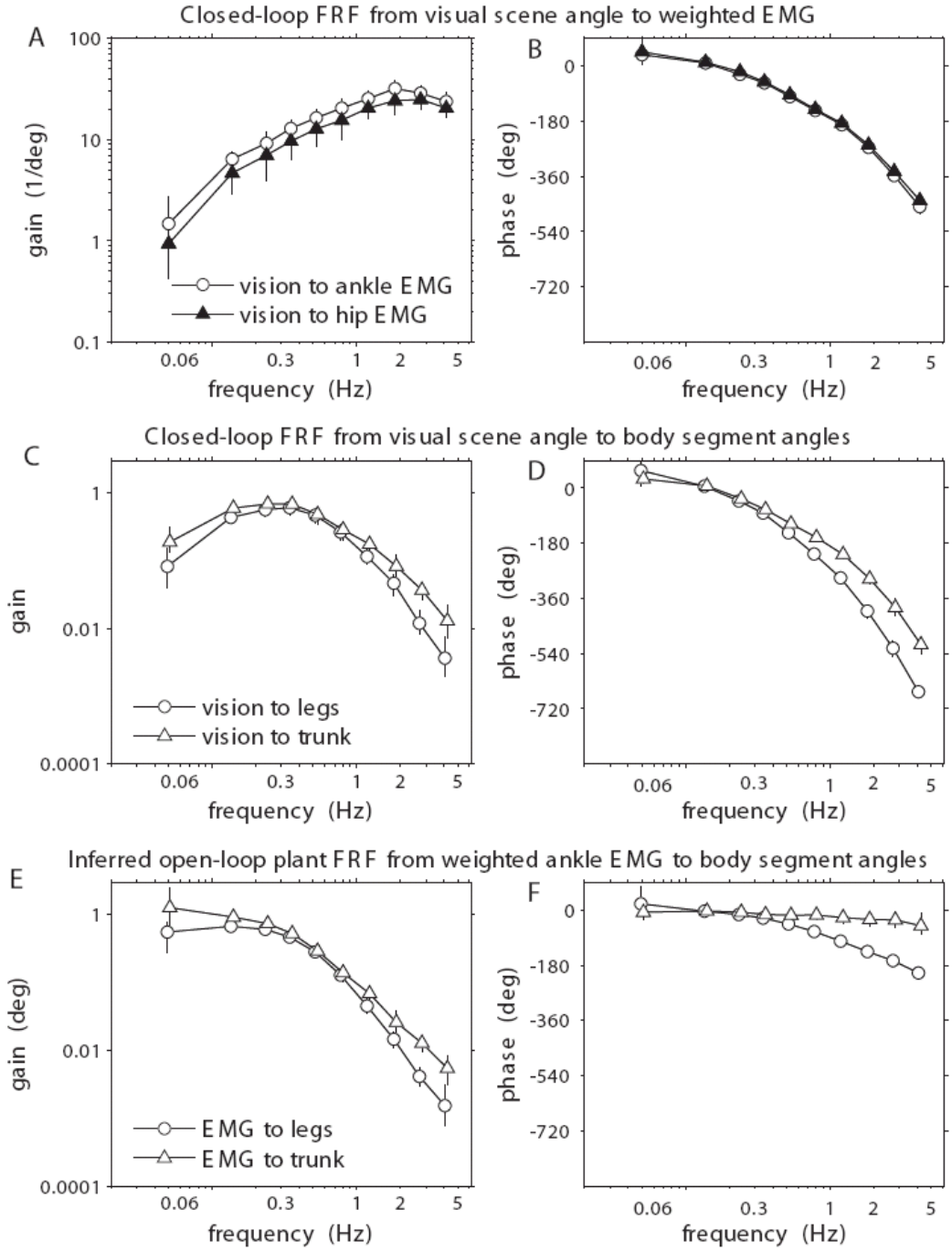

Figure 7.5. Closed-loop responses to visual scene and inferred open-loop plant (average across subjects). Error bars are 95% bootstrap confidence intervals.

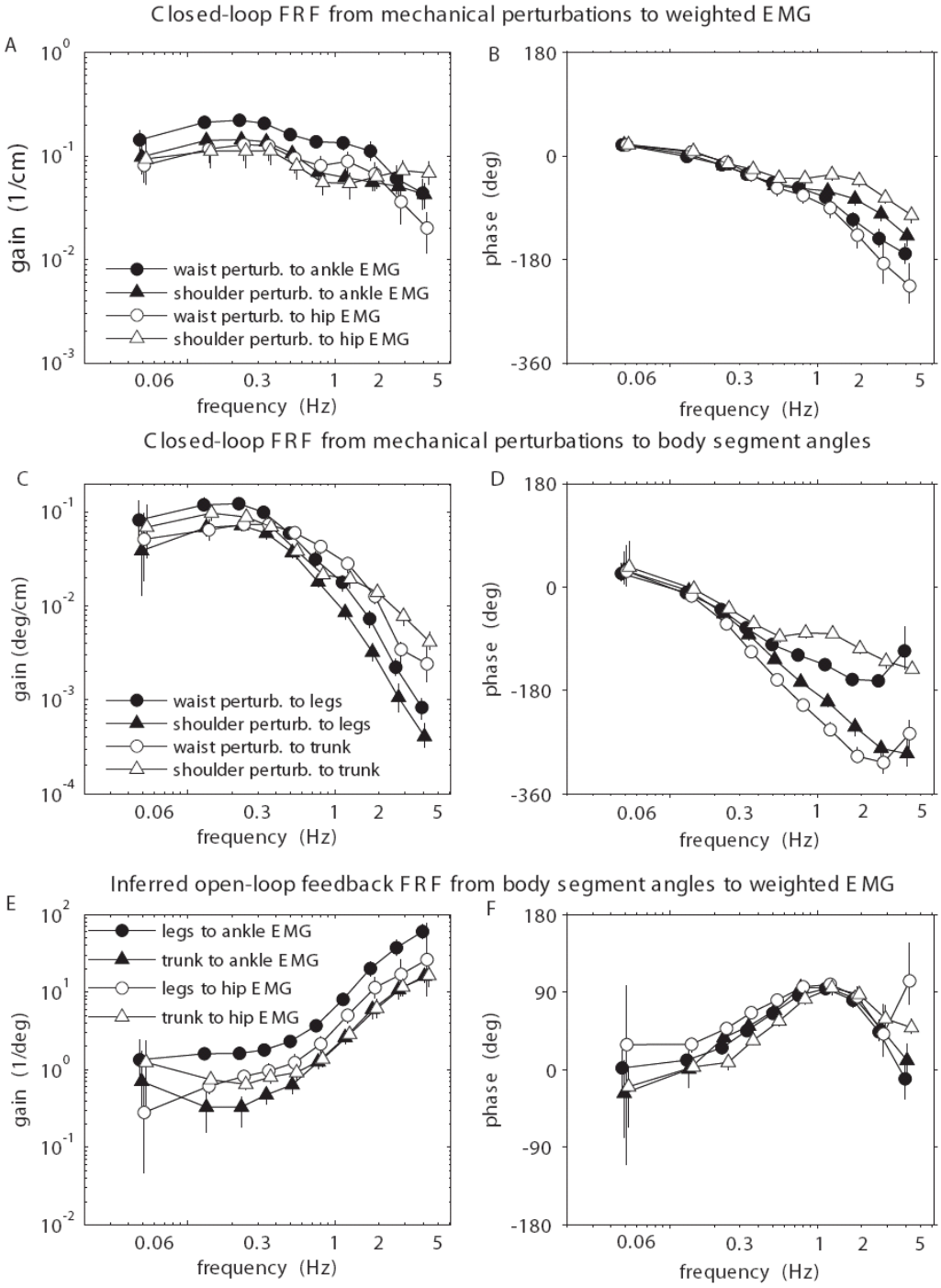

Figure 7.6. Closed-loop responses to mechanical perturbations and inferred open-loop Feedback (average across subjects). Error bars indicate 95% boot strap confidence intervals.

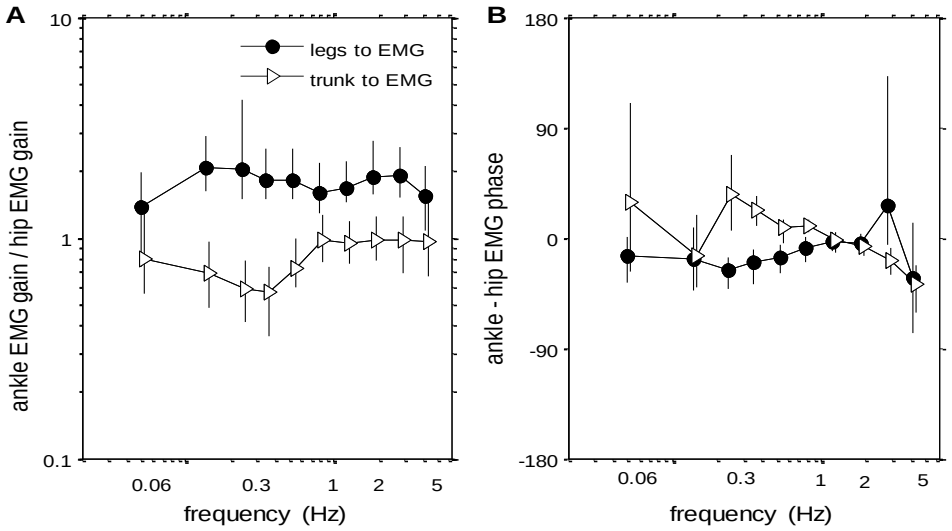

Figure 7.7. Comparison of the inferred open-loop feedback FRF using ankle and hip EMG.

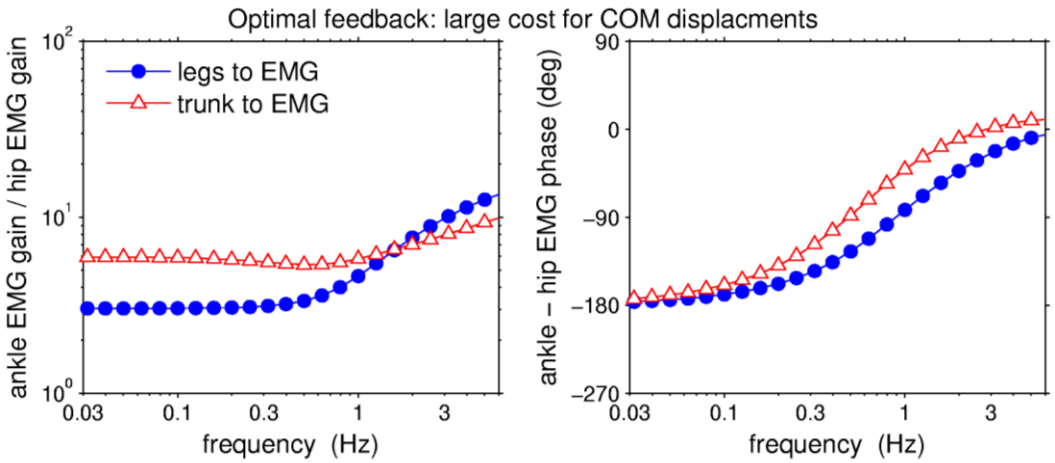

Figure 7.8. Optimal feedback with a cost function of minimizing the COM displacements.

REFERENCE

Alexandrov, A. V., Frolov, A. A., & Massion, J. (2001). Biomechanical analysis of movement strategies in human forward trunk bending. I. modeling. *Biological Cybernetics, 84,* 425-434.

Andersen, R. A., Snyder, L. H., Bradley, D. C., & Xing, J. (1997). Multimodal Representation of Space in the Posterior parietal Cortex and Its Use in Planning Movements. *Annu.Rev.Neurosci., 20,* 203-230.

Angelaki, D. E., McHenry, M. Q., Dickman, J. D., Newlands, S. D., & Hess, B. J. (1999). Computation of inertial motion: neural strategies to resolve ambiguous otolith information. *Journal of Neuroscience, 19,* 316-327.

Bardy, B. G., Marin, L., & Stoffergen, T. A. (1999). Postural coordination modes considered as emergent phenomena. *Journal of Experimental Psychology: Human Perception and Performance, 25,* 1284-1301.

Benjamini, Y. & Hochberg, Y. (1995). Controlling the False Discovery Rate: A Practical and Powerful Approach to Multiple Testing. *Journal of the Royal Statistical Society, 57,* 289-300.

Berthoz, A., Lacour, M., Soechting, J. F., & Vidal, P. P. (1979). The role of vision in the control of posture during linear motion. *Progress in Brain Research, 50,* 197-209.

Bizzi, E., Polit, A., & Morasso, P. G. (1976). Mechanisms Underlying Achievement of Final Head Position. *Journal of Neurophysiology, 39,* 435-444.

Buchanan, J. & Horak, F. B. (1999). Emergence of Postural Patterns As a Function of Vision and Translation Frequency. *Jouranl of Neurobiology, 81,* 2325-2339.

Carver, S., Kiemel, T., van der Kooij, H., & Jeka, J. J. (2005). comparing internal models of the dynamics of the visual environment. *Biological Cybernetics, 92,* 147-163.

Creath, R., Kiemel, T., Horak, F. B., Peterka, R. J., & Jeka, J. J. (2005). A unified view of quiet and perturbed stance: Simultaneous co-existing excitable modes. *Neuroscience Letters, 377,* 75-80.

Dai, T. H., Liu, J. Z., Sahgal, V., Brown, R. W., & Yue, G. H. (2001). Relathionship Between Muscle Output and Functional MRI-measured Brain Activation. *Experimental Brain Research, 140,* 290-300.

Dichgans, J., Held, R., Young, L. R., & Brandt, T. (1972). Moving Visual Scenes Influence the Apparent Direction of Gravity. *Science, 178,* 1217-1219.

Elahi, A., Kiemel, T., Saffer, M., & Jeka, J. J. (2005). The Effect of Shifted COM on Co-existing Coordination Patterns during Quiet Stance. In Washington DC.

Fitzpatrick, R. C., Burke, D., & Gandevia, S. C. (1996). Loop Gain of Reflexes Controlling Human Standing Measured With the Use of Postural and Vestibualr Disturbances. *Journal of Neurophysiology, 76,* 3994-4008.

Fujisawa, N., Masuda, T., Inaoka, H., Fukuoka, Y., Ishida, A., & Minamitani, H. (2005). Human Standing Posture Control System Depending on Adopted Strategies. *Medical & Biological Engineering & Computing, 43,* 107-114.

Gibson, J. J. (1952). The visual field and the visual world: a reply to Professor Boring. *Psychological Review, 59,* 149-151.

Guerraz, M., Shallo-Hoffmann, J., Yarrow, K., Thilo, K. V., Bronstein, A. M., & Gresty, M. A. (2000). Visual control of postural orientation and equilibrium in congenital nystagmus. *Invest Ophthalmol Vis Sci., 41,* 3798-3804.

Henry, S. M., Fung, J., & Horak, F. B. (1998). EMG Responses to Maintain Stance During Multidirectional Surface Translations. *Journal of Neurophysiology, 80,* 1939-1950.

Horak, F. B., Dickstein, R., & Peterka, R. J. (2002). Diabetic Neuropathy and Surface Sway-referencing Disrupt Somatosensory Information for Postural Stability in Stance. *Somatosenory & Motor Research, 19,* 316-326.

Horak, F. B. & Diener, H. C. (1994). Cerebellar control of postural scaling and central set in stance. *Journal of Neurophysiology, 72,* 479-493.

Horak, F. B., Diener, H. C., & Nashner, L. M. (1989). Influence of central set on human postural responses. *Journal of Neurophysiology, 62,* 841-853.

Horak, F. B. & Macpherson, M. (1996). Postural orientation and equilibrium. In J.Shepard & L. Rowell (Eds.), *Handbook of Physiology* (pp. 255-292). New York: Oxford University Press.

Horak, F. B. & Nashner, L. M. (1986). Central programming of postural movements: adaptation to altered support-surface configurations. *Journal of Neurophysiology, 55,* 1369-1381.

Horak, F. B., Nashner, L. M., & Diener, H. C. (1990). Postural strategies associated with somatosensory and vestibular loss. *Experimental Brain Research, 82,* 167-177.

Horak, F. B., Nutt, J., & Nashner, L. M. (1992). Postural inflexibility in parkinsonian subjects. *J.Neurol.Sci, 111,* 46-58.

Horak, F. B. & Shupert, C. L. (1994). Role of the Vestibular System in Postural Control. In S.J.Herman (Ed.), *Vestibular Rehabilitation* (pp. 22-46). Philadelphia: F.A.Davis Company.

Hsu, W., Scholz, J. P., SchÖner, G., Jeka, J. J., & Kiemel, T. (2007). Control and Estimation of Posture During Quiet Stance Depends on Multijoint Coordination. *Journal of Neurophysiology, 97,* 3024-3035.

Ishida, A., Masuda, T., Inaoka, H., & Fukuoka, Y. (2008). Stability of the Human Upright Stance Depending on the Frequency of External Disturbances. *Medical & Biological Engineering & Computing, 46,* 213-221.

Jeka, J. J., Kiemel, T., Creath, R., Horak, F. B., & Peterka, R. (2004). Controlling Human Upright Posture: Velocity Information is More Accurate Than Position or Acceleration. *Journal of Neurophysiology, 92,* 2368-2379.

Jeka, J. J., Oie, K. S., & Kiemel, T. (2000). Multisensory information for human postural control: integrating touch and vision. *Experimental Brain Research, 134,* 107-125.

Jeka, J. J., Ribeiro, P., Oie, K. S., & Lackner, J. R. (1998). The Structure of Somatosensory Information for Human Postural Control. *Motor Control, 2,* 13-33.

Jeka, J. J., SchÖner, G., Dijkstra, T., Ribeiro, P., & Lackner, J. R. (1997). Coupling of fingertip somatosensory information to head and body sway. *Experimental Brain Research, 113,* 475-483.

Johansson, R., Magnusson, M., & Akesson, M. (1988). Identification of Human Postural Dynamics. *IEEE Trans Biomed Eng., 35,* 858-869.

Kandel, E. R., Schwartz, J. H., & Jessell, T. M. (2000). *Principles of Neural Science*. (4 ed.).

Kawato, M. (1999). Internal Models for Motor Control and Trajectory Planning. *Current Opinion in Neurobiology, 9,* 718-727.

Khoo, M. C. K. (1999). Identification of Physiological Control System. In *Physiological Control Systems: Analysis, Simulation, and Estimation* (.

Kiemel, T., Elahi, A., & Jeka, J. J. (2008a). Identification of the Plant for Upright Stance in Humans: Multiple Movement Patterns from a Single Neural Strategy. *Journal of Neurophysiology*.

Kiemel, T., Elahi, A. J., & Jeka, J. J. (2008b). Identification of the Plant for Upright Stance in Humans: Multiple Movement Patterns From a Single Neural Strategy. *Journal of Neurophysiology*, 3394-3406.

Kiemel, T., Oie, K. S., & Jeka, J. J. (2002). Multisensory fusion and the stochastic structure of postural sway. *Biological Cybernetics, 87,* 262-277.

Kiemel, T., Oie, K. S., & Jeka, J. J. (2006). Slow Dynamics of Postural Sway Are in the Feedback Loop. *J Neurophysiol, 95,* 1410-1418.

Kuo, A. D. (2005). An Optimal State Estimation Model of Sensory Integration in Human Postural Balance. *Journal of Neural Engineering,* S235-S249.

Kuo, A. D. (1995). An optimal control model for analyzing human postural balance. *IEEE Trans Biomed Eng., 42,* 87-101.

Kuo, A. D. (2007). Choosing Your Steps Carefully: Trade-offs between Economy and Versatility in Dynamic Walking Bipedal Robots. *IEEE Robotics and Automation Magazine, 14,* 18-29.

Kuo, A. D. & Zajac, F. E. (1993). Human standing posture: multi-joint movement strategies based on biomechanical constraints. *Progress in Brain Research, 97,* 349-358.

Lashley, K. (1951). The Problem of Serial Order in Behavior. In *The Hixon Symposium* New York: John Wiley.

Latash, M. (1993). What Muscle Parameters Are Controlled by the Nervous System? In *Controlled of Human Movement* (pp. 1-48). Champaign, ILL: Human Kinetics.

Leigh, R. J., Newman, S. A., Zee, D. S., & Miller, N. R. (1982). Visual Following During Stimulation of an Immobile Eye (the Open Loop Condition). *Vision Research, 22,* 1193-1197.

Lenzi, D., Cappello, A., & Chiari, L. (2003). Influence of Body Segment Parameters and Modeling Assumption on the Estimate of Center of Mass Trajectory. *Journal of Biomech, 36,* 1335-1341.

Loram, I. D. & Lakie, M. (2002). Direct measurement of human ankle stiffness during quiet standing: the intrinsic mechanical stiffness is insufficient for stability. *Journal of Physiology, 545,* 1041-1053.

Loram, I. D., Maganaris, C. N., & Lakie, M. (2005). Active, Non-spring-like Muscle Movements in Human Postural Sway: How Might Paradoxical Changes in Muscle Length Be Produced? *Journal of Physiology, 564,* 281-293.

Luporini, I., Fleury, A., & Weber, H. (2003). Biomechanical Modeling and Optimal Control of Human Posture. *Journal of Biomech, 36,* 1701-1712.

Masani, K., Popovic, M. R., Nakazawa, K., Kouzaki, M., & Nozaki, D. (2003). Importance of Body Sway Velocity Information in Controlling Ankle

Extensor Activities During Quiet Stance. *Journal of Neurophysiology, 90,* 3774-3782.

Matthews, P. B. C. (1988). Proprioceptors and Their Contribution to Somatosensory Mapping: Complex Messages Requires Complex Processing. *Canadian Journal of Physiological Pharmacology, 66,* 430-438.

Maurer, C., Mergner, T., Bolha, B., & Hlavacka, F. (2001). Human balance control during cutaneous stimulation of the plantar soles. *Neuroscience Letters, 302,* 45-48.

McCollum, G. & Leen, T. K. (1989). Form and Exploration of Mechanical Stability Limits in Erect Stance. *Journal of Motor Behavior, 21,* 225-244.

McIlroy, W. E. & Maki, B. E. (1997). Preferred Placement of the Feet During Quiet Stance: Development of a Standardized Foot Placement for Balance Testing. *Clinical Biomechanics, 12,* 66-70.

McMahon, T. A. (1984). *Muscles, Reflexes, and Locomotion*. Princeton, NJ: Princeton University Press.

Mergner, T., Maurer, C., & Peterka, R. J. (2003). A multisensory posture control model of human upright stance. *Progress in Brain Research, 142,* 189-201.

Mergner, T. & Rosemeier, T. (1998a). Interaction of vestibular, somatosensory and visual signals for postural control and motion perception under terrestrial and microgravity conditions -- a conceptual model. *Brain Research Reviews, 28,* 118-135.

Mergner, T. & Rosemeier, T. (1998b). Interaction of vestibular, somatosensory and visual signals for postural control and motion perception under terrestrial and microgravity conditions -- a conceptural model. *Brain Research Reviews, 28,* 118-135.

Miall, R. C. & Wolpert, D. M. (1996). Forward models for physiological motor control. *Neural Networks, 9,* 1265-1279.

Morasso, P. G. & Sanguineti, V. (2003). Modelling motor control paradigms. In Jiangfeng Feng (Ed.), *Computational neuroscience - A comprehensive approach* (Champman & Hall /CRC.

Morasso, P. G. & Schieppati, M. (1999). Can muscle stiffness alone stablize upright standing? *Journal of Neurophysiology, 83,* 1622-1626.

Nashner, L. M. (1977). Fixed patterns of rapid postural responses among leg muscles during stance. *Experimental Brain Research, 30,* 13-24.

Nashner, L. M. (1981). Analysis of stance posture in humans. In A.L.Towe & E. S. Luschei (Eds.), *Handbook of Behavioral Neurobiology: Motor Coordination* (pp. 527-565). New York: Plenum Press.

Nashner, L. M. & Berthoz, A. (1978). Visual contribution to rapid motor responses during posture control. *Brain Research, 150,* 403-407.

Nashner, L. M., Black, F. O., & Wall, C. I. (1982). Adaptation to altered support and visual conditions during stance: patients with vestibular deficits. *Journal of Neuroscience, 2,* 536-544.

Nashner, L. M. & Woollacott, M. (1979). The organization of rapid postural adjustments of standing humans: an experimental-conceptual model. In R.E.Talbott & D. R. Humphrey (Eds.), *Posture and movement* (pp. 243-257). Raven Press.

Oie, K. S., Kiemel, T., & Jeka, J. J. (2002). Multisensory fusion: simultaneous re-weighting of vision and touch for the control of human posture. *Cognitive Brain Research, 14,* 164-176.

Patterson, S. W., Piper, H., & Starling, E. H. (1914). The Regulation of the Heart Beat. *Journal of Physiology (London), 48,* 465.

Peterka, R. J. (2004). Dynamic regulation of sensorimotor integration in human postural control. *Journal of Neurophysiology, 91,* 410-423.

Peterka, R. J. (2002). Sensorimotor integration in human postural control. *Journal of Neurophysiology, 88,* 1097-1118.

Peterka, R. J. (2000). Postural control model interpretation of stabilogram diffusion analysis. *Biological Cybernetics, 82,* 335-343.

Peterka, R. J. & Benolken, M. S. (1995). Role of Somatosensory and Vestibular Cues in Attenuating Visually Induced Human Postural Sway. *Experimental Brain Research, 105,* 101-110.

Popovic, M., Pappas, I., Nakazawa, K., keller, T., Morari, M., & Dietz, V. (2000). Stability Criterion for Controlling Standing in Able-bodies Subjects. *Journal of Biomech, 33,* 1359-1368.

Runge, C. F., Shupert, C. L., Horak, F. B., & Zajac, F. E. (1998). Role of vestibular information in initiation of rapid postural responses. *Experimental Brain Research, 122,* 403-412.

Runge, C. F., Shupert, C. L., Horak, F. B., & Zajac, F. E. (1999). Ankle and Hip Postural Strategies Defined by Joint Torque. *Gait & Posture, 10,* 161-170.

Saffer, M., Kiemel, T., & Jeka, J. J. (2005). Co-existing Patterns of Sway, Co-existing Modes of Control. In Washington DC.

Saffer, M., Kiemel, T., & Jeka, J. J. (2008). Coherence Analysis of Muslce Activity during Quiet Stance. *Experimental Brain Research, 185,* 215-226.

SchÖner, G. (1991). Dynamic Theory of Action-Perception Patterns: the "Moving Room" Paradigm. *Biological Cybernetics, 64,* 455-462.

Shumway-Cook, A. & Woollacott, M. H. (2000). *Motor Control: Theory and Pratical Applications*. (2 ed.) Baltimore: Lippincott Williams & Wilkins.

Shupert, C. L., Black, F. O., Horak, F. B., & Nashner, L. M. (1988b). Coordination of The Head And Body in Response to Supprot Surface Translations in Normals And Patients with Bilaterally Reduced Vestibular Functions. In B.Amblard, A. Berthoz, & F. Clarac (Eds.), *Posture And Gait: Development, Adaptation And Modulation* (pp. 281-289). Amsterdam: Elsevier.

Shupert, C. L., Black, F. O., Horak, F. B., & Nashner, L. M. (1988a). Coordination of The Head And Body in Response to Support Surface Translations in Normals And Patients with Bilaterally Reduced Vestibular Functions. In B.Amblard,

A. Berthoz, & F. Clarac (Eds.), *Posture And Gait: Development, Adaptation And Modulation* (pp. 281-289). Amsterdam: Elsevier.

Stark, L. & Baker, F. (1958). Stability and Oscillations in a Neurological Servomechanism. *Journal of Neurophysiology, 22,* 156-164.

Stein, B. E. (1998). Neural mechanisms for synthesizing sensory information and producing adaptive behavior. *Experimental Brain Research, 123,* 124-135.

Stein, R. B. (1982). What Muscle Variable(s) Does the Nervous System Control in Limb Movements? *The Behavioral And Brain Science, 5,* 535-577.

Stoffergen, T. A. (1985). Flow structure versus retinal location in the optical control of stance. *J Exp Psychol Hum Percept Perf, 11,* 554-565.

Sugrue, L. P., Corrado, G. S., & Newsome, W. T. (2005). Choosing the Greater of Two Goods: Neural Currencies for Valuation and Decision Making. *Nature Reviews: Neuroscience, 6,* 363-375.

Todorov, E. (2004). Optimality Principles in Sensorimotor Control. *Nature Neuroscience, 7,* 907-915.

van der Kooij, H., Jacobs, R., Koopman, B., & Grootenboer, H. (1999). A multisensory integration model of human stance control. *Biological Cybernetics, 80,* 299-308.

van der Kooij, H., Jacobs, R., Koopman, B., & van der Helm, F. (2001). An adaptive model of sensory integration in a dynamic environment applied to human stance control. *Biological Cybernetics, 84,* 103-115.

van der Kooij, H., van Asseldonk, E., & van der Helm, F. (2005). Comparison of Different Methods to Identify and Quantify Balance Control. *Journal of Neuroscience Methods, 145,* 175-203.

van Iersel, M. B., Ribber, H., Munneke, M., Borm, G. F. B., & Olde Rikkert, M. G. (2007). The Effect of Cognitive Dual Tasks on Balance During Walking in Physically Fit Elderly People. *Arch Phys Med Rehabil, 88,* 187-191.

Winter, D. A., Patla, A. E., Prince, F., & Ishac, M. (1998). Stiffness of control of balance in quiet standing. *Journal of Neurophysiology, 80,* 1211-1221.

Winter, D. A., Prince, F., Frank, J. S., Powell, C., & Zabjek, K. F. (1996). Unified Theory Regarding A/P and M/L balance in Quiet Stance. *Journal of Neurophysiology, 57,* 1-10.

Wolpert, D. M. & Ghahramani, Z. (2000). Computational Principles of Movement Neuroscience. *Nature Neuroscience Supplement, 3,* 1212-1217.

Wolpert, D. M., Ghahramani, Z., & Jordan, M. I. (1995). An internal model for sensorimotor integration. *Science, 269,* 1880-1882.

Woollacott, M. & Shumway-Cook, A. (2002). Attention and the control of posture and gait: a review fo an emerging area of research. *Gait & Posture, 16,* 1-14.

Zhang, Y., Kiemel, T., & Jeka, J. J. (2007). The Influencce of Sensory Information on Two-Component Coordination During Quiet Stance. *Gait & Posture, 26,* 263-271.

Zhang, Y., Kiemel, T., & Jeka, J. J. (2006). The Influencce of Sensory Information on Two-Component Coordination During Quiet Stance. *Gait & Posture, in submission*.